The development of ion mobility-mass spectrometry for complex mixture analysis

Emma. L. Harry

Centre for Analytical Science
Department of chemistry
Loughborough University

LIST OF ABBREVIATIONS

IM	Ion mobility
IMS	Ion mobility spectrometry
MS	Mass spectrometry
FAIMS	Field asymmetric ion mobility spectrometry
CV	Compensation voltage
DV	Dispersion voltage
DMS	Differential mobility spectrometry
LC	Liquid chromatography
HPLC	High performance liquid chromatography
UHPLC	Ultra high performance liquid chromatography
GC	Gas chromatography
TLC	Thin layer chromatography
RP-TLC	Reversed phase-thin layer chromatography
DESI	Desorption electrospray ionisation
ESI	Electrospray ionisation
HESI	Heated electrospray ionisation
CRM	Charge residue model
IEM	Ion evaporation model
FAB	Fast atom bombardment
MALDI	Matrix assisted laser desorption ionisation
ToF	Time of flight
Q-ToF	Quadrupole time-of-flight
FT-ICR	Fourier transform-ion cyclotron resonance
RF	Radio frequency
DC	Direct current
NMR	Nuclear magnetic resonance spectrometry
PCA	Principle component analysis
ANNs	Artificial neural networks
DNA	Deoxyribonucleic acid
LOD	Limit of detection
R_f	Retention factor
QC	Quality control
m/z	Mass-to-charge
RMS	Root mean square

LIST OF FIGURES

ABSTRACT

Multidimensional ion mobility (IM) and mass spectrometry separations have been applied successfully to the analysis of a wide range of analytes and demonstrate potential as a selective and high throughput analytical technique.

The direct analysis of pharmaceutical formulations from non-bonded reversed-phase thin layer chromatography (RP-TLC) plates by desorption electrospray ionisation (DESI) combined with drift tube ion mobility-mass spectrometry (IM-MS) has been investigated. The detection of active pharmaceutical ingredients is demonstrated with, and without, chromatographic separation of the active ingredients and formulation excipients. Varying the solvent composition of the DESI spray using a gradient allows selective desorption of pharmaceutical ingredients from the surface of the RP-TLC plate.

The potential of IM-MS in combination with high performance liquid chromatography (LC) for the metabonomic analysis of rat urine is reported. The approach allowed the acquisition of nested data sets, with mass spectra acquired at regular intervals during each IM separation and several IM spectra acquired during the elution of an LC peak. The application of LC combined with field asymmetric waveform ion mobility spectrometry (FAIMS) and ion trap mass spectrometry to a metabonomic study of rat urine, with subsequent data mining by artificial neural networks, allowed discrimination between young and old rats on the basis of LC-FAIMS-MS profiles.

The application of IM-MS to real-time reaction monitoring has also been investigated. Real-time reaction monitoring was carried out over a period of several hours, with the reaction mixture sampled and analysed at intervals of several minutes. Results indicate that spectral quality is improved when employing IM-MS, compared to mass spectrometry alone, as the complexity of the reaction mixture increases with time. The combined IM-MS approach has potential as a rapid and selective technique to aid pharmaceutical process control and for the elucidation of reaction mechanism.

ACKNOWLEDGEMENTS

I would like to thank dearly my supervisor professor Colin Creaser for his continued support, encouragement, guidance and patience during the entirety of my PhD and for being so generous and tireless in helping me, both professionally and personally. I would also like to thank the rest of my supervisory team, Tony Bristow, Ian Wilson and Paul Thomas for their continued support, advice, and regular uplifting phone calls and emails. For the stream of ideas and suggestions which came my way, thank you. I would also like to acknowledge the collaborating establishment, AstraZeneca, UK, for financial support.

It is rare the person who can call all of her colleagues friends, Jim, Dan, Gavin, Mark, Little Vic, Big Vic, Lauren, Nikki, Neil, Helen, Matt, Vicky, Christina, Aadi, Ran, Andrea. Thank you all.

I would like to say a big "thank you" to all of my family and friends, especially, Pamela, Charlotte, Nad, Kelly, Debbie & Tracy. And to Lynn, whose continued support many years ago has drove me along the way, deepest thank you. I wish to thank Damian, for moving across country from university to university and making it possible for me to carry out my studies, for your encouragement and non faltering belief that I could do this. And finally and most of all, to my beautiful little girl who has been the greatest and most unexpected motivator, Beau, thank you.

CONTENTS

CHAPTER ONE

Introduction

1.1 Ion mobility spectrometry

Objects suspended in a gas or liquid medium experience spontaneous diffusion due to Brownian motion at finite temperature. With no other forces exerted the diffusion has no preferred direction, however when an external force is applied (electrical, magnetic or gravitational) an object will move along its vector with a speed controlled by the characteristic known as mobility.[1] The application of an electric field creates a Coulomb force which is exerted onto charged particles causing them to move along field lines, towards increasing potential. Both the diffusion and mobility properties of an ion are dependant upon the nature of the ion. The study of ions in an electric field is termed ion mobility spectrometry (IMS). IMS is a gas phase electrophoretic technique, first introduced in 1970 by Karasek[2] under the name plasma chromatography, IMS has since developed considerably over the last decade and now branches into two subfields; drift tube ion mobility spectrometry (IMS), where a constant electric field is applied to a drift tube and methods are based upon absolute ion transport properties measured using a time-independent electric field, and field asymmetric waveform ion mobility spectrometry (FAIMS), or differential mobility spectrometry (DMS) where a change in ion transport properties is a function of a time-dependent electric field.

IMS allows analytes to be distinguished on the basis of their ion mobility defined by their reduced mass, charge and collision cross section (*i.e.*, size and shape).[3] Ion mobility is determined by the velocity of an ion under the influence of the electric field gradient and in the presence of a buffer gas, measured using a drift tube. Ion mobility is therefore characteristic of the analyte and the buffer gas, and hence can provide a means for the detection and identification of single component ions within a

mixture. The electric field accelerates ions, while collisions with the buffer gas decelerate them, leading to a constant drift velocity.[4] IMS allows for the study of a wide range of chemical species, from aggregates of carbon and silicon clusters through to studies of volatile and semi-volatile compounds, biomolecules and synthetic polymers. [3,5,6,7]

1.1.1 Theoretical principles of ion mobility spectrometry

Free molecular diffusion is governed by Fick's law of diffusion:

$$J_M = -D\nabla_N \qquad \text{Equation 1.1}$$

Where J_M represents the number of molecules flowing through a unit area per unit time, ∇_N is the concentration gradient and D the diffusion coefficient which is a molecular characteristic. A molecule will diffuse differently in different media and so D is a property of both the diffusing molecules and the media. The velocity of the diffuse flow, v_D, is proportional to D:

$$v_D = -(D/N)\,\nabla_N \qquad \text{Equation 1.2}$$

Where N is the number density of the gas (the number of molecules per unit volume) for diffusion in gases, D is determined by:

$$D = \frac{3}{16N}\left(\frac{2\pi k_B T}{\mu}\right)^{1/2}\frac{1}{\Omega} \qquad \text{Equation 1.3}$$

Where *k*B is the Boltzmann constant, *T* is the gas temperature and μ = (Mm/m+M*)* is the reduced mass of the diffusing ion (M) and the drift gas molecule (m). The quantity Ω is the collision integral of both the diffusing molecule and the diffusing media molecule and is termed the collision cross section. Of the variables acting upon a diffusing molecule Ω is the only variable that depends on the structure of the gas molecule and the diffusing molecule and therefore unknown molecules can be characterised based upon measuring the speed of diffusion in a known gas at standard temperature and pressure and is the basis for ion mobility spectrometry. When a coulombic force is applied, analyte ions reach a terminal velocity v or the drift velocity, in IMS different species have different drift velocities depending on their ions mobility K. [1]

Ion mobility spectrometry (IMS), formerly known as plasma chromatography,[2] is based on determining the drift velocities (υ_d) attained by ionised sample molecules in the weak electric field of a drift tube containing a gas. Therefore, ions have to be formed from sample molecules to measure ion mobilities.[8] The drift velocity of an ion is described by:

$$\upsilon_d = KE \qquad \text{Equation 1.4}$$

Where υ_d is the ion drift velocity (cm s^{-1}), *K* the mobility of an ion (cm^2 V^{-1} S^{-1}) and *E* is the electric field strength (V cm^{-1}).

Ion mobility is further influenced by the operational parameters as well as by the structural features of the ions, described by the Mason-Schamp equation:

$$K = \frac{3ze}{16N}\left(\frac{2\pi}{\mu k_B T}\right)^{1/2}\frac{1}{\Omega} \qquad \text{Equation 1.5}$$

Where z is the charge on the ion, N the density of drift gas molecules, μ = (m xM)/(m+M) the reduced mass of the ion (m) and drift gas molecule (M), k the Boltzmann constant, T the temperature and Ω is the average ionic collision cross-section. Ω includes structural parameters (size and shape)[4]. The mobility of an ion at a given temperature and buffer gas pressure is therefore determined by the mass, charge and, most importantly, the collision cross section of the ion. This relationship only holds true at the low field limit, where the ratio of *E/N* is ≤ 2 Td, (where 1Td (Townsend) = 10^{-17} C cm^2). At higher values of *E/N* the mobility is no longer constant but becomes field dependant, which is the main principle of FAIMS or DMS as described in Section 1.3.[9] Ions in this regime effectiviely have no inertia and hence mobility of an ion will stop if the field is switched off, ions can be further decelerated by collisions with the buffer gas molecules with the velocity loss being dependant upon the m/M ratio and hence velocity is a function of the reduced mass of drift gas molecules. The acceleration of an ion between braking events or collisions is proportional to E and their frequency is proportional to N. [1] Hence, V is proportional to *E/N* and *K* is proportional to *K=v/E* or *1/N*. The absolute mobility scale enabling comparisons between IMS data at different *N* is attainable by calculating reduced mobilities**.** Reduced mobility (K_0) is the ion mobility corrected to standard

conditions of temperature (T in Kelvin) and pressure (p_b in Torr), as an increase in temperature, or a decrease in pressure, causes ions to travel faster and hence increase ion mobilities:

$$K_0 = K(273/T)\,(p_b/760) \qquad \text{Equation 1.6}$$

Ions in gases diffuse regardless of the presence of an electric field described previously and governed by Brownian motion and hence resolution in IMS is limited mostly by diffusion of the ion packets along the drift tube. Ion packets placed in a uniform electric field steadily broaden while drifting along E, the diffusion at low field limits is isotropic with packets which are initially spherical diffusing equally in all directions and thus remain spherical. Non spherical packets though initially retain their shape become increasingly spherical as they drift along E. [1] Diffusion is a critical parameter in IMS in regards to resolution, if two ion packets diffuse and overlap then resolution of the two species is not attainable. The resolution (R) is therefore defined by the intensities of the peaks relative to the baseline:

$$R = \frac{^{2}\left(td_B - td_A\right)}{\left(wt_A + wt_B\right)} \qquad \text{Equation 1.7}$$

And is defined through the full width at half maximum (FWHM) of peak:

$$R = \frac{td}{w_{1/2}} \qquad \text{Equation 1.8}$$

The resolving power in conventional IMS depends on the electric field strength, gas temperature and pressure, ion charge state, drift tube length and the ion injection gate width. The non-zero width of ion packets at the start of IMS separations and broadening mechanisms such as coulomb repulsion, diffusion broadening and also field heterogeneity, capacitive coupling between approaching ions and the detector and ion molecule reactions within the drift region all reduce resolution in IMS separations. Improvements in resolution have been investigated by extending the separation time of the analysis employing gas flows in addition to electric fields.[10] In order to increase resolving power it is necessary to increase the voltage across the drift tube. However, it is desirable to keep the ions within the low field limit, low E/N, where the mobility is independent of the drift field, E. [11] At high fields the mobility depends on the drift voltage and alignment of the drifting ions may occur. To overcome this problem and in order to increase the voltage across the drift tube it is necessary to also increase the buffer gas pressure. Temperature effects resolution in IMS and the resolving power (Rp) is inversely proportional to the square root of the drift gas temperature or resolving power decreases when the temperature is increased. By reducing the overall temperature the diffusion limit can be reduced, however at extremely low temperatures an increase in ion clustering with water is observed leading to a decreases in Rp. Cases of increasing resolution with increasing temperature have also been reported. The increase or decrease in resolution at

elevated temperatures has been attributed to the changes in separation factor (α) which is governed by the different hydration and clustering tendency of ions.[12] Temperature reduces resolving power but can increase α – depending on hydration tendencies of the analyte ions. An increase in de-clustering reduces ion size and hence reduces collisions and Ω of the ion, leading to the potential shift of the ion drift time which results in the possibility of changing the selectivity of an ion.

Increasing the electric field strength results in relatively higher resolution whereby diffusion theory predicts that IMS resolving power increases with the square root of the voltage applied across the drift tube. For example Clemmer *et al.*[13] obtained a resolving power of 172 for fullerene by increasing the voltage across the drift tube (10 000V) by developing a new high resolution IMS apparatus. However, a consequence of high electric field strength is that the drift gas pressure must be increased proportionally to maintain a low *E*/*N* ratio also electrical breakdown within gases can occur at high electric field strengths which caps the maximum E attainable. However, higher polarisable gases can withstand higher voltages before electrical breakdown occurs and hence can extend the value of E which can be applied. The ion injection gate width is an important factor in relation to IMS resolution, with longer pulse widths resulting in peak broadening at the start of the IMS separation and a decrease in resolution. The width of the initial ion packet also determines the shape and width of an IM peak whilst also preventing diffusion of neutral species into the drift region. Figure 1.1 displays the effects of initial ion pulse width on resolution at different pressures. It can be seen that resolution decreases as the gate width increases.[14]

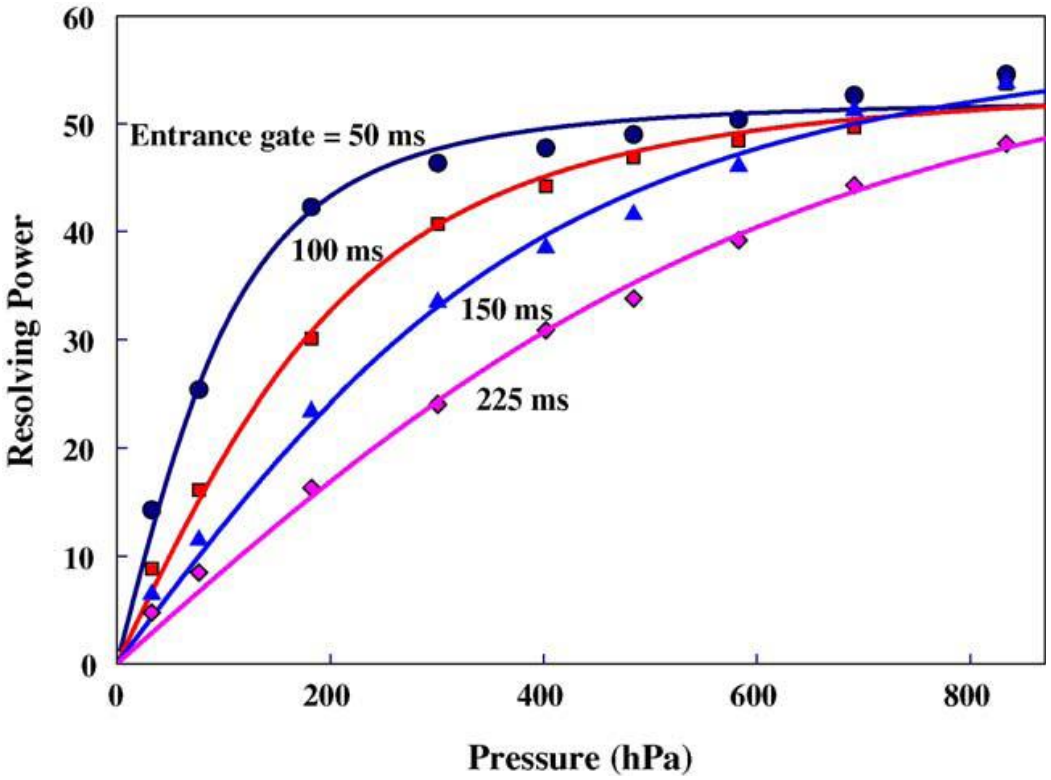

Figure 1.1. Predicted and measured resolving power with different gate widths at various pressures. [14]

At zero pressure resolution is equal to zero. Increasing pressure has no effect on separation factors however, increasing pressure increases resolution. The decrease in resolution at low pressures can be compensated by shortening the ion pulse width since reducing pressure results in a higher ion current (E/N). Resolving power increases with pressure however it cannot exceed a certain value which is termed the diffusion limited resolving power. Tabrizchi *et al.* [14] investigated the effects of pressure in IMS and showed that reducing pressure has no effect on separation factors but decreases the resolving power and resolution.

1.1.2 IMS instrumentation

The basic components of an IMS consist of a sample inlet system, an ionisation region, a reaction region (for ^{63}Ni and CI ionisation processes), an ion gate, a drift region and an ion collector. Figure 1.2 illustrates these components in a conventional stacked ring drift tube design. Sample product ions are formed and directed toward the drift region by an applied electric field. A narrow pulse of ions is injected into the drift region using an ion shutter grid. In the drift region, ions of different identities are separated based upon, charge, mass and collision cross section. The analytical signal is obtained when ions strike a conducting plate and the resulting current amplified.[15]

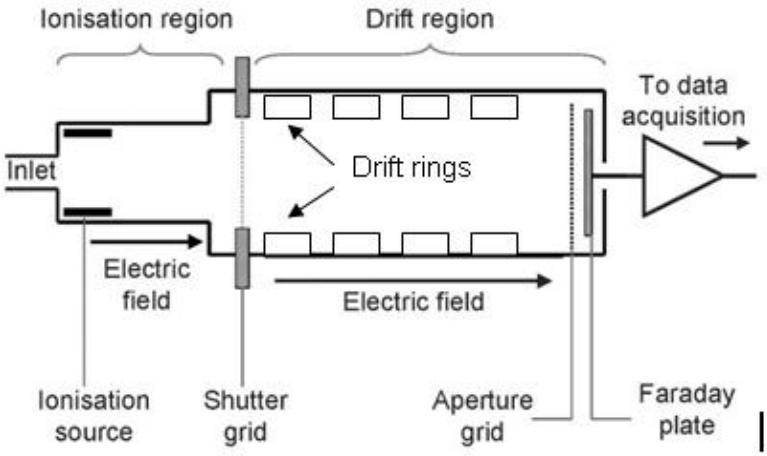

Figure 1.2. Schematic diagram of an ion mobility spectrometer taken from reference[3]

1.1.2.1 Sample introduction and ionisation

Ions may be generated by numerous ionisation techniques but most commonly externally using electrospray ionisation (ESI)[16] or within the ionisation region of the IMS drift cell via atmospheric pressure chemical ionisation (APCI) using a ^{63}Ni source. [17] On entering the drift region ions are subjected to a uniform weak electric field, which accelerates them towards a detector situated at the end of the drift region. A buffer gas is also present within the drift cell which is held at a constant pressure, typically 1-760 Torr[2]. Ions passing through the drift region experience collisions with the buffer gas molecules impeding their progression towards the detector. Ions with larger collision cross sections (Ω) experience more collisions with the buffer gas molecules compared to those with smaller collision cross sections and, therefore take longer to transverse the drift tube. As discussed previously collision cross section includes size and shape and hence separation of ions differing in size and shape (not necessarily mass).

Numerous sample introduction techniques have been developed and are employed in IMS. One method, described by Karpas[18], involved the adsorption of sample vapour onto a nickel wire. The wire was then inserted, through a septum into the heated ionisation region. This heated region allows the adsorbed sample to volatilise from the wire's surface and be ionised by the ^{63}Ni source. Further methods of sample introduction include headspace analysis,[19] diffusion tubes,[20] permeation tubes,[21] membrane inlet, [22,23] syringe injection,[24] and laser desorption/ablation.[25]

The coupling of chromatography with IMS has also been described,[26,27,28,29] providing an additional separation. IMS was first evaluated as a detector for liquid

chromatography (LC) in 1973[30]. The sample was introduced with the moving wire technique described above by Karpas.[18] Spectra were successfully obtained for halogenated benzenes, DDT, Endrin, and Dieldrin. Spectral collection times averaged two minutes, though no chromatograms were shown, eventually electrospray probes (described in section 1.4.1.1) were developed over time in order to allow successful coupling.[31] Gas chromatography (GC) however, proved to be a more attainable coupling strategy with IMS. Sample analytes are already within the gas-phase and sample sizes are considerably smaller than for LC. In hyphenated GC-IM the capillary column is inserted into the ionisation region allowing the eluent to be directly ionised within its own carrier gas.[32]

1.1.2.2 The drift region

Once sample ions have been generated they enter the drift region of the IMS cell where separation can occur (see Figure 1.2). Ions may either be gated into the drift region electronically or pulsed in by some other means. In both cases, a trigger is required to synchronise the detector with the entry of the ions allowing accurate drift times to be recorded. A typical ion gate, or shutter grid as employed in atmospheric pressure IMS consists of a series of parallel wires held at a potential to prevent entry of the ions into the drift region. Potential changes across the wires to match that of the drift field, opens the gate, allowing the ions to enter the drift region. The two main shutter grids employed are the Tyndall gate[33] and the Bradbury/Neilson gate.[34]

The Tyndall gate[33] consists of two grids separated by <1mm placed across the entrance of the drift tube. When a voltage is applied across the two grids the gate is closed the closed grid also attracts the ions which are neutralised upon impact.

The Bradbury/Neilson gate[34] is composed of a single shutter grid in which the shutter grid consisting of alternate wires is held at opposite polarity to one another. The gate is opened when an applied voltage to all the wires equals that of the drift field.

Once the ions have been gated into the drift region, they experience a uniformed electric field gradient created by a series of metal drift rings (Figure 1.2). Each drift ring is connected to the next by a resistor, which acts as a voltage divider. When a voltage is applied to the first and last drift ring in the cell, the potential difference between these voltages is spread evenly across the whole stack of drift rings creating a constant field gradient. The strength of the field gradient varies between instruments, but is typically in the range of 1-500 Vcm^{-1}.

1.1.2.3 The drift gas

The common drift gases employed in IMS are nitrogen and control air, other less commonly used gases includes helium,[35] argon[36] and carbon dioxide.[27] The use of different drift gases and their effects on ion mobility have been well documented.[37,38] Ions have been found to travel faster in the lighter gases with lower polarisabilities such as helium.[37] Helium also proves valuable in the measurement of collision cross sections in the gas phase. Due to the low polarisability of helium, molecular

modelling and the associated theoretical calculations become simplified. A loss in sensitivity with heavier gases has also been reported primarily due to the longer periods of time the ions spend in the drift region resulting in ion scattering. However, resolving power has been found to increase due to the ions travelling more slowly.[37]

The separation of two analytes is dependant upon the separation factor (α) which is described by:

$$\alpha = K_1/K_2 \qquad \text{Equation 1.9}$$

Where $K_1$is the mobility of the faster moving ion and K_2 is the mobility of the more slowly moving ion. Therefore, a separation factor of 1 is indicative that two ions have the same drift velocity and hence are not resolved.[39] Changing drift gas composition, temperature or pressure can alter the mobility of ions and in turn change the separation factor. Addition of a chiral modifier to the drift gas has also been investigated[40] to separate atenolol enantiomers. The chiral reagent was studied employing (s)-(+)-2-butanol to demonstrate enantiomeric separations of serine, methionine, theronine, glucose, penicillamine, valinol, phenylalanine and tryptophan from their respective racemic mixtures. The versatility of using different buffer gases or buffer gas modified by the addition of volatile compounds can affect the interaction of the ion with the buffer gas. The exploration of crown ethers and polyethyleneglycol as shift reagents has been carried out. In this approach crown ether

is added to the sample to form a complex that is electrosprayed into the gas phase. The resulting complex has a different mobility than the original analyte ion.[41,42]

1.1.2.4 The aperture grid

In order to maintain spectral resolution an aperture grid must be placed approximately 1mm in front of the ion collector. The grid design is similar to a Bradbery/Neilson ion gate. A voltage is applied to the aperture grid to maintain a drift field near the collector. The function of this grid is to capacitively decouple the collector from the approaching ion swarm, without the grid the ion swarm is felt coulombicly by the collector several millimetres prior to its actual arrival resulting in broadening of the ion peaks. Increase in sensitivity of up to 2.5 times has been described.[43]

1.2 Applications of IMS

IMS has several strengths that enhance its suitability as an analytical technique. Firstly, it has a selectivity factor based on ion mobility that allows ions to be distinguished by collision cross section. Secondly, it is an extremely sensitive technique with sub-parts-per-billion or picogram detection limits for many compounds. Thirdly, IMS has continuous real-time monitoring capabilities and, fourthly, the system can be easily automated. Due to these advantages use of IMS has increased during the past decade and has become a widely used analytical method, with more than 50,000 stand-alone ion mobility spectrometers currently employed throughout the world for the detection of explosives, drugs and chemical warfare

agents.[44] With the development of electrospray[45] as an ion source for IMS applications have expanded from those limited to vapour-phase samples. IMS when coupled to MS offers additional data not possible from MS alone. Separation of isomers, isobars and conformers; reduction in chemical noise and measurement of ion size are possible.

IMS was first coupled to a gas chromatograph in 1972[46]. The experiment was designed to enable comparison of both a flame ionization detector (FID) and an IMS detector. FID response and IMS spectra were recorded and compared from the gas chromatographic analysis of musk ambrette. GC–IMS was further used in 1976[47] for the determination of part-per-million levels of *sec*-butyl chlorodiphenyl oxides in biological tissues. IMS was demonstrated to be as a selective and non-selective detector for GC in another report by Baim *et al.* who analysed terpenes from orange extracts by monitoring responses for all product ions having drift times between specific intervals.[48] Recently techniques that utilize a multi-capillary column in combination with IMS equipped with a radioactive and UV ionization sources have been developed for the determination of MTBE and BTX in gaseous and aqueous matrices,[49] rapid on-site detection of ground and surface water contaminants,[50] chemical warfare detection,[32] detection of health relevant analytes from surfaces[51] and detection of volatile organic metabolites in human breath.[52] IMS was first evaluated as a detector for liquid chromatography in 1973 as previously stated. Since then the application of IMS coupled with LC has emerged as a powerful analytical technique coinciding with the development of electrospray ionisation (1972[53]) as a sample ionisation source for ion mobility spectrometry. Although this work utilised two separation steps, it did not make full use of both dimensions of separation because

limitations in electronics required that at least one dimension of the system be operated in a scanning rather than dispersive mode.[54]

In the late 1990s advances in electronics and data acquisition systems enabled the development of the first multiply dispersive ion mobility-mass spectrometry (IM-MS) method, with IMS coupled to time-of-flight MS.[55] IMS has since been interfaced to a variety of mass spectrometers including, time-of-flight,[56] quadrupole,[57] ion-trap,[58] ion-cyclotron[59] and magnetic sector mass spectrometers.[60] Ion mobility cells can also be interfaced to other ion mobility cells producing IMS^n type analysis.[61] Early stand alone IMS investigations were conducted by McDaniel in low field drift cells to study the ion mobilities and ion molecule reactions in gases.[62] Throughout the 1970s and 1980s ion mobility-mass spectrometry was dominated by the use of MS to identify mobility selected ions from ion mobility spectrometers. Development of modern instruments to investigate ion structure was investigated by Jarrod *et al.*[63] and Kemper and Bowers.[64] While initial investigations focused on the studies of ion neutral reactions of ion clusters, IMS is now employed to study the gas-phase structures of a wide variety of molecules and application areas. IMS has since been applied to the study of alkanes, alkenes and cycloalkanes,[65] the detection of biogenic amines in food products,[66] the detection of drugs from hair,[67] identification of structural motifs of DNA,[68] the determination of ammonia,[69] the detection of explosive,[70] for use within the pharmaceutical industry,[71] the detection of pesticides[72] and environmental soil contaminants.[73]

The coupling of IMS to MS afforded greater analytical power through the added dimension of mobility combined with mass measurement. One unique feature of IM-

MS spectra is the mass-mobility correlation observed for classes of ions with spectra plotted with mass as a function of drift time.[44] One practical advantage of employing IMS in combination with mass spectral analysis is the ability to separate multiply charged ions, as seen in the experiments conducted by Clemmer *et al.* for protein digest, whereby a clear separation of charge state was observed.[74] Another advantage of combined IM-MS is that fragmentation of a mobility separated ion can be achieved. The application of IM-MS is a growing field with a large number of application areas. The study of proteins[75] and amino acids has been reported,[76] as well as carbohydrates, lipids, nucleotides and other bio-molecules,[77,78,79] chemical warfare degradation products,[80] drugs of abuse,[81] hydrocarbons[82], halogenated compounds[83] and proteome profiling[84].

The separation of small molecules in complex mixtures is an area where IM-MS offers advantages over MS alone, primarily the combination of IM-MS offers a rapid method for the analysis of small molecules in which isobars may by separated in mobility space before mass analysis. Biological process and samples typically contain a complex matrix making it difficult to detect the many components present. IMS shows potential to enhance selectivity and detect as many sample components as possible. The detection of bacteria was achieved by Nicholson *et al.* for food safety purposes in 1995.[85] In 2005 Baumbach and co workers described the detection of human metabolites using multi-capillary columns coupled to IMS to gain information about different metabolic processes of the body.[86] During this study it was shown that volatile compounds could potentially carry important information about the health status of humans. The metabolic profiling of E.coli[87] by IMS highlighted the advantages of employing IMS compared to MS alone, in that it was not essential for

the metabolite to be volatile whilst employing ESI, separations were faster, and the study showed that sensitivity was sufficient to monitor 500 metabolites at the μM level. Overall this study showed the promising nature of employing IM-MS for metabonomic studies.

As IM-MS instruments become more commercially available the mobility advantage in mass analysis will continue to grow, developments in multidimensional IMS, novel interface technologies and ionisation sources may lead to enhanced sensitivity, quantification, resolving power and separation selectivity. This in turn will lead to the increased detection and separation of complex samples.

1.3 Field asymmetric waveform ion mobility spectrometry (FAIMS)

Studies have shown that FAIMS can separates isobaric ions[88] including diastereoisomers,[89] separate isomers, reduce background signals by isolating ions of interest and simplifying spectra of complex mixtures by dividing the mixture into a series of simpler subsets of ions.[90] Applications ranging from quantitative analysis of inorganic and organometallic compounds, to studies of the conformers of intact proteins, have been reported [91] (Table 1.1).

If the ratio of electric field strength (E) to buffer gas number density (N) exceeds the low-field limit (E/N is $\leq$ 2 Td), the mobility of an ion, K, is no longer constant (Section 1.1.1) and the gas-phase mobility of the ion becomes dependant upon electric field strength:

$$K(E) = K(0)\ (1 + a\ (E/N)^2 + b(E/N)^4 + c(E/N)^6 + \ldots\ldots \qquad \text{Equation 1.10}$$

In a typical FAIMS regime the terms up to $b(E/N)^4$ generally represent $K(E)$ with sufficient accuracy. Depending on the relative values of a and b coefficients, $K(E)$ may increase, decrease, or first increase and then decrease, with corresponding ions classified as types A/C, and B respectively (Figure 1.3). [92] These designations are not absolute but are dependant on the buffer gas employed for example; A type behaviour in one gas may become C type in another.

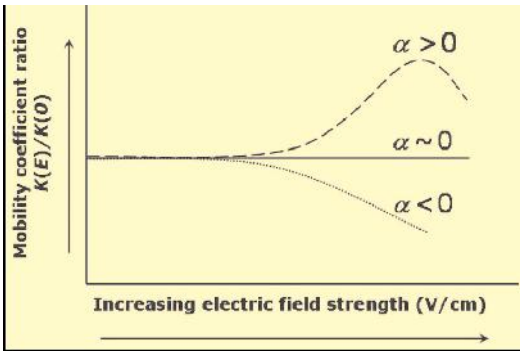

Figure 1.3 Schematic of three possible examples of dependence of ion mobility on electric field strength [93]

Resolution and sensitivity within FAIMS is also somewhat buffer gas dependant, and using binary and ternary mixtures is often better than that with any individual gas component. [94] The alpha function in Equation 1.10 describes how the mobility of an ion varies with increasing electrical field strength, and is independent of both the instrumentation and the applied waveform. However, the exact composition of the buffer gas is required as buffer gas composition can alter the nature of the ion neutral clusters. Positive alpha values are indicative of small ions forming adducts with water and other neutrals at low electric fields (-CV) and negative alpha values are indicative of decreasing ion mobility with increasing field strength (+CV). Large ions forming adducts results in smaller effects on mobility compared to small ions forming adducts.

FAIMS technology originated in Russia during the early 1980s.[95] The first refereed reference to FAIMS was reported by Buryakov *et al.* in 1993[96] in which the general principles were discussed and applied to the separation of tertiary alkylamines. The technique of FAIMS was further developed by Purves and Guevremont [97] and has since been applied to various effects as described in Table 1.1

Table 1.1 Applications of ESI-FAIMS-MS [98]

Area of interest	Analytes	FAIMS electrode design	Important result
Drinking water disinfection products	Bromate, chlorate, iodate	Cylindrical	LOD = 3–71 ng L^{-1}
	Perchlorate, bisulfate, dihydrogen phosphate	Cylindrical	LOD = 1 nM
	Perchlorate	Dome	LOD = 0.050–4.8 ppb in matrix
	Halogenated acids	Cylindrical	LOD = 0.5 to 4 ng mL^{-1}
	Halogenated acids	Dome	LOD = 5–36 parts per trillion
	Haloacetic acids	Dome	LOD = 0.6–0.5 ng mL^{-1}
	Highly polar, non-target analytes	Dome–Q-TOF	Structural determination
Pharmaceuticals	Amphetamine, methamphetamine, derivatives	Dome	LOD = 0.2–7.5 ng mL^{-1}
	Morphine, codeine	Dome	LOD = 20–60 ng mL^{-1}
	Ephedra alkaloids	Dome	LOD = 0.1–3 mg mL^{-1}
	Cisplatin and its hydrolysis products	Dome	LOD = 0.7 ng mL^{-1}
	Theophylline, paraxanthine	Cube	FAIMS separated isomers, improved quantification
	Amine drug and its *N*-oxide metabolite	Cube	FAIMS allowed accurate quantification
Separation of isomers and isobaric peaks	Leucine enkaphalin clusters	Cylindrical	FAIMS separated clusters by charge state
	Leucine/isoleucine	Cylindrical	Isomers well-separated by FAIMS
	Ortho-, *meta-*, *para*-phthalic acids	Dome	Good separation, better S/N
	Microcystin	Dome	Good separation, reduced background
	Disaccharides	Dome	Isomers well-separated by FAIMS
	Naphthenic acids	Dome	Determined elemental composition
	Underivatized amino acids	Dome	Best, simplest overall compound analysis
	Poly(ethylene glycol) isomers	Dome	Observation of conformers
	Liposaccharides	Dome	First coupling to capillary electrophoresis
Metal speciation	Organoarsenic compounds	Dome	Arsenocholine, tetramethylarsinic acid identified
	Stable isotope separation	Dome	Isolation of specific isotopes of chlorine
Protein conformer identification	Bovine ubiquitin	Cylindrical	Resolve conformers of same charge state
	Bovine ubiquitin	Dome	Separate inter- and intra-charge state conformers
	Bradykinin	Dome	Separate inter- and intra-charge state conformers
	Gramicidin S	Dome	Separate inter- and intra-charge state conformers
	Cytochrome c	Dome	Separate inter- and intra-charge state conformers
	β-Microglobulin	Cube	3-D plots (intensity *vs* pH and CV and *vs* charge state, CV)
	Prostanoids	Cube	Separate interconverting low MW species
	Ubiquitin/cytochrome c	Dome/ion funnel	Isolate more conformers
	Bradykinin	Planar FAIMS/ion funnel	Isolated unknown conformers
	Ubiquitin	Dome	Correlation of conformer to ECD efficiency
	Lysozyme, PEG ions	Dome	Develop algorithm to determine number of conformers
Tryptic peptides	Pig hemoglobin peptides	Cylindrical	Orthogonal *m/z* ratio and CV
	Pig hemoglobin peptides	Dome	Separation of peptides by charge state
	Enolase I tryptic peptides	Dome	More peptides identified
	Complex tryptic digests, various proteins	Dome	Coupled to nanoLC, less abundant peptides identified
	Study of dipole alignment in proteins with FAIMS	Dome	Better able to separate large proteins

FAIMS devices uses a flowing a gas stream to transport ions through the space between two electrodes or plates termed the analytical gap. The ions in the gap are subjected to alternating strong and weak electric fields by the application of an asymmetric waveform to the electrodes. Ions are separated by the difference between their mobilities at high and low electric fields (E) that differ as ion mobilities in gases depend on the field (E/N is $\leq$ 2 Td). Therefore, it can be said that FAIMS measures the mean derivative of mobility with respect to field (over a certain range of E), in contrast to conventional IMS that determines absolute ion mobility, (K).[99] The

FAIMS device as stated previously consists of two electrodes which may be two parallel plates (planar FAIMS) or two concentric cylinders (c-FAIMS, Figure 1.4) between which ions are introduced. The asymmetric waveform voltage is applied across the two plates with a high positive voltage applied for a short period of time and a low negative voltage is applied for a longer time period (Figure 1.5). This is termed the dispersion voltage (DV). If the mobility of an ion under low field conditions <200 volts/cm is different from its mobility at (> 5000 volts/cm) then the application of the waveform may cause the ions to drift towards one of the plates.[92]

.

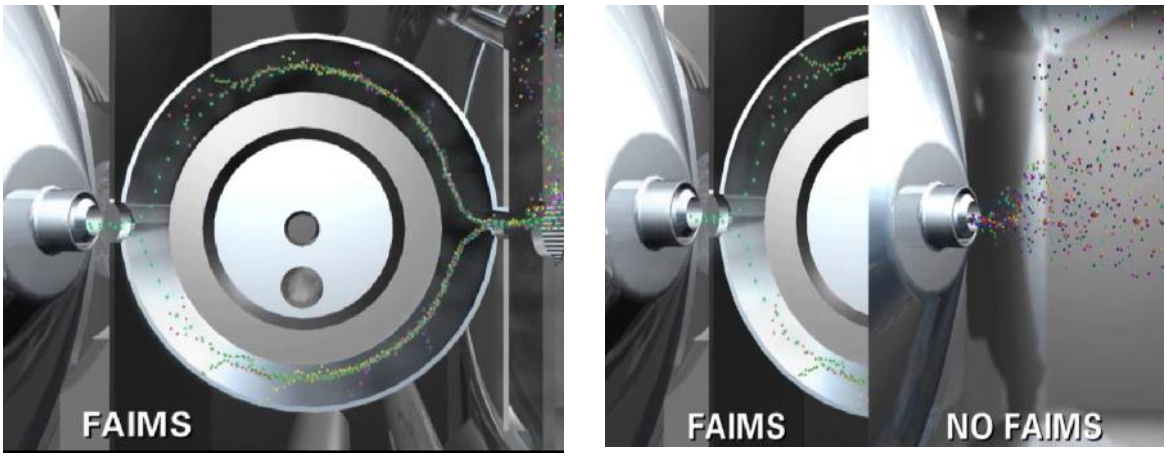

Figure 1.4 Separation of ions using FAIMS taken from Thermo Scientific.

The reason the ion will drift towards a plate is that if the ion mobility is different when the electric field is high to when it is low, the ion will move proportionally farther in one field than the other resulting in a net drift towards one of the electrodes. This drift of an ion can be corrected by the application of a small dc voltage to either plate, termed the compensation voltage (CV). The CV is therefore, used within

FAIMS to scan the FAIMS spectrum and control ion separation. By fixing the CV value, a subset of ions is allowed to pass through the FAIMS device by controlling the ions drift, whereas other ions are lost to the walls of the device and neutralised. A mixture of ions carried by a gas flow can therefore be transmitted selectively by scanning the CV and detecting the ions travelling between the plates (Figure 1.5). Each ion type travels through the device at a characteristic value of CV.

(a)

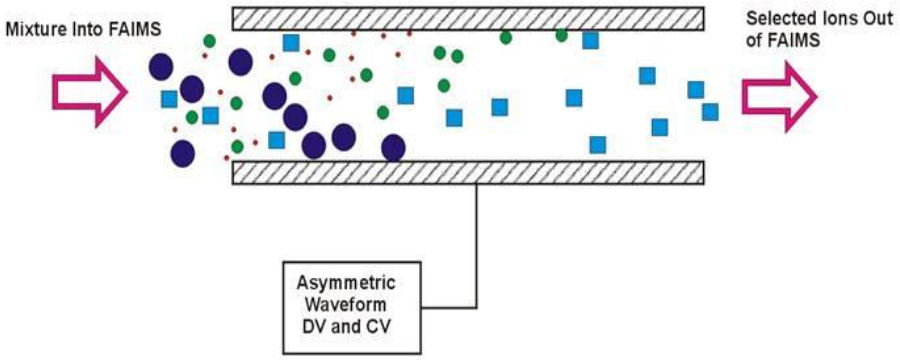

Dispersion voltage (DV)

(b)

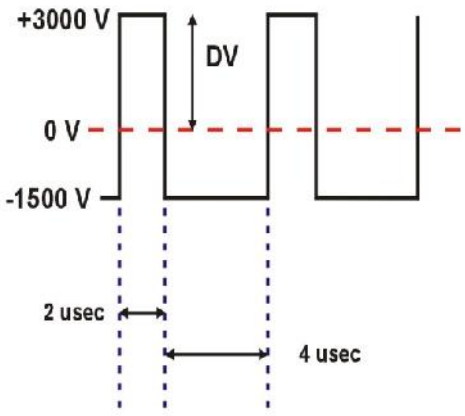

Figure 1.5 Schematic representation of the FAIMS device showing (a) the separation process and (b) a schematic of the applied waveform.

1.4 Mass spectrometry

"Mass spectrometry (MS) enjoys a rich heritage dating back more than a hundred years" (R.M. Caprioli, 2002). Since the first studies of J.J. Thomson (1912), mass spectrometry has since undergone countless improvements including the coupling with GC in the late 1950s, the discoveries of electrospray ionisation by Dole *et al.*[100] and matrix-assisted laser desorption[101] allowing molecules with high molecular weights to be analysed and also the coupling of other separation techniques, LC[102], capillary electrophoresis,[103] IMS[44] and FAIMS.[98] These advancements have allowed for significant information including structure, composition and purity to be derived from various sample types, chemical and biological, allowing mass spectrometry to become an important and powerful analytical tool with limits of detection in the femtomole/attomole range.

Mass spectrometry is a technique in which gaseous ions formed from the molecules or atoms of a sample are separated in space or time and detected according to their mass-to-charge ratio, *m/z*. The number of ions of each mass detected constitutes a mass spectrum, or in other words the peaks in a mass spectrum represent the ion current measured by the instrument at a specific *m/z* ratio. A mass spectrometer consists of a sample introduction system, ionisation source, mass analyser and a detector (Figure 1.6)

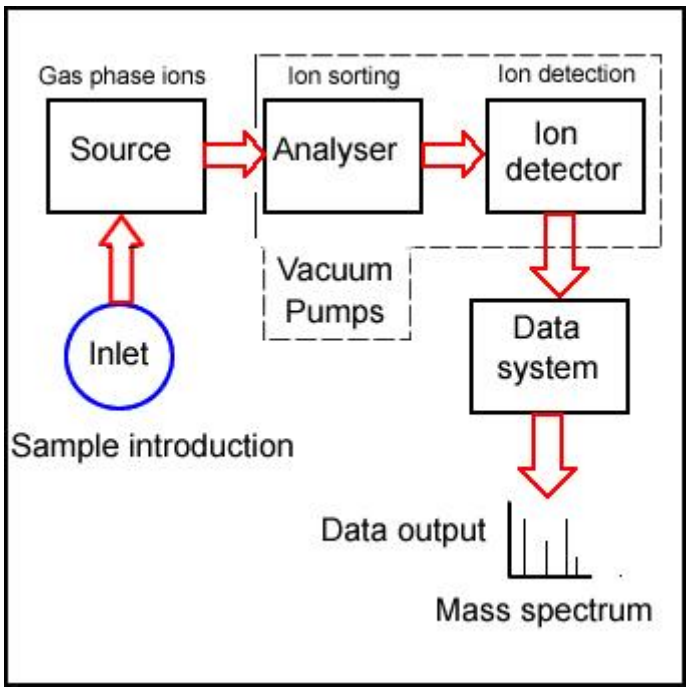

Figure 1.6 Simplified block diagram of a mass spectrometer [104]

The sample is introduced into the ionisation region where gas phase analyte ions are formed, these ions are then directed into the mass analyser which separates ions according to their *m/z* ratio, and finally ions strike the detector, producing an ion current.

1.4.1 Ionisation techniques

The function of the ionisation source is to produce gas phase ions from the sample molecules, which can then be separated by the mass analyser. The ionisation source may be held at either atmospheric pressure or under vacuum. Several techniques have been developed to overcome the problem of introducing the sample in a suitable form. The research presented in this thesis used electrospray and desorption electrospray ionisation. These are discussed in section 1.4.1.1 and 1.4.1.2.

1.4.1.1 Electrospray ionisation

Electrospray ionisation was introduced by Dole in 1968, [105] but only after development in the 1980s by Fenn *et al.* [106] was success gained in the analysis of a wide variety of biological molecules. Electrospray ionisation also facilitated the efficient interfacing of liquid chromatography with mass spectrometry. Electrospray ionisation further lends itself to producing multiply charged ions and hence can greatly extend the mass range of existing instruments. More recently, low flow rate variations such as nano electrospray[107] have proved capable of excellent performance with high sensitivity.

The electrospray interface operates at atmospheric pressure. The sample is dissolved with a solvent and sprayed from a narrow tube or metal capillary tube into an electric field obtained by applying a potential difference of 3-6kV between the tube and a counter electrode. Electrospray is the result of charging such a liquid at the needle tip

by the application of a high potential between the needle and counter electrode (the cone). The formation of the aerosol depends on the competition between coulomb repulsion and surface tension. When no potential is applied to the liquid flow, drops fall off due to gravity and no electrospray is achieved, with the increase in potential droplet size reduces, a liquid elongated liquid column forms with a sharp tip at its point, the so called Taylor cone. When the potential is further increased accumulation of charge on the surface coupled with evaporation (aided by a desolvation gas) of the solvent, force the droplets to diminish is size until the Rayleigh limit is reached. At this point the force of coulombic repulsion between the ions in the droplet is equal to the surface tension of the liquid. As a result of these forces, the droplet breaks up producing a number of smaller droplets. This process is repeated until the ions are fully desolvated, producing protonated or cationised ions in the gas phase.

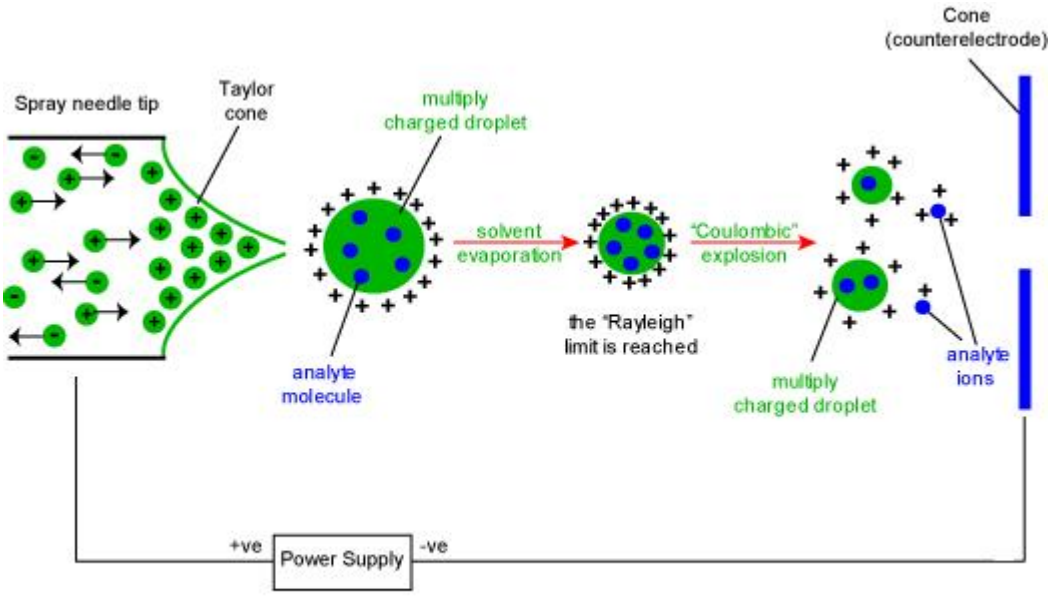

Figure 1.7 Droplet formation in electrospray ionisation [108]

In positive ion mode an enrichment of positive electrolyte ions occurs at the solution meniscus (Figure 1.7). Charge balance is maintained by electrochemical oxidation at the capillary tip and reduction at the counter electrode. When the Rayleigh limit is reached, the droplets become unstable and undergo disintegration into smaller droplets as described previously and produce the Taylor cone from which smaller offspring droplets are formed.

There are two theories describing how gas phase ions may be produced from the charged droplets. The charge residue model (CRM) proposed by Dole *et al*.[109] proposes that the ion is converted to a gas phase ion by evaporation of solvent from a droplet containing a single ion. A sequence of Rayleigh instabilities (where columbic repulsion becomes greater than the surface tension) coupled with solvent evaporation produce the final droplets which contain only one ion each. The ion evaporation model (IEM) introduced by Iribarne and Thomsom[110] assumes that before a droplet reaches the final stages in the CRM model, the increased charge density or field on the droplets surface coupled with solvent evaporation causes coulombic repulsion to overcome the surface tension, resulting in an ion escaping from the droplet surface and enter the gas phase.

1.4.1.2 Desorption Electrospray Ionisation

Desorption electrospray ionisation (DESI) was introduced by Takats and co-workers[111] in 2004 and has proved successful for producing gas phase ions directly from the surface of samples, under ambient conditions, and without the need for a matrix (MALDI) or sample pre-treatment. DESI uses fast moving charged solvent

droplets from an ESI probe to extract analytes from surfaces under interrogation and eject the secondary ions towards the mass spectrometer. Interaction between the spray and the surface ionises the sample and the gas phase analyte ions are then transported into the mass spectrometer. A schematic representation of the DESI process is displayed in Figure 1.8.

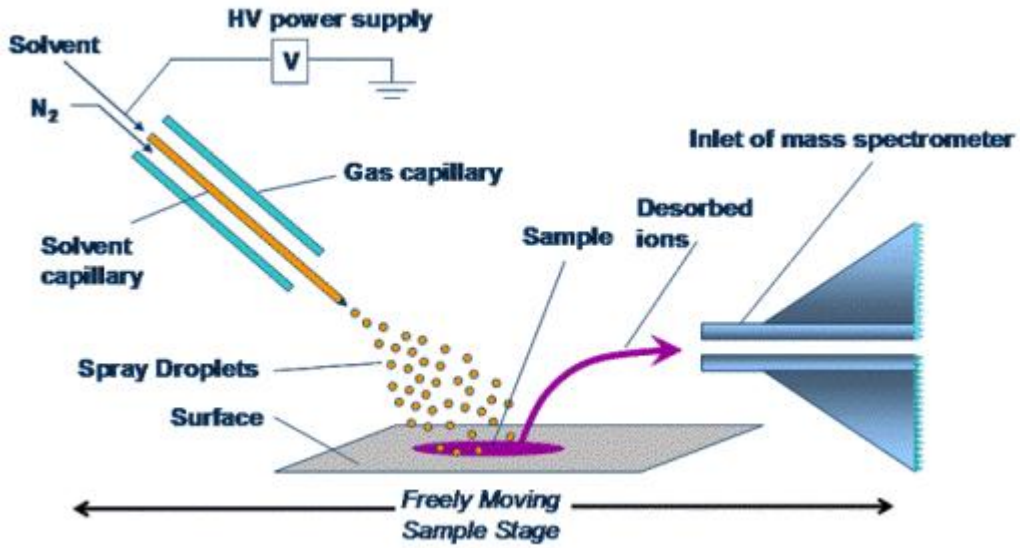

Figure 1.8 Schematic representation of the DESI process[112]

There is no requirement for sample preparation or matrix addition required with MALDI and, as a result, analysis is rapid, making DESI a high throughput technique with total analysis speed typically less than 5 seconds, or the time taken to present the sample to the ESI spray. DESI can also be said to be a soft ionisation method similar to that seen in ESI with internal energy distributions of ions produced around 2 eV, with little fragmentation occurring.[113]

Currently the ionisation processes in DESI are not fully understood. However, a number of ion formation mechanisms have been proposed, including the droplet pick up mechanism, chemical sputtering[114] and volatilisation of neutral species from the

analyte surface. The main DESI mechanism has been described as the 'droplet pick-up'.[115] The droplet pick up process is shown in Figure 1.9.

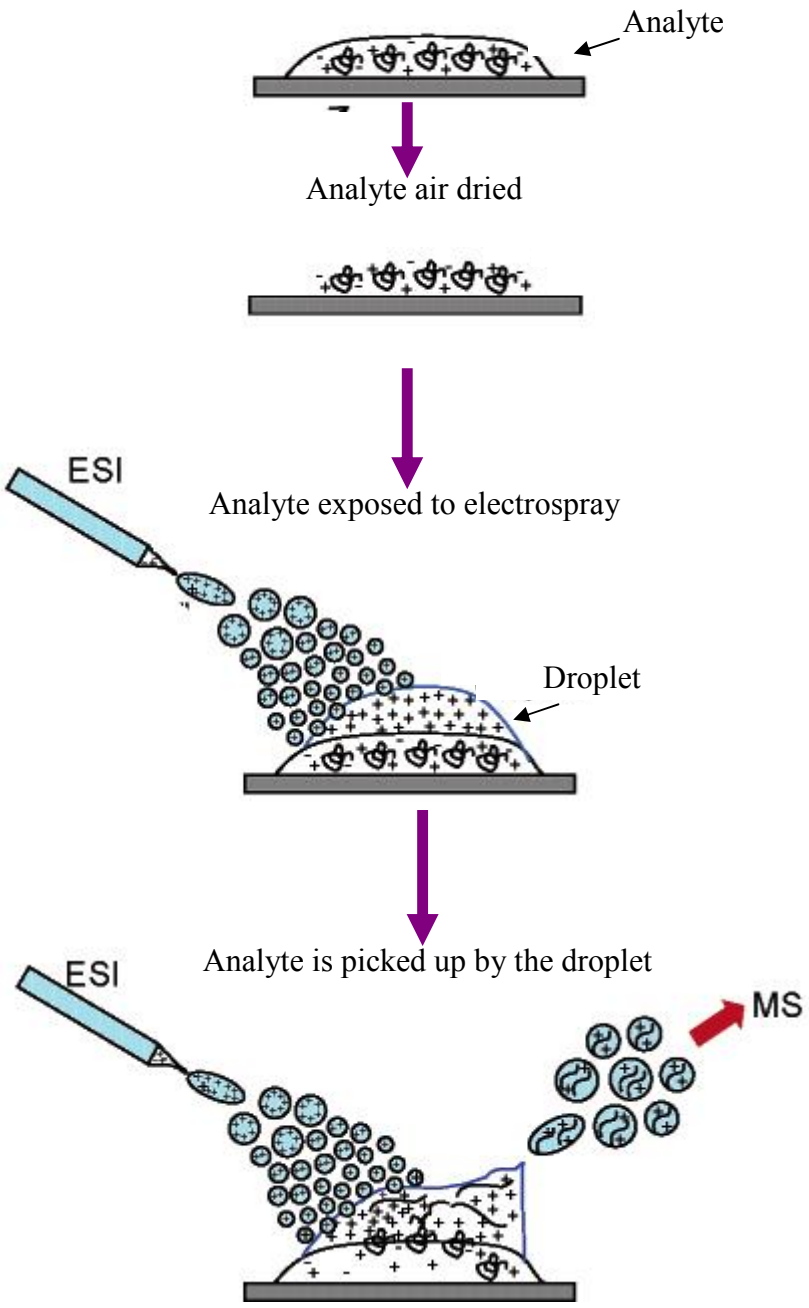

Figure 1.9 Schematic representation of the proposed droplet pick-up process for DESI modified from reference [161]

Measurements of droplet size and velocity distributions, as well as simulations and other evidence based on spectral characteristics, including the strong similarity in charge-state distributions, indicate that a droplet pick-up mechanism probably operates under most circumstances. It is believed to involve the initial wetting of the surface under interrogation whereby surface analytes dissolve or otherwise collect in the solvent layer, followed by splashing on the arrival of subsequent droplets with emission of secondary droplets containing the dissolved surface material and analyte of interest. The wetting effect can often be visualised during the DESI experiment as a build up of a surface liquid layer. Muddiman *et al.*[116] also indicated what was called a 'solvation delay' in the ion intensities, observed when initially switching on the DESI spray. The total ion current detected in the mass spectrometer was low at the onset of the spray for 1-2s. This delay could account for the time required for the dissolution of analytes from the surface into the thin film layer. Further evidence for this mechanism comes from simulations and experiments on the velocity and diameter of the droplets as determined by phase Doppler particle analysis. [117] Simulations of the DESI process showed the formation of microdroplets resulting from a single droplet-thin film collision event and significant macro droplet expulsion from the surface as seen in Figure 1.10.[118]

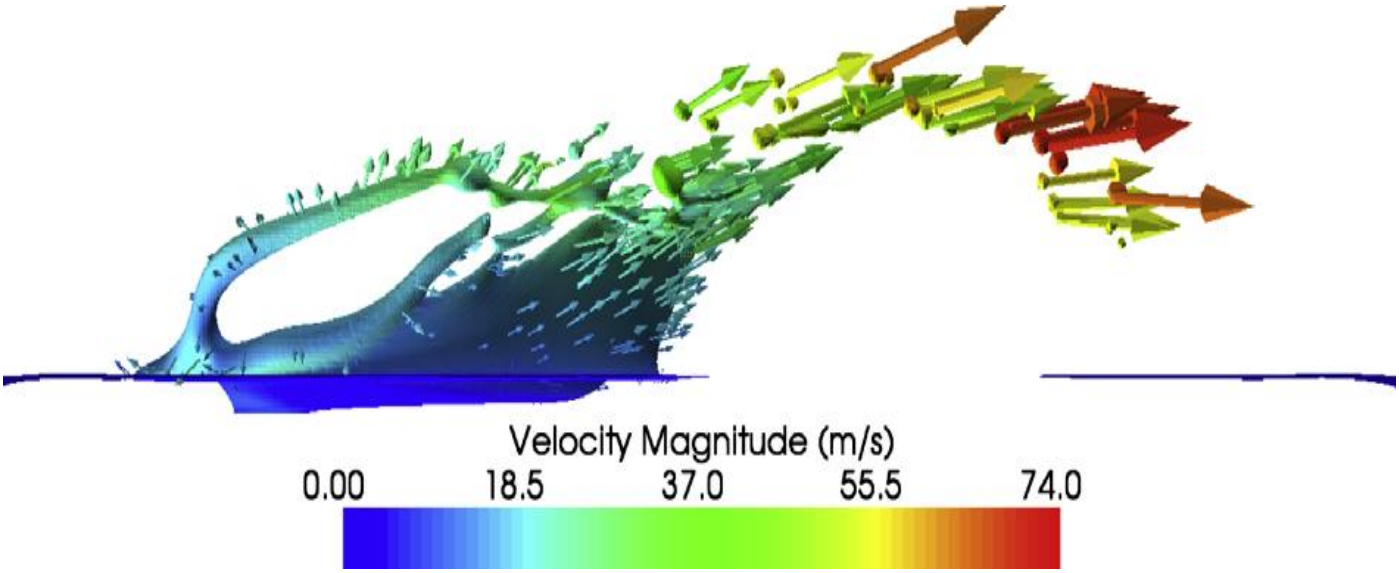

Figure 1.10 Side view of contours for DESI [118]

The last stage of analyte liberation from a droplet is proposed to be identical in DESI to that observed in ESI. This hypothesis is supported by experimental measurement of the internal energies of analyte ions in DESI through thermometer ion method and comparison of internal energies from ESI .[119]

DESI ion sources can be easily constructed by modification of an atmospheric pressure ESI interface, by introduction of a DESI target close to the ESI spray. DESI conditions have been reported to influence the ionisation efficiency, analyte specificity and overall signal intensity. These parameters include solvent, substrate and geometrical positioning of the sample. Solvent choice has been shown to greatly affect the DESI ionisation efficiency as dissolution of the analyte is a key requirement

in the droplet pick-up mechanism. Selected solvents and addition of modifiers to the solvent spray provides specificity for the ionisation of analytes of interest. A correlation between the solubility of a compound in a particular solvent and the signal response in DESI is seen and hence suitable solvents should be selected based upon the sample under interrogation. The use of aqueous solvents increases the signal of polar analytes, whereas organic additives enhance the signal of non polar analytes. [120] The addition of surfactant to the solvent spray was investigated with observations indicating an increase in detection limits, with the effect being ascribed to the reduction in surface tension.[121] The addition of a reagent to the solvent can be employed to modify the analyte via a chemical reaction at the sample surface, such modification may involve derivatisation and is generally termed 'reactive DESI'. The potential value of reactive DESI was demonstrated by Cooks and co workers for the DESI-MS analysis of a tissue section the resulting spectrum showed no signal for cholesterol but gave a strong signal for the cholesterol derivative when betaine aldehyde was added to the spray solvent.[122] Other examples of reactive DESI include anion addition[123] and redox reactions.[124] Investigations have also been carried out to eliminate the formation of salt adducts. This work demonstrated that the addition of 0.1% ammonium acetate (7M) to the standard methanol:water (1:1) DESI solvent spray, increased the salt tolerance of the DESI technique and displayed increased signal-to-noise in comparison to ESI.[125] Geometric parameters include the positioning of the sample surface including the position of the incident and collection angles (α and β respectively), the sprayer tip-to-sample surface (d_1) and the sample surface-to-MS inlet distance (d_2). α and d_1 are known to have a direct effect on the ionisation process whilst β and d_2 influence the collection efficiency. Optimum geometric parameters vary depending on sample type with an increased α angle

typically lending to ESI type analytes, lower values of α typically lend to polar and ionic compounds.[126] Other important parameters influencing efficiency of DESI process are displayed in Figure 1.11

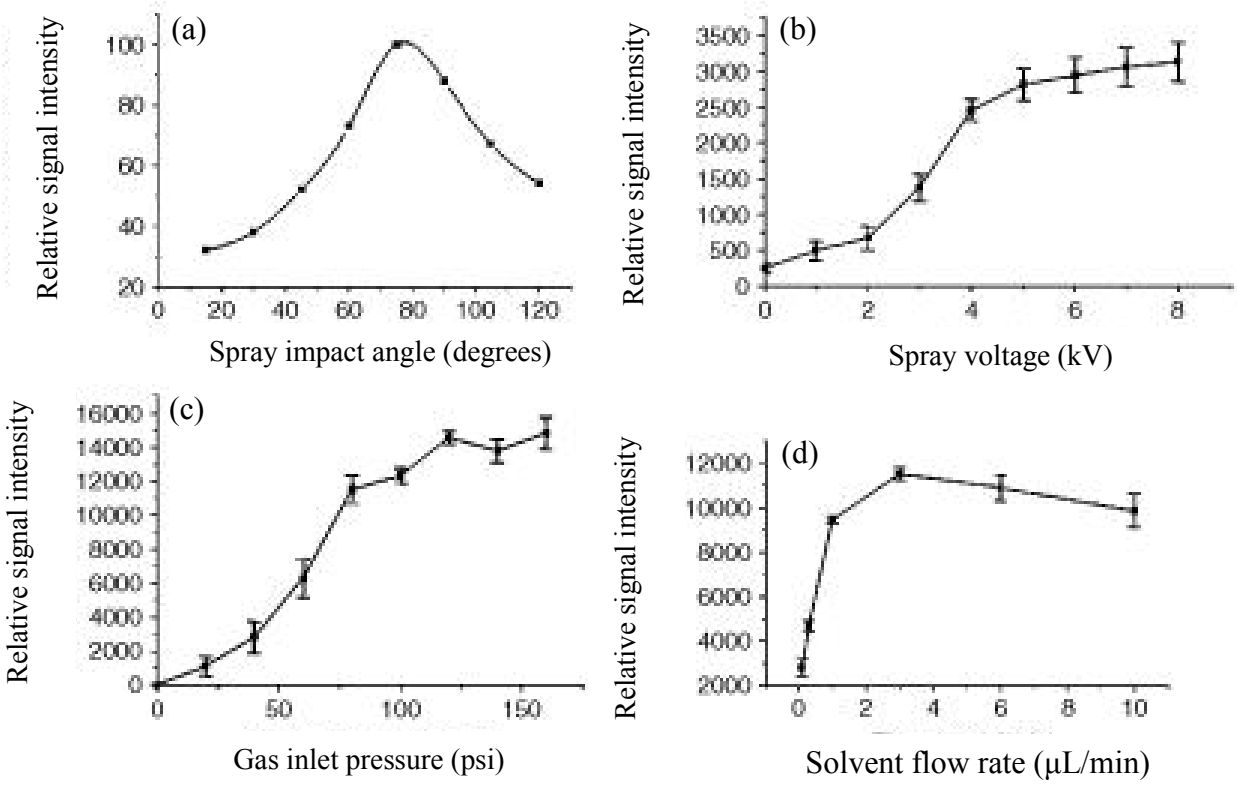

Figure 1.11 Dependence of signal intensity of triply charged melittin ions on (a) spray impact angle, (b) spray high voltage (c) nebulizing gas inlet and (d) solvent flow rate.

Surface temperature and surface potential has also been shown to have an affect on signal intensity, increasing surface temperature results in an increase in ionisation efficiency. APCI type analytes are affected to a greater degree by surface potential, and are typically ionised when the potential difference between the spray tip and surface is greater than 2 kV.

Due to the advantageous properties of DESI over other ionisation techniques the application of DESI has grown considerably since its introduction in 2004. The application of DESI to pharmaceutical preparations, such as the desorption of active pharmaceutical ingredients from tablets, patches and creams[127,128,129,130] at levels as low as 0.14% (w/w). Illicit drug detection has also been investigated with high sensitivity and throughput for the screening of Ecstasy.[131] The technique has shown promise for the analysis of chemical warfare agents[132] and the detection of explosives (TNT, RDX, TATP)[133,134,135] in forensic[136] and public safety applications, with analytes desorbed and detected at the low to mid femtogram level from a variety of surfaces including, paper, plastic, metal and leather. The in-vivo sampling of tissues by DESI, including the detection of pharmaceutical products or metabolites directly from skin, saliva and bodily fluids (urine and blood)[111,137,138,139] provides a non-invasive alternative for bio-analysis with little or no sample pre-treatment. The capability of DESI imaging had also been explored in the forensic analysis of inks as a non-destructive method for detecting fraudulent documents.[122] The imaging of biological systems has been investigated to identify potential biomarkers of disease in thin sections of rat brain tissue.[140] Profiling of intact and untreated micro-organisms has also been investigated.[141] Combination with TLC and its use has been described with normal phase silica gel[142] and cellulose[143] plates for the study of medicinal ingredients,[144] dyes,[145] alkaloids,[146] proteins and peptides[147] and pharmaceutical

formulations.[148] The application of DESI to the analysis of analytes from hydrophobic, reversed-phase TLC plates with bonded silica phases has been investigated for the analysis of dyes.[149,150,151] More recently, Wiseman *et al.* reported the use of pressurised planar electrochromatography using reversed-phase C_{18} plates for the study of steroids.[152] DESI/MS has also been employed for the chemical imaging of dyes separated on TLC plates[138] and the desorption of analytes from non-bonded, reversed-phase TLC plates by DESI. Other applications include the analysis of bio-molecules, such as proteins[153], tryptic and other peptides[126,154,155] and carbohydrates.[156]

DESI has been implemented as the ionisation source with many mass spectrometers, including ion traps,[157] orbitrap[158], triple-quadrupoles and a hybrid quadrupole time-of-flight (Q-ToF).[159] DESI has also been coupled to IMS and has been reported for the direct analysis of active ingredients in pharmaceutical formulations, demonstrating the benefits offered by the additional dimension of IM.[127] Further studies described the use of DESI/IM-MS for the analysis of peptides[160] and conformational studies of folded and denatured states of proteins.[161] In more recent investigations, DESI was coupled with a travelling-wave based ion mobility-mass spectrometer for the analysis of drugs.[162]

A DESI source has now been commercialised as the Omni Spray (Prosolia) developed by Cook *et al*.[163]

1.4.2 Mass analysers

The mass analyser region of the spectrometer separates ions according to their mass-to-charge ration, *m/z*. Ions generated in the source are accelerated into the analyser chamber by applying potentials to a series of lenses through which they pass. There are several different types of mass analyser available, including magnetic sector,[164] time-of-flight (ToF),[165] Fourier Transform-Ion Cyclotron Resonance (FT-ICR)[166] and quadrupole devices.[167] ToF, quadrupole and ion trap analysers were used in this work.

1.4.2.1 Time-of-Flight (ToF) mass analyser

During the late 1950s the Cincinnati Division of the Bendix Aviation Corporation introduced the first commercial time-of-flight mass spectrometer.[168] In ToF instruments the ions are formed in the source and ion bunches are accelerated into the analyser, which is a field free region (Figure 1.12) Since all the ions are accelerated by the same voltage and therefore, have the same kinetic energy, their velocity will be a function of their mass. Lighter ions will transverse the field free region more rapidly than the heavier ions. The time an ion takes to transverse the flight tube is termed the flight time (t). The *m/z* ratio of an ion can then be calculated from the measured flight time.

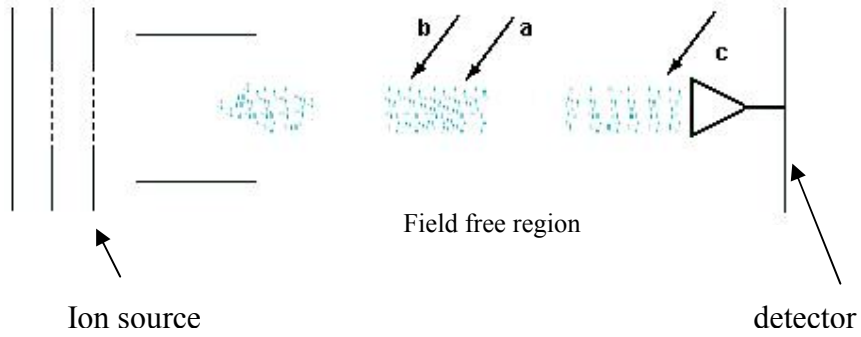

Figure 1.12 Schematic representation of a ToF flight tube. Where; a corresponds to the light ions, b to the heavier ions and c shows the ions becoming separated into individual packets.[169]

The kinetic energy of an ion following acceleration from the source is given by the equation:

$$KE = zeV_{acc} = mv^2/2 \qquad \text{Equation 1.11}$$

Where z is the charge residing upon the ion, e equals the fundamental unit of charge (1.602×10^{-19} C), V_{acc} is the accelerating voltage, v is velocity and m is the ion mass.

This equation can be rearranged to determine velocity of the ion in the flight tube described by:

$$v = (2zeV_{acc}/m)^{1/2} \qquad \text{Equation 1.12}$$

The velocity of an ion is related to the flight time (t) and the length (d) of the flight tube employing the equation:

$$v = d/t \qquad \text{Equation 1.13}$$

By further rearrangement of the equations and substituting for v the *m/z* ratio can be calculated from the measured flight time:

$$m/z = \frac{t^2(2eN)}{d^2} \qquad \text{Equation 1.14}$$

However, many ToF spectrometers are fitted with reflectron lenses to improve resolution by increasing the ions flight path, and hence the calculation of *m/z* becomes more difficult.

In practice the simplified equation (1.15) is employed to determine *m/z* ratios from measured flight times:

$$m/z = at^2 + b \qquad \text{Equation 1.15}$$

Where a and b refer to constant values obtained from reference compounds of known molecular weight for a given set of instrument conditions.

ToF spectrometers have, theoretically, an unlimited mass range however, in practice very large ions may not generate a significantly large enough current when they hit the detector plate. Nevertheless, ToF analysers are capable of detecting molecules with a molecular mass in excess of 300kDa.

The introduction of an electrostatic reflector or reflectron into the ToF was used to overcome poor resolution seen in the linear ToF (Figure 1.13). Ions that have higher kinetic energies will arrive at the reflectron before ions of the same mass, but with lower kinetic energy. However, they will also penetrate further into the electrostatic field than the lower kinetic energy ions, this results in their flight time in the reflectron increasing compared to low kinetic energy ions. The delay of high kinetic energy ions enables the slower moving ions to arrive at the detector at the same time as the high kinetic energy ions due to the fact that they spend less time in the electrostatic field.

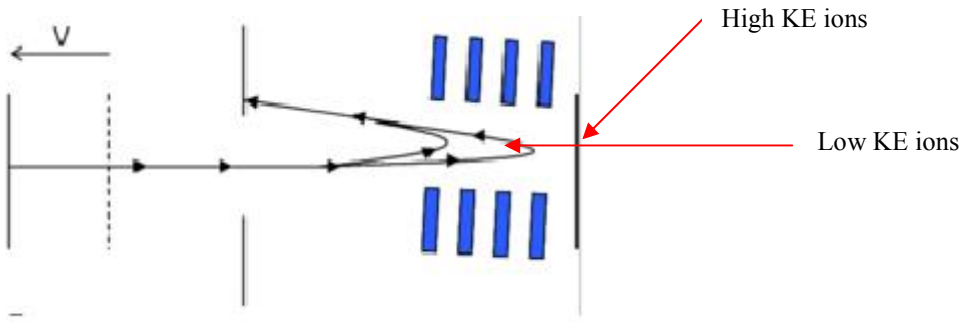

Figure 1.13 schematic of reflectron ToF instrument showing focusing of ions of similar mass but different kinetic energy.[170]

The reflectron focuses the kinetic energy distribution of the ions and hence the reflectron ToF gives mass resolution in the range of >10000 compared to >1000 with a linear ToF.

1.4.2.2 Quadrupole mass analysers

The concept of quadrupole mass spectrometers, which utilise electrical fields to separate ions based upon their *m/z* ratio, was introduced in the early 1950s by Wolfgang Paul, who shared the 1989 Nobel prize for physics.[171] Paul showed that ions in quadrupole fields were either stable or unstable depending on their *m/z* ratio and the geometrical structure and electrical parameters of the field. In a linear quadrupole, the fields could be adjusted to allow transmission of an ion with a specific *m/z* ratio from one end of the quadrupole to the other. It was also shown that a cubic quadrupole could be employed to either trap a single ion of *m/z* ratio or a

range of ions and that the later ions could be ejected in sequence by modification of the field.

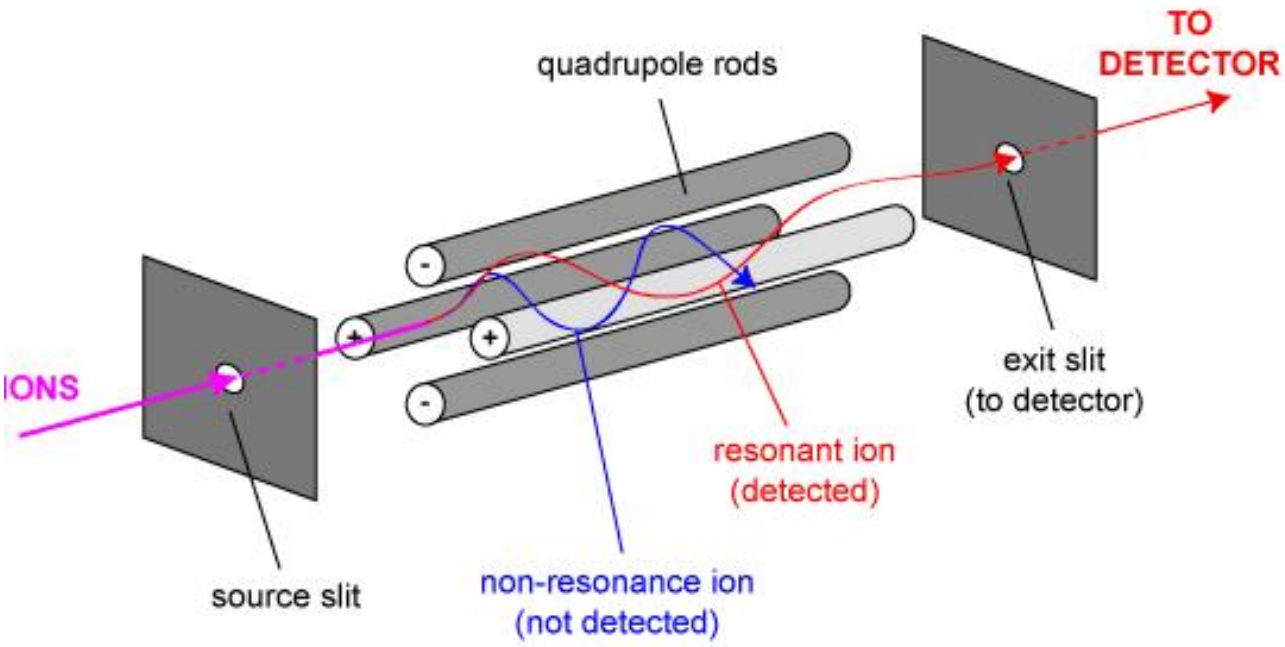

Figure 1.14 Schematic representation of a linear quadrupole taken from reference [172]

The quadrupole itself consists of four rods (Figure 1.14), which are either circular or hyperbolical in cross section. Superimposed RF and DC voltages are applied to these rods, which are electrically connected in opposing pairs. Ions passing through the quadrupole may have resonant or non-resonant frequencies; only ions with resonant frequencies will have a stable trajectory and be transmitted through the quadrupole to the detector.

The stability of an ion can be determined from Newton's second law (force = mass x acceleration) which gives equation 1.16. This equation is also termed the Mathieu equation:

$$D^2u/d\xi^2 + (a_u - 2q\cos 2\xi)u = 0 \qquad \text{Equation 1.16}$$

Where u = x or y and $\xi = \pi$ ft (f=frequency, t=time). The a and q terms are dimensionless and for ions within a quadrupole field are:

$$a_x = -a_y = 8eU/mr_0^2\Omega^2 \qquad \text{Equation 1.17}$$

$$q_x = -q_y = -4eV/mr_0^2\Omega^2 \qquad \text{Equation 1.18}$$

Where m is the mass of an ion travelling through a quadrupole of radius r_0. The quadrupole is operated with RF (V) and DC (U) potentials and a main RF angular drive frequency

$$(\Omega = 2\pi f) \qquad \text{Equation 1.19}$$

Ion trajectories can be further described by the Mathieu stability diagram. Ions must have stable trajectories in both the x and y directions to transverse the quadrupole and ions whose working point lies within the boundaries are stable in both directions and hence will pass through the quadrupole. Ions lying outside this boundary have non-

resonant trajectories in either both or one direction and hence will not transverse the quadrupole and be detected.

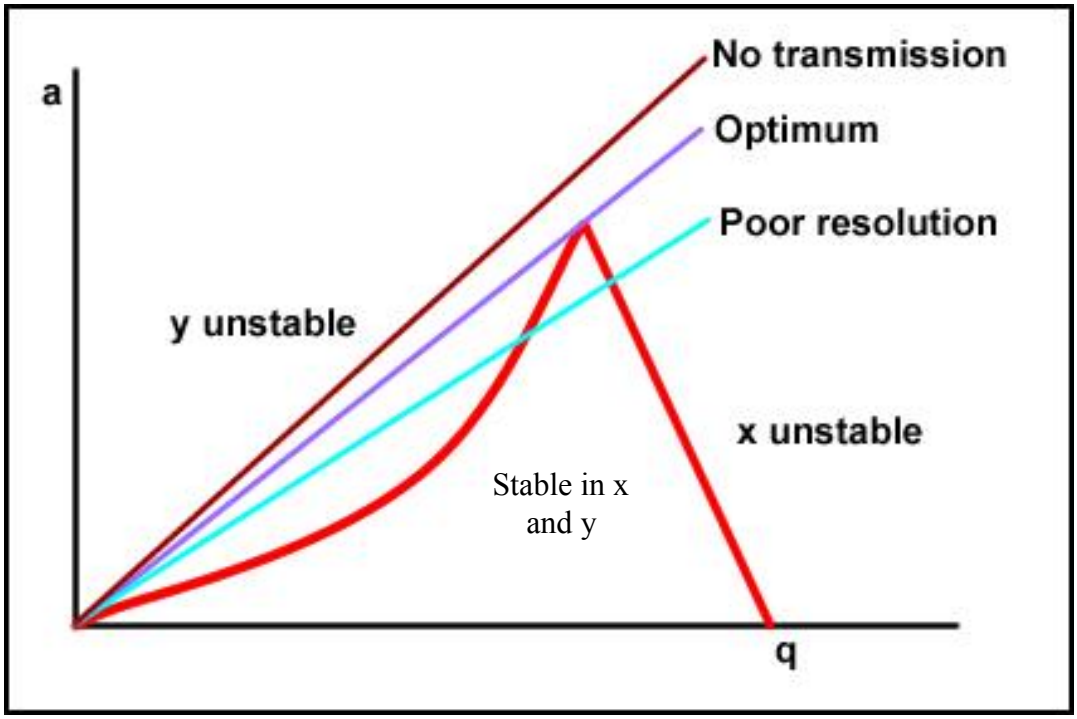

Figure 1.15 Linear quadrupole stability diagram modified from reference [104]

As the RF and DC voltages increase the working point of an ion will move along one of the lines indicated in Figure 1.15 under optimum conditions. Ions of increasing *m/z* will pass through the apex of the stability diagram where they have stable a and q values. Ions of lower or higher *m/z* will not have stable trajectories at this same point. The quadrupole mass anlyser separates ions only on the basis of their *m/z* ratio, it therefore can be said that instruments that use this concept act as true mass filters.

In a linear quadrupole ion trap, ions are introduced into the quadrupole and retained in stable trajectories by applying a potential to each end of the device. Ions are ejected by a mass-selected instability scan to obtain a mass spectrum. A significant problem with ion tap technology is that peak broadening can occur due to overloading of the trap itself with analyte ions, leading to space charging effects. The ions retained in the trap repel like charged ions so that ions of the same *m/z* occupy different working points on the stability diagram and are ejected at slightly different times during the analytical scan and hence causing broadening of the spectral peaks. To overcome this problem a software modification known as automatic gain control (AGC) was devised, which performs a short pre-scan before the main scan and thus measures the number of ions entering the trap. The analytical scan ion time can therefore be calculated so that an overload of ions does not occur, preventing space charging effects.

Quadrupole instruments have been further developed utilising multiple quadrupoles and allowing for tandem mass spectrometry to be performed. In a triple quadrupole the first quadrupole is employed as a mass filter to select precursor ions , the second is operated in RF mode only to ensure all ions are transmitted. This second quadrupole is maintained at a constant pressure with a suitable gas, primarily He or Ar to act as a collision cell where the precursor ions undergo fragmentation. The third quadrupole is used to scan the mass spectrum of the fragment ions. Quadrupoles have also been coupled to ToF instruments whereby the third quadrupole is replaced with ToF flight tube giving a Q-ToF configuration.

1.4.3 Detection systems

Several different types of detector are used within mass spectrometry however, they can be further categorised into two components, the Faraday plate,[173] which directly measures the current of the ions striking a metal plate and the other detectors. Other detector types include such detectors as the array detector,[174] electron multipliers[175] and photomultiplier tubes[176] which all increase the intensity of the original signal producing much higher measured currents.

1.5 Introduction to Metabonomics

Since the 1990s, there has been a revolution in the techniques and approaches used in molecular biology and biochemistry directly following the human genome project[177,178] and the subsequent decoding of the human genome. This change, led to the idea that genetic differences might be able to account for all disease processes, and in turn led to the discipline of transcriptomics. Further advancements in the ability to assay and identify proteins using mass spectrometry and other techniques led to the term proteomics. However, during the past few years the full complexity of molecular biology has been realised and the complex interactions between genetic make-up and environmental factors have now been recognised. It is now accepted that a full understanding of these interactions is not possible at the transcriptomic and proteomic level alone. Even in combination, genomics and proteomics do not provide the range of information needed for an understanding of the integrated cellular function in living systems, since both ignore the dynamic metabolic status of the

whole organism.[179] A further point is that the number of metabolites is around 5000, compared with 1,000,000 estimated proteins and over 20,000 genes in humans.[180]

Small molecules involved in biochemical processes provide information on the status and functioning of a living system, both from effects caused by changes in gene expression and also by differences in life style, diet, and environmental factors. The process of monitoring and evaluating such changes is termed metabonomics.[181]

The field of metabonomics grew out of work carried out in the mid 1980s [182,183,184,185] and which was subsequently combined with pattern recognition and multivariate statistic investigation of the data sets to yield possible biomarkers. However, the term metabonomics was not suggested until 1999 and was defined by Nicholson *et al.* as "the quantitative measurement of the dynamic multiparametric metabolic response of living systems to pathophysiological stimuli or genetic modification".[179] There is also a related concept of the metabolome or metabolomics, which has been consistently used interchangeably with metabonomics throughout many texts. However, the metabolome represents the total small molecule complement of a cell, whereas metabonomics refers to the process of quantifying, identifying, and cataloguing the history of time related metabolic changes in an integrated biological system rather than an individual cell.[179]

1.5.1 Samples for metabonomics

Metabonomic studies of biomedical relevance generally use biofluids, cell or tissue extracts. These include, breath, urine, sputum, (Figure 1.16) and can provide an integrated view of the whole systems biology. Urine and plasma are obtained essentially non-invasively and hence lend themselves for disease diagnosis and clinical trail settings. However, a wide range of fluids and sample type have been investigated including, seminal fluids, amniotic fluid, digestive fluids, lung aspirate and dialysis fluid. Analysis of tissue biopsy has also been conducted employing NMR spectroscopy in studies of atherosclerosis.[186] Metabonomics can also be applied to characterising in vitro systems for example, tumour cells.

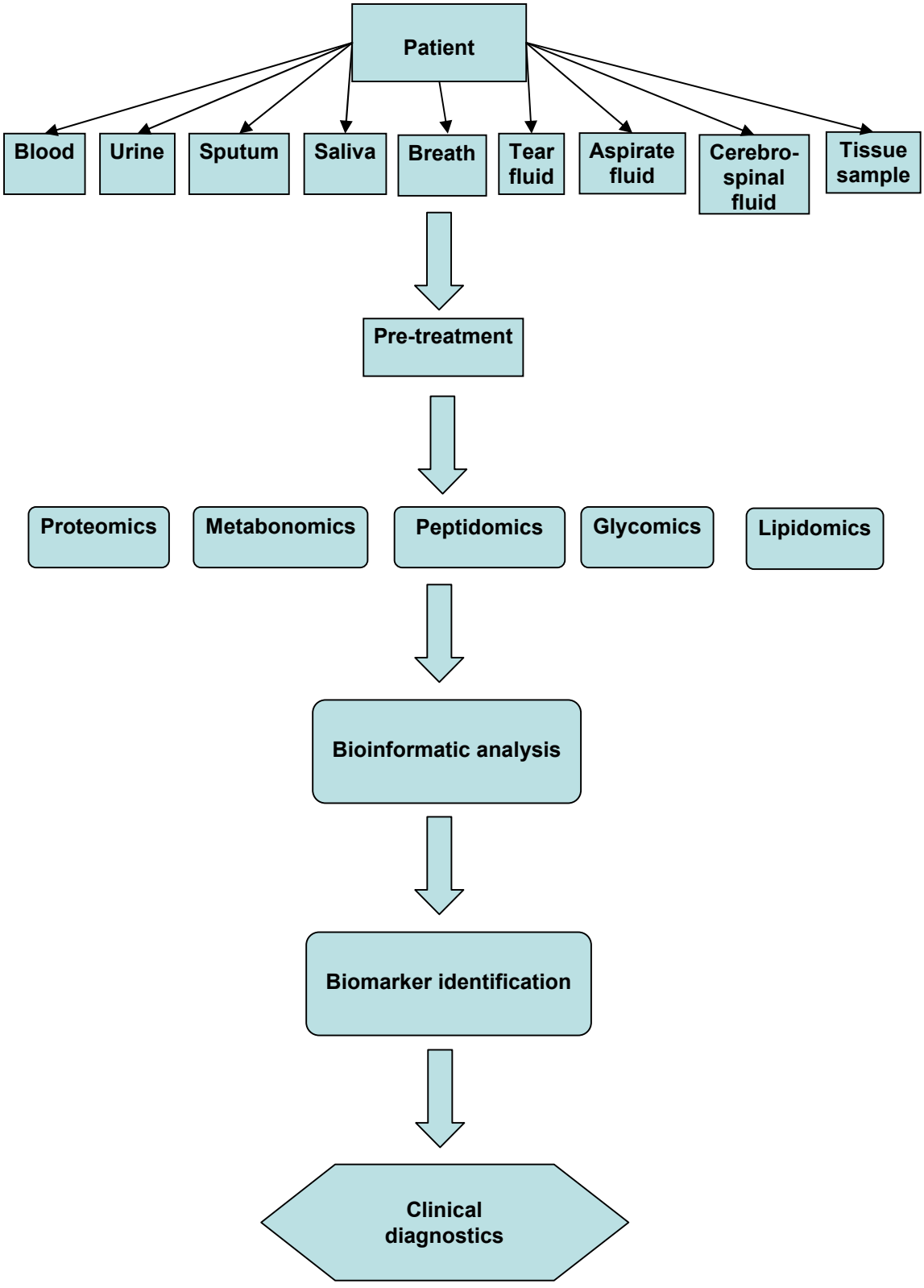

Figure 1.16 Scheme for mass-spectrometry based omics technologies modified from reference [187]

1.5.2 Analytical Techniques for metabonomic analysis

A number of analytical methods can be employed to produce metabolic signatures of biomaterials, including high resolution ^{1}H nuclear magnetic resonance (NMR) spectroscopy,[188] gas chromatography-mass spectrometry (GC-MS),[189] liquid chromatography-mass spectrometry (LC-MS),[190] ultra high performance liquid chromatography- mass spectrometry (UHPLC-MS)[191] and capillary electrophoresis-mass spectrometry (CE-MS).[192] All metabonomic studies result in complex multivariate data sets, which in turn require bioinformatic methods for visualisation and interpretation. High resolution ^{1}H nuclear magnetic resonance (NMR) spectroscopy has proved to be one of the most valuable and most powerful technologies for biofluids due to its non-destructive nature, application to intact biomaterials, tissues and cells, and the elucidation of molecular structure.[193] NMR spectroscopy is capable of recording many metabolites either in vivo or in vitro. However, there are limitations for NMR-based metabonomic studies including low resolution and sensitivity (>1 nmol metabolite for ^{1}H-NMR detection) and the inability to detect NMR inactive nuclei (e.g. O & S) and difficulties in absolute metabolite quantification. MS is inherently more sensitive than NMR, but is a destructive technique. MS is also a major technique for molecular identification, especially through tandem MS fragmentation studies or measurement.

1.5.3 Overview of metabonomics

Nicholson *et al.* used NMR spectroscopy to study multicomponent metabolic composition of biofluids. A typical example is the extensive study of the toxicity of the model hepatotoxin, hydrazine, in the rat by analysis of urine and blood.[194] Dose dependant trajectory plots showed increasing metabolic insult and recovery with Krebs cycle intermediates being shown to decrease in dosed animals. NMR spectroscopy continues to be a valuable tool within metabonomics but due to sensitivity issues mass spectrometry is quickly becoming a powerful method of choice either used in combination with NMR or alone. Due to the scope of this research, emphasis will be directed towards MS only applications.

MS has been widely used in metabonomics for metabolic fingerprinting, identification and the elucidation of biomarkers as well as becoming the "powerhouse"[195] of the pharmaceutical and biotechnology industry for metabolic fingerprinting of drugs. The majority of MS-based studies within the literature have been directed towards plant extract studies.[196,197] However, the application of MS to mammalian studies is increasing. For metabonomic applications on biofluids such as urine,[198] an HPLC chromatogram is generated with MS detection, usually employing electrospray ionisation and both positive and negative ion spectra can be measured. At each point in the chromatogram, there is a full mass spectrum, providing retention time, mass, and intensity data sets. UPLC has enabled better chromatographic peak resolution, increased speed and sensitivity to be obtained for complex mixture analysis. A comparison of HPLC and UPLC for mouse urine samples was investigated by Wilson *et al*.[199] The study showed that UPLC offers significant advantages, including more

than a doubling of peak capacity, an almost 10-fold increase in speed and a 3-5-fold increase in sensitivity.

Early developments of metabonomic studies included the chemotaxonomic discrimination of Pencillium cultures via identification of strain specific metabolites.[200] Bacterial characterisation and identification on free cell extracts has been studied and species specific peaks identified *for Escherichia coli, Bacillus spp and Brevibacillus laterosporus*.[201] Metabonomic studies have been used to investigate the effects of aging and development in Wister-derived rats by analysis of urinary profiles and the endogenous metabolites excreted. It was found that, through multivariate data analysis which enables visual clustering effects, that urine collected at 4-6 weeks of age showed the greatest differences in metabolite profiling for example carnitine was found to increase with age.[202] Clinical diagnostic applications provide screening of large number of samples through targeted analyses of specific metabolites indicative of metabolism disorder. Postmortem diagnosis by analysis of bile fluid or urine have indicated metabolic disorders that may have resulted in sudden infant death syndrome.[203] The combined approach of coupling IMS to MS for metabonomic analysis has also been investigated. The mobility dimension provides additional information, which can be generated and gathered from the metabonomic data and hence provide a novel technique for metabonomic investigations. The metabolic profiling of *E.coli*[87] and drug metabolites[204] have been investigated and the metabonomic study of rat urine reported.[205] More recently the metabolic profiling of blood by IM-MS has been reported.[205]

It seems likely that ultimately a combination of technologies will prove to be the most useful in the exploration of metabonomics. However, the additional dimension of IMS is being realised, demonstrating the potential to enhance metabonomic coverage by the introduction of a gas-phase electrophoretic separation.

1.6 Introduction to data mining methods

Data mining can be defined as the process of extracting patterns from large data sets. Data mining is seen as an increasingly important analytical tool as modern analysis methods provide opportunities to generate huge volumes of data with every analysis. It has become routine that spectroscopic methods provide analytical data on many components of a single sample, where several variables are measured. A spectrum would normally be characterised by several hundred to several thousand *m/z* and intensity measurements. The aim of data mining methods is to reduce the volume data whilst maintaining the relevant information and to find patterns and relationships within the vast quantity of data generated. Data mining can only uncover patterns already present in the data; the target dataset must be representative to contain these patterns while remaining concise enough to be mined in an acceptable timeframe.[206] Before data mining algorithms can be used, a target data set must be assembled, with noise and missing data points removed. Data is reduced into feature vectors, one vector per observation which dramatically reduces the size of the dataset to be mined, and hence reducing the processing timeframe. The feature(s) selected will depend on what the objective(s) is/are; obviously, selecting the "right" feature(s) is fundamental

to successful data mining[207]. The feature vectors are divided into two sets, the "training set" and the "test set". The training set is used to "train" the data mining algorithm(s), while the test set is used to verify the accuracy of any patterns found. The final step of data mining is to verify the patterns produced by the data mining algorithms occur in the wider data set. It is common for the data mining algorithms to find patterns in the training set which are not present in the general data set, this is called over fitting. To overcome this, the evaluation uses a test set of data which the data mining algorithm was not trained on. The learnt patterns are applied to this test set and the resulting output is compared to the desired output. If the learnt patterns meet the desired standards the interpretation of the data can be carried out.

1.6.1 Principal component analysis.

Principal component analysis (PCA) is a technique for reducing the amount of data when there is correlation present, with the prime objective to find principle components. PCA is a mathematical procedure that transforms a number of (possibly) correlated variables into a (smaller) number of uncorrelated variables called principal components. The objective of principal component analysis is to reduce the dimensionality (number of variables) of the dataset but retain most of the original variability in the data.[208] Principal components are chosen so that the first principal component (PC1) accounts for most of the variation in the data set, the second (PC2) accounts for the next largest variation and so on. When significant correlation occurs the number of useful PCs is reduced and far fewer than the original variables and hence reduces the amount of data. Each component accounts for a maximal amount of variance in the observed variables that was not accounted for by the preceding

components, and is uncorrelated with all of the preceding components. A principal component analysis proceeds in this fashion, with each new component accounting for progressively smaller and smaller amounts of variance.[209] As variance is a measure of the spread of data in a data set, PCA can be employed to determine whether an experimental study has remained within control limits and if the data shows correlation. For example a full metabonomic study data set will contain 1000's of variables in order to determine if correlation is observed PCA analysis could be employed. Throughout this research PCA analysis was employed to determine if the analytical system remained within control limits and hence to determine the validity of the generated data.

1.6.2 Artificial Neural Networks

In a simple form ANNs attempt to imitate the operation of neurons in the brain. Such networks are constructed of linked layers of artificial neurons which includes an input and output layer, Figure 1.17.[210] Variables are presented to the input layer and processed by one or more of the hidden layers to produce one or more outputs. The network is trained by employing a training set, where the system will adapt based upon the training information. Discrepancies between the observed and predicted values during the training phase are used to adjust internal parameters in the network. These steps, prediction and adjustment, are repeated until the desired outcome is achieved. The performance of the network is evaluated employing a training set, though care is needed to ensure that over fitting has not occurred. ANNs are normally employed to find patterns in large data sets containing many variables.

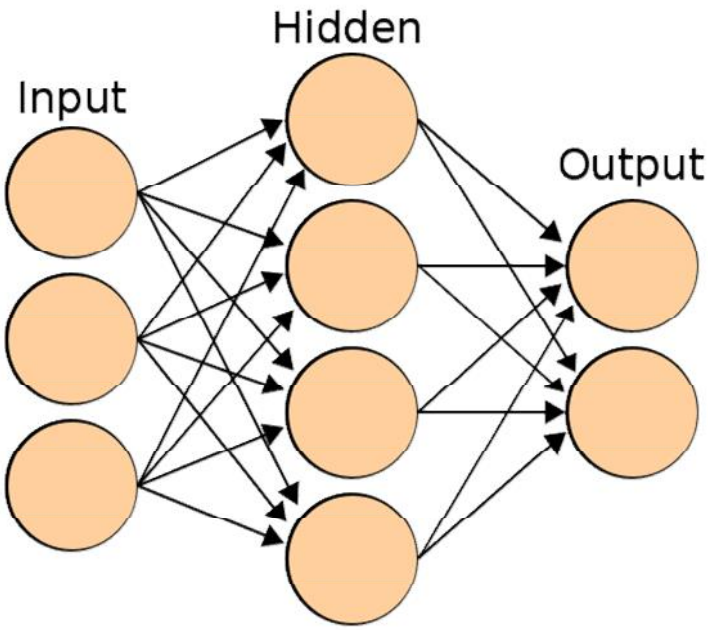

Figure 1.17 Example of a neural network[211]

The neural network does not start by assuming a particular type of relationship between the input and output variables, it is therefore useful when the underlying mathematical model is uncertain.[206] ANNs are versatile and flexible tools for modelling complex relationships between variables. During this research ANNs were employed to find correlation between age groups of rats from their urinary profile.

1.7 REFERENCES

1. Shvartsburg A.A. *Differential ion mobility spectrometry*. 2009, Boca Raton: CRC press.
2. Karasek F.W. *Anal. Chem*. 1974; **46**: 710-716.
3. Creaser C.S, Griffiths J.R, Bramwell C.J, Noreen S, Hill C.A & Thomas C.L.P. *Analyst*. 2004; **129**: 984-994.
4. Clemmer D.E & Jarrold M.F. *J. Mass Spectrom*. 1997; **32**: 577-592.
5. Jackson A, Hovoi M, Chaudhuri I, Frauenheim T & Shvartsburg A.A. *APS Physics, physical Review Letters*. 2004; **93**: 013401/1-013401/4.
6. Kanu A.B, Hill H.H Jr, Gribb M.M &Walters R.N. *J. Enviro. Monit*. 2007; **9**: 51-60.
7. Helden G.V, Hsu M.T, Kemper P.R & Bowers M.T. *J. Chem. Phys*. 1992; **93**: 3835-3843.
8. Borsdorf H, Stone J.A & Eiceman G.A. *Int. J. Mass spectrom*. 2005; **426**, 19-28.
9. Eiceman G.A & Karpas Z. *Ion mobility spectrometry.* 2005, CRC press.
10. Laiko V.V. *J. Am. Soc. Mass Spectrom*. 2006; **17**: 500-507.
11. Mason E.A & McDaniel E.W. *Transport properties of ions in Gases*. 1988, New York, Wiley.
12. Tabrizchi M. *Talanta*. 2003; **62**; 65-70.
13. Dugourd P, Hudgins R.R & Clemmer D.E. *Rev. Sci. Instrum*. 1997; **68**: 1122-1129.
14. Tabrizchi M & Rouholahnejad F. *Talanta*. 2006; **69**: 87–90.
15. St. Louis R.H & Hill H.H Jr. *Critical reviews in analytical chemistry*. 1990;**15**: 321-353.
16. Zhou L, Collins D.C, Lee E.D & Lee M.L. 2007; **388**; 1618-2650.
17. Zhang M & Wexler A.S. *Int. J. Mass spectrom*. 2006; **258**; 13-20.
18. Karpas Z. *Anal. Chem*. 1989; **61**: 684-689.
19. Pozzi R, Pinelli F, Bocchini P & Galletti G.C. *Analytica Chimica Acta.* 2004; **504**: 313-317.
20. Borsdorf H & Rudolph M. *Int. J. Mass. Spectrom*. 2001; **208**: 67-72.
21. Preston J.M & Rajadhyax L. *Anal. Chem*. 1988; **60**: 31-34.
22. Kim S.M & Spangler G.E. *Anal. Chem*. 1985; **57**: 567-569.

23. Bocos-Bintintan V, Brittain A & Thomas C.L.P. *Analyst*. 2001; **126**: 1539-1544.
24. Meytro M.M & Keller R.A. *J. Chromatogr. Sci*. 1973; **11**: 520-528.
25. Simpson M, Anderson D.R, McLeod C.W, Cooke M & Saatchi R. *Analyst*. 1993; **118**: 1293-1298.
26. Karasek F.W, Hill H.H Jr, Kim S.H & Rokushika S. *J. Chromatogr*. 1977; **135**: 329-339.
27. Hill H.H Jr, Siems W.F & St.Louis R.H. *Anal. Chem*. 1990; **62**: 1201-1209.
28. Atkinson D.A & Hill H.H. *J. Chromatogr*. 1993; **617**: 173-179.
29. Matz L.M, Dion H.M & Hill H.H Jr. *J. Chromatogr*. 2002; **946**: 59-68.
30. St.Louis R.H & Hill H.H Jr. *Anal. Chem*. 1990; **21**: 321-354.
31. Wu C, Siems W.F, Klasmeier J & Hill H.H Jr. *Anal. Chem*. 2000; **72**: 391-395.
32. Erickson R.P, Tripathi A, Maswadeh W.M, Snyder P.A, Smith P.A. *Analytica Chimica Acta*. 2006; **556**: 455-461.
33. Tyndall A.M. *The mobility of positive ions in gases*. 2003. Cambridge University press, Cambridge.
34. Bradbury N.E & Neilson R.A. *Phys. Rev*. 1936; **49**: 388-393.
35. Von Helden G, Wyttenbach T & Bowers M.T. *Science*. 1995; **267**: 1483-1485.
36. Rokushika S, Hatano H & Hill H.H Jr. *Anal. Chem*. 1987; **59**: 8-12.
37. Asbury G.R & Hill H.H Jr. *Anal. Chem*, 2000; **72**: 580-584.
38. Matz L.M, Hill H.H Jr, Beegle L.W & Kanik I. *J. Am. Soc. Mass Spectrom*. 2002; **13**: 300-307.
39. Beegle L.M, Kanik I, Matz L.M & Hill H.H Jr. *Int.J.Mass.Spectrom*. 2002; **216**: 257-268.
40. Dwivedi P, Wu C, Matz L.M, Clowers B.H, Siems W.F & Hill H.H. *Anal. Chem*. 2006; **78**: 8200-8206.
41. Hilderbrand A.E, Myung S & Clemmer D.E. *Anal. Chem*. 2006; **78**: 6792-6800.
42. Howdle M.D, Eckers C, Laures A.M.F & Creaser C.S. *J. Am. Soc. Mass Spectrom.*, 2009; **20**: 1-9.
43. Siems W.F, St Louis R.H & Hill H.H. Jr. unpublished data.
44. Kanu A.B, Dwivedi P. Tam M, Matz L & Hill H.H Jr. *J. Mass Spectrom*.

2008; **43**: 1-22

45. Shumate C.B. *Anal Chem*. 1989; **61**: 601-606.
46. Karasek F.W & Keller R.A. *J. Chromatogr. Sci.* 1972; **10**: 626-633.
47. Tou J.C & Boggs G.U, *Anal. Chem.* 1976; **48**: 1351-1357.
48. Baim M.A, Schuetze F.J, Frame J.M & Hill H.H Jr. *Am. Lab.* 1982; **31**: 59-70.
49. Baumbach J.I, Sielemann S, Xie Z & Schmidt H. *Anal. Chem.* 2003; **75**: 1483-1490.
50. Walendzik G, Baumbach J.I & Klockow D. *Anal. Bioanal. Chem.* 2005; **382**: 1842-1847.
51. Wolfgang V, Baumbach J.I & Uhde E. *Anal. Bioanal. Chem.* 2006; **384**: 980-986.
52. Ruzsanyi V, Baumbach J.I. *International Society for Ion Mobility Spectrometry.* 2005; **8**: 5-8.
53. Gieniec J, Cox L.H, Teer D & Dole M. *Abstracts, 20th annual conference on MS and allied topics*, Dallas, TX, 1972: **276**
54. Valentine S.J, Liu X, Plasencia M.D, Hilderbrand A.E, Kurulugama R.T, Koeniger S.L & Clemmer D.E. *Expert Rev. proteomics*. 2005; **2**: 553-565.
55. Hoaglund C.S, Valentine S.J, Sporleder C.R, Reilly J.P & Clemmer D.E. *Anal. Chem.* 1998; **70**: 2236-2242.
56. Mc Afee K.B, Spider D.P & Edelson D. *Physical Review*. 1967; **160**: 130-135.
57. Martin D.W, McDaniel E.W. *Atlanta*, 1970; **45**: 531-534.
58. Hoaglund C.S, Valentine S.J & Clemmer D.E. *Anal. Chem*. 1997; **69**: 4156-4161.
59. Parent D.C & Bowers M.T. *Chemical Physics*. 1981; **60**: 257-275.
60. Tang X, Bruce J.E & Hill H.H Jr. *Rapid Commun Mass Spectrom*. 2007; **21**: 1115-1122.
61. Koeniger S.L, Merenbloom S.I, Valentine S.J, Jarrold M.F, Udeth H.R, Smith R.D & Clemmer D.E. *Anal. Chem*. 2006; **78**: 2802-2809.
62. Kanu A.B, Dwivedi P, Tam M, Matz L & Hill Jr H.H. *J. Mass Spectrom*. 2008; **43**: 1-22.
63. Kuk Y, Jarrod M.F, Silverman P.J, Bowers M.T, Brown W.L. *Physical review B: Condensed matter*. 1989; **39**: 11168-11170.
64. Kemper P.R & Bowers M.T. *J. Am. Soc. Mass Spectrom*. 1990; **1**: 197-207.

65. Bell S.E, Ewing R.G, Eiceman G.A & Karpas Z. *J. Am. Soc. Mass Spectrom.* 1993; **5**: 177-185.

66. Bota G.M & Harrington P.B. *Talanta*, 2006; **68**: 629-635.

67. Keller T, Miki A, Regenscheit P, Dirnhofer R, Schneider A & Tsuchihashi H. *Forensic science international*, 1998; **94**: 55-63.

68. Gidden J, Baker E.S, Ferzoco A & Bowers M.T. *Int. J. Mass spectrom*. 2005; **240**: 183-193.

69. Przybylko A.R.M, Thomas C.L.P. Anstice P.J, Fielden P.R, Brokenshire J & Irons F. *Analytica Chimica Acta*. 1995; **311**: 77-83.

70. Wu C, Steiner W.E, Tornatore P.S, Matz L.M, Siems W.F, Atkinson D.A & Hill H.H Jr. *Talanta.* 2002; **57**: 123-134.

71. Debono R, Stefanou S, Davis M & Walia G. *Pharmaceutical technology*. 2002

72. Jafari M.T. *Talanta*. 2006; **69**: 1054-1058.

73. Kanu A.B, Hill H.H Jr, Gribb M.M & Walters R.N. *J. Environ. Monit*. 2007; **9**: 51-60.

74. Kindy J.M, Taraszka J.A, Regnier F.E & Clemmer D.E. *Anal. Chem*. 2002; **74**: 950-958.

75. Hill H.H Jr, Hill C.H, Asbury G.R, Wu C, Matz L.M & Ichiye T. *Int. J. Mass spectrom*. 2002; **219**: 23-37.

76. Colgrave M.L, Bramwell C.J & Creaser C.S. *Int. J. Mass spectrom*. 2003; **229**: 209-216.

77. Clowers B.H, Dwivedi P, Steiner W.E & Hill H.H Jr. *J. Am. Soc. Mass Spectrom*. 2005; **16**: 660-669.

78. Ugarov M, Egan T, Koomen J, Gillig K.J, Fuhrer K, Gonin M & Schultz J.A. *Anal. Chem*. 2004; **76**: 2187-2195.

79. Hoaglund C.S, Valentine S.J, Sporleder C.R, Reily J.P & Clemmer D.E. *Anal. Chem*. 1998; **70**: 2236-2242.

80. Asbury G.R, Wu C, Siems W.F & Hill H.H Jr. *Analytica Chimica Acta*. 2000; **404**: 273-283.

81. Matz L.M & Hill H.H Jr. *Anal. Chem*. 2001;**73**; 1664-1669.

82. Borsdorf H, Nazarov E.G & Eiceman G.A. *J. Am. Soc. Mass Spectrom*. 2002; **13**: 1078-1087.

83. Borsdorf H, Nazarov E.G & Miller R.A. *Talanta*. 2006; **3**: 815-822.

84. Valentine S.J, Plasencia M.D, Liu X, Krishnan M, Naylor S, Udseth H.R, Smith R.D & Clemmer D.E. *Journal of Proteome Research*. 2008;**7**;1109-1117.

85. Strachen N.J.C, Nicholson F.J & Ogden I.D. *Analytica Chimica Acta*. 1995; **313**: 63-67.

86. Ruzsanyi V, Baumbach J.I, Sielemann S, Litterst P, Westhoff M & Freitag L. *Journal of Chromatography A*. 2005; **1084**: 145-151.

87. Dwivedi P, Wu P, Klopsch S.J, Puzon G.J, Xun L & Hill H.H Jr. *Metabolomics.* 2008; **4**: 63-80.

88. Barnett D.A, Purves R.W, Ells B & Guevremont R, *J. Mass Spectrom.* 2000; **35**: 976.

89. McCooeye M.A, Ding L, Gardner G.J, Fraser C.A, Lam J, Sturgeon R.E & Mester Z. *Anal. Chem.* 2003; **75**: 2538-2542.

90. Kapron JT, Jemal M, Dunca G, Kolakowski B & Purves R. *Rapid Commun. Mass Spectrom*. 2005; **19**: 1979-1983.

91. Guevremont R. *J.Chromatogr.A*. 2004; **1058**: 3-19.

92. Shvartsburg A.A, Keqi F, Tang L & Smith R.D. *Anal.Chem*. 2006; **78**: 3706-3714.

93. Rearden P & Harrington P. *LabPlus international*. 2006; **1**: 20-24.

94. Ells B, Barnett D.A, Purves R.W & Guevremont R. *Anal.Chem*. 2002; **72**: 4555-4559.

95. Gorshkov M.P. *Inventors Certificate*, SU 955683. 1982

96. Buryakov I.A, Krylov E.V, Nazarov E.G & Rasulev U.K. *Int.J.Mass.Spectrom*. Ion Processes. 1993; **128**: 143-148.

97. Guevremont R. *High-Field Asymmetric Waveform Ion Mobility Spectrometry (FAIMS)*. May 20, 2005.

98. Kolakowski B.M & Mester Z. *Analyst*.2007;**132**:842-864.

99. Scvartsburg A.A, Tang K & Smith R.D. *J. Am. Soc. Mass Spectrom*. 2005; **16**:1447-1445.

100. Dole. M. Hines R.L. Mack R.C. Mobley Ferguson L.D & Alice M.B. *J. Chem. Phys*. 1968; **49**: 2240-2249.

101. Karas, M. Bachmann, D. Hillenkamp, F. *Anal. Chem.* 1985; **57**: 2935–9

102. Arpino P. *Mass Spectrometry Reviews*, 1992; **11**: 3-40.

103. Loo J.A, Udseth H.R, Smith R.D. *Anal. Biochem.* 1989; **179**: 404–12.
104. http://www.hull.ac.uk/chemistry/masspec3/principles%20of%20ms.html. Date accessed; 08/11/07
105. Dole M, Hines R.L, Mack R.C, Mobley R.C, Ferguson L.D & Alice M.B. *Chem. Phys*. 1968; **49**: 2240-2249.
106. Fenn J.B, Mann M, Meng C.K & Whitehouse C.M. *Science*. 1989; **246**: 49
107. Wilm M, Mann M. *Anal. Chem.*1996; **68**: 1–8.
108. Gates P. University of Bristol, Department of Chemistry, 2004.
109. Dole M, Hines R.L, Mack L.L, Mobley R.C, Ferguson L.D & Alice M.B. *Macromolecules*. 1968; **1**: 96-101
110. Iribarne J.V & Thomson B.A. *J. Chem. Phys*. 1976; **64**: 2287-2296
111. Takats Z, Wiseman J.M, Gologan B & Cooks R.G. *Science*. 2004; **306**: 471-473.
112. http://www.prosolia.com/DESI.html. Date accessed; 08/11/07
113. Ifa D.R, Wu C, Ouyang Z & Cooks R.G. *Analyst*. 2010; **135**: 669-681.
114. Vincenti M, Cooks R.G, *Org. Mass Spectrom*. 1988; **23**:317-326.
115. Cooks R.G, Ouyang Z, Takats Z & Wiseman J.M. *Science.* 2006;**311**: 1566-1570.
116. Bereman M.S & Muddiman D.C. *J. Am. Soc. Mass Spectrom*. 2007; **18**: 1093-1096.
117. Venter A, Sojka P.E & Cooks R.G. *Anal. Chem*. 2006; **78**: 8549-8555.
118. Cost A.B & Cooks R.G. *Chem. Phys. Lett*. 2008; **464**: 1-8.
119. Nefliu M, Smith J.N, Venter A, Cooks R.G. *J. Am. Soc. Mass Spectrom*. 2007; **19:** 420-427.
120. Kaupilla T.J. *Analyst*. 2007; **132**: 868-875.
121. Collins R.T, Jones J.J, Harris M.T, Basaran O.A. *Nat. Phys. 4* 2008; **4**:149-154.
122. Ifa D.R, Gumaelius L.M, Eberlin L.S, Manicke N.E, Cooks R.G. *Analyst.* 2007; **132**: 461-467.
123. Kauppila T.J, Wiseman J.M, Ketola R.A, Kotiaho T, Cooks R.G & Kostiainen R. *Rapid Commun. Mass Spectrom*. 2006; **20**: 387-392.
124. Pan Z et al., *Anal. Bioanal. Chem*. 2007; **387**: 539-549.
125. Jackson A.U et al. *J. Am. Soc. Mass Spectrom*. 2007;**11**:464–67.

126. Takats Z, Wiseman J.M & Cooks R.G. *Journal of mass spectrometry*. 2005; **40**:1261-1275.

127. Weston D.J, Bateman R, Wilson I. D, Wood T. R &Creaser, C. S. *Anal Chem*, 2005; **77**: 7572-7580.

128. Chen H. Talaty N.N. Takats Z & Cooks R.G. *Anal Chem*, 2005; **77**: 6915-6927.

129. Leuthold L.A, Veressio E & Hopfgartner G, *Spectroscopy Europe*. 2006; **18**: 8-12.

130. Rodriguez-Cruz S.E. *Rapid Commun Mass Spectrom*, 2006; **20**: 53-60.

131. Leuthold L.A, Mandscheff, J.F, Fathi M, Giraud C, Augsburger M, Varesio E & Hopfgartner G *Rapid Commun Mass Spectrom*, 2006; **20**: 103-110.

132. D'Agostino P.A, Chenier C.L, Han- cock J.R & Lepage C.R.J. *Rapid Commun Mass Spectrom*, 2007; **21**: 543-549.

133. Misharin A. S, Laughlin B. C, Vilkov A, Takats Z, Zheng O. Y & Cooks R. G. *Chemical Communications*, 2005; **15**: 1950-1952.

134. Cotte-Rodriguez I, Chen H & Cooks R.G. *Chemical Communications*, 2006; **9**: 953-955.

135. Cotte-Rodriguez I, Takats Z, Talaty N, Chen H.W & Cooks R.G. *Anal Chem*. 2005; **77**: 6755-6764.

136. Ifa D.R, Gumaelius L.M, Eberlin L.S, Manicke N.E & Cooks R.G. *Analyst*, 2007; **132**,:461-467.

137. Kauppila T.J, Talaty N, Kuuranne T, Kotiaho T & Kostiainen R. *Analyst*, 2007; **132**: 868-875.

138. Williams J.P, Patel V.J, Holland R, Scrivens J.H. *Rapid Commun Mass Spectrom*. 2006; **20**: 1447-1456.

139. Chen H.W, Pan Z, Talaty N, Cooks R.G & Raftery D. *Anal Bioanal Cem*. 2007; **387**: 539-49.

140. Wiseman J.M, Ifa D.R, Song Q.Y & Cooks R.G. *Angew Chem, Int Ed Engl*, 2006; **45**: 7188-7192.

141. Song Y.S et al. *Chemical Communications*. 2007; **223**: 61-63.

142. Van Berkel G.J, Ford M.J, Deibel. *Anal. Chem*. 2005; **77**: 1207-1215.

143. Pasilis S.P, Kertesz V, Van Berkel G.J, Schulz M, Schorcht S. *Anal Bioanal Chem*. 2008; **391**: 317-324.

144. Pasilis S.P, Kertesz V, Van Berkel G.J. *Anal. Chem*. 2007; **79**: 5956-5962.
145. Kertesz V, Van Berkel GJ. *Rapid Commun. Mass Spectrom* . 2008; **22**: 2639-2644.
146. Van Berkel G.J, Tomkins B.A, Kertesz V. *Anal. Chem*. 2007; **79**: 2778-2789.
147. Pasilis S.P, Kertesz V, Van Berkel G.J, Schulz M, Schorcht S. *J. Mass Spectrom*. 2008; **43**: 1627-1635.
148. Lin S.Y, Huang M.Z, Chang H.C, Shiea J. *Anal. Chem*. 2007; **79**: 8789-8795.
149. Van Berkel G.J, Kertesz V. *Anal. Chem*. 2006; **78**: 4938-4977.
150. Ford M.J, Van Berkel G.J. *Rapid Commun. Mass Spectrom*. 2004; **18**; 1303-1309.
151. Ford M.J, Kertesz V, Van Berkel G.J. *J. Mass Spectrom*. 2005; **40**: 866-875.
152. Janecki D.J, Novonty A.L, Woodward S.D, Wiseman J.M, Nurok D. *Journal of Planar Chromatography*. 2008; **21**: 11-14.
153. Shin Y.S, Drolet B, Mayer R, Dolence K & Basile F. *Anal Chem*, 2007; **79**: 3514-3518.
154. Kaur-Atwal G, Weston D.J, Green P.S, Crosland S, Bonner P.L, Creaser C.S. *Rapid Commun. Mass Spectrom,* 2007; **21**: 1131-1138.
155. Hu Q, Talaty N, Noll R.J & Cooks R.G. *Rapid Commun. Mass Spectrom.* 2006; **20**: 3403-3408.
156. Bereman M.S, Williams T.I & Muddiman D.C. *Anal Chem*. 2007; **79**: 8812-8815.
157. Dixon R.B, Sampson J.S & Hawkridge A.M. *J. Am. Soc. Mass Spectrom*, 2007; **18**: 1844-1847.
158. Hu Q, Talaty Z.N, Noll R.J & Cooks R.G. *Rapid Commun. Mass Spectrom*. 2006; **20**: 3403-3408.
159. Williams J.P. *J Mass Spectrom*, 2006; **41**: 1277-1286.
160. Kaur-Atwal G, Weston D.J, Green P.S, Crosland S, Bonner P.L.R & Creaser C.S. *Rapid Commun. Mass Spectrom.* 2007; **21**: 1131-1138.
161. Myung S, Wiseman J.M, Valentine S.J, Takats Z, Cooks R.G & Clemmer D.E. *J. Phys. Chem. B*. 2006; **110**: 5045-5051.
162. Williams P & Scrivens J.H. *Rapid Commun. Mass Spectrom*. 2008; **22**: 187-196.

163. Takáts Z, Wiseman J.M, Gologan B & Cooks G.R. *Science*. 2004; **306** : 471-473.
164. Gabler H.E. *Journal Of Geochemical Exploration*. 2002; **75** :1-15.
165. Lenz E.M, Bright J, Knight R, Wilson I.D & Major H. *Analyst*. 2004; **129**: 535-541.
166. Jarrold M.F. *Ann. Rev. Phys. Chem*. 2000; **51**: 179-207.
167. Hoffmann de E & Stroobant V. *Mass Spectrometry Principles and Applications,* Second Edition, 2002, Wiley, England.
168. Grayson M.A. *Measuring Mass, From Positive Rays to Proteins. American Society for Mass Spectrometry*. 2002. USA
169. http://www.rmjordan.com/Resources/Tutorial.pdf. Date accessed 8/11/07
170. http://en.wikipedia.org/wiki/File:TOF-reflectron.png. Date accessed; 08/11/07
171. Wolfgang P. Nobel Lecture, December 8, 1989
172. www.chm.bris.ac.uk/ms/theory/quad-massspec.html. Date accessed; 8/11/07
173. Brown K.L & Tautfest G.W. *Review of Scientific Instruments* 1956; **27** ;696-702.
174. Taylor L.C, Brent D.A, Cottrell J.S. *Biochem. Biophys. Res. Commun*. 1987; **145**: 542-548.
175. Allen J. S. *Review of Scientific Instruments* 1947; **18**: 739-749.
176. Lubsandorzhiev, B. *Nuclear Instruments and Methods in Physics Research Section A: Accelerators, Spectrometers, Detectors and Associated Equipment* 2006; **567**: 236.
177. http://www.ornl.gov/sci/techresources/Human_Genome/home.shtml. Date accessed; 08/11/07
178. The Genome International Sequencing Consortium Initial sequencing and analysis of the human genome. *Nature* 2001; **409**, 860-921.
179. Nicholson J.K, Lindon J.C & Holmes E. *Xenobiotica*, 1999; **29**: 1181-1189.
180. Ginsburg G.S & Haga S.B. *Expert Rev Mol Diagn*. 2006; **6**: 179-191.
181. Lindon L.C, Nicholson J.K & Holmes E. 2007, *The Handbook of Metabonomics and Metabolomics*. Elsevier, London.
182. Nicholson J.K, Buckingham M.J & Sadler P.J. *Biochemical Journal*. 1983; **211**; 605-615.
183. Nicholson J.K, Timbrell J.A & Sadler P.J. *Molecular Pharmacology*. 1985; **27**: 644-651.

184. Nicholson J.K & Wilson I.D. *Progress in NMR Spectroscopy*. 1989; **21**; 449-501.

185. Bales J.R, Higham D.P, Howe I, Nicholson J.K & Sadler P.J. *Clinical Chemistry.* 1984; **30**; 426-432.

186. Mayer M, Chung Y.L, Mayer X.K, Ly L, Troy H, Fredericks S, Yu Y.H, Griffiths J.R & Xu Q.B. *Arterioscl. Thromb. Vasc. Biol*. 2005; **25**: 2135-2142.

187. Zhang X, Wei D, Yap Y, Li L, Guo S & Cheng F. *Mass Spectrometry reviews*. 2007; **26**: 403-431.

188. Robertson D.G, Reily M.D, Sigler R.E, Wells D.F, Paterson D.A & Braden T.K. *Toxicol. Sci*. 2000; **57**: 326-337.

189. Roessner U, Wagner C, Kopka J, Trethewey R.N & Willmitzer L. *Plant J*. 2000; **23**: 131-142.

190. Wilson I.D, Plumb R, Granger J, Major H, Williams R & Lenz E.M. *J. Chromatogr B*. 2005; **817**: 67-76.

191. Plumb R.S, Granger J.H, Stumpf C.L, Johnson K.A, Smith B.W, Gaulitz S, Wilson I.D & Castro-Perez J. *Analyst*. 2005; **130**: 844-849.

192. Soga T. Ohashi Y, Ueno Y, Naraoka H. Tomita M & Nishioka T. *J. Proteome Res*. 2003; **2**: 488-494.

193. Lindon J. *Business Briefing; Future Drug Discovery.* 2004

194. Nicholls A.W, Holmes E, Lindon J.C, Shockor J.P, Farrant R.D, Haselden J.N. Damment S.J.P. Wterfield C.J. *Chem. Res. Toxicol*. 2001; **14**: 975-987.

195. Ginsburg G.S & Haga S.B. *Expert Rev Mol Diagn*. 2006; **6**: 179-191.

196. Goodacre R, York E.V, Heald J.K & Scott I.M. *Phytochemistry*. 2003; **62**: 859-863.

197. Mauri P & Pietta P. *J. Pharm. Biomed. Anal*. 2000; **23**: 61-68.

198. Pitt J.J, Egginton M & Kahler S.G. *Clin. Chem*. 2002; **48**: 1970-1980.

199. Wilson I.D, Nicholson J.K, Castro-Perez, Granger J.H, Johnson K.A, Smith B.W &. Plumb R.S. *J. Proteome Res*. 2005; **4**:591-598.

200. Smedsgaard J & Frisvad J.C. *J. Microbiol. Methods*. 1996; **25**: 5-17.

201. Vaidyanathan V, Kell D.B & Goodacre R. *J. Am. Soc. Mass Spectrom*. 2002; **13**: 118-128.

202. Williams R,E, Lenz E.M, Lowden J.S, Rantalainen M & Wilson I.D. *Mol. BioSyst.* 2005; **1**: 166-175.

203. Rashed M.S, Ozand P.T, Bennet M.J, Barnard J.J, Govindaraju D.R & Rinaldo P. *Clin. Chem*. 1995, **41**: 1109-1114.

204. Chan E.C.Y, New L.S, Yap C.W & Goh L.T. *Rapid Commun. Mass Spectrom*. 2009; **23**: 384-394.

205. Dwivedia P, Schultzb A.J & Hill H.H Jr. *Int. J. Mass spectrom* 2010; **298**: 78–90.

206. Miller J.N & Miller J.C. *Statistics and Chemometrics for Analytical Chemistry.* Fifth edition. 2005. Pearson Education Limited. England.

207. Kantardzic M. *Data Mining: Concepts, Models, Methods, and Algorithms*. Second edition. 2003. John Wiley & Sons. New York.

208. http://www.resample.com/xlminer/help/PCA/pca_intro.htm. Date accessed: 02/03/11

209. http://support.sas.com/publishing/pubcat/chaps/55129.pdf. Date accessed; 02/03/11

210. http://en.wikipedia.org/wiki/File:Artificial_neural_network.svg. Date accessed; 02/03/11

211. Balabin R.M & Lomakina E.I. *J. Chem. Phys.* 2009; **7**: 074104-074108.

CHAPTER TWO

The application of desorption electrospray ionisation-ion mobility-mass spectrometry for pharmaceutical analysis.

2.1 INTRODUCTION

Studies investigated the direct analysis of pharmaceutical formulations and active ingredients in caplet form and from non-bonded reversed-phase thin layer chromatography (RP-TLC) plates by desorption electrospray ionisation (DESI) combined with ion mobility-mass spectrometry (IM-MS) is reported. The analysis of formulations containing analgesic (paracetamol), decongestant (ephedrine),anti-foaming (Simethicone), opioid (Codeine/Loperamide) and stimulant (Caffeine) active pharmaceutical ingredients is described, with and without chromatographic development to separate the active ingredients from the excipient formulation. Selectivity was enhanced by combining ion mobility and mass spectrometry to characterise the desorbed gas-phase analyte ions on the basis of mass-to-charge (*m/z*) ratio and gas-phase ion mobility (drift time). Varying the solvent composition of the DESI spray using a step gradient was employed to optimise the desorption of active pharmaceutical ingredients from the RP-TLC plates. The combined RP-TLC/DESI/IM-MS approach has potential as a rapid and selective technique for pharmaceutical analysis by orthogonal gas-phase electrophoretic and mass-to-charge separation.

2.2 CHAPTER TWO AIMS AND OBJECTIVES

This chapter describes an investigation to develop a fast, novel method on the detection of pharmaceutical formulations employing desorption electrospray ionisation (DESI) coupled with ion mobility – mass spectrometry (IM-MS). Active pharmaceutical ingredients were analysed directly from tablets and in combination with reversed phase thin layer chromatography plates (RP-TLC).

Thin layer chromatography (TLC) remains a widely used technique for the separation of mixtures for both qualitative and quantitative analysis, but has limitations with respect to the identification of the separated analytes. To overcome this limitation there have been many attempts to couple TLC with MS using ionization techniques such as fast atom bombardment (FAB) and matrix assisted laser desorption ionisation (MALDI).[1] In this context, DESI as a sample introduction method for MS seems ideally suited to combination with TLC and its use has been described with normal phase silica gel[2] and cellulose[3] plates for the study of medicinal ingredients,[4] dyes,[4,5] alkaloids,[6] proteins and peptides[7] and pharmaceutical formulations.[8]

The application of DESI to the analysis of analytes from hydrophobic, reversed-phase TLC plates with bonded silica phases has been investigated for the analysis of dyes.[9,10,11] More recently, Wiseman *et al.* reported the use of pressurised planar electrochromatography using reversed-phase C_{18} plates for the study of steroids.[12] DESI/MS has also been employed for the chemical imaging of dyes separated on TLC plates.[9] The desorption of analytes from non-bonded, reversed-phase TLC plates by DESI has not been previously reported and presents additional challenges because the plates cannot be pre-cleaned to reduce background contamination prior to analyte deposition and there may be interference from stationary phase molecules being desorbed together with the analyte.

The specific objectives were:

- To investigate the potential of DESI/IM-MS analysis of pharmaceutical drug formulations to increase selectivity and to characterise and separate analytes of interest with little or no sample preparation.

- To investigate the application of DESI for the direct, rapid ion mobility mass spectrometric analysis of active pharmaceutical ingredients from the surface of bonded and non-bonded RP-TLC plates, with or without separation from the excipient components.

- To evaluate the potential of ion mobility as a pre-separation technique for gas phase ions generated by DESI for active-pharmaceutical ingredients.

- To asses the potential of RP-TLC/DESI-IM-MS for chemical imaging.

- To investigate the potential of varying the solvent composition of the DESI solvent spray to provide on-line optimisation of the method for reduced analysis times.

2. 3 EXPERIMENTAL

2.3.1 Chemicals

Acetonitrile (HPLC gradient grade), methanol (HPLC gradient grade) and water (HPLC grade) were purchased from Thermo Fisher Scientific (Loughborough, UK). Mass spectrometry grade (puriss, p.a) formic acid was purchased from Sigma-Aldrich (Gillingham, UK). Generic Co-codamol tablets containing 500 mg paracetamol and 8 mg codeine, generic cold and flu tablets containing 250 mg paracetamol, 25 mg caffeine and 8 mg ephedrine and Sleepeaze (Boots, Nottingham, UK) containing diphenhydramine 25 mg were purchased over the counter. Imodium plus caplets (Johnson & Johnson, MSD) containing Loperamide hydrochloride (1) and Simethicone (2) were purchased over the counter.

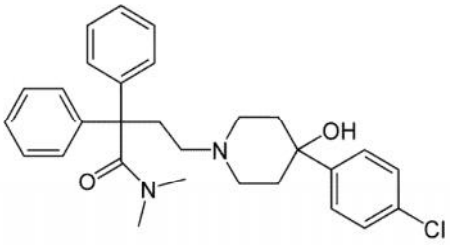

(1)

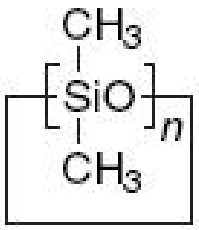

(2)

2.3.2 Desorption electrospray ionisation/ ion mobility-mass spectrometry analysis of Imodium plus caplets.

All experiments were carried out employing a prototype IM-quadrupole time-of-flight mass spectrometer (Waters Corporation, Manchester). The atmospheric pressure ionisation (API) region of a Z-spray electrospray ionisation source was modified for DESI by attaching a section of TLC plate to a manipulator, allowing horizontal, vertical and rotational manipulation of the plate, which was located in the atmospheric pressure ionisation region of the mass spectrometer at an approximate 45° angle relative to the spray tip and cone, Figure 2.1. A Waters Alliance 2790 chromatograph (Waters Corporation, Manchester, UK) was coupled to the modified DESI ion source of the IM-Q-ToFMS spectrometer to provide the DESI solvent flow.

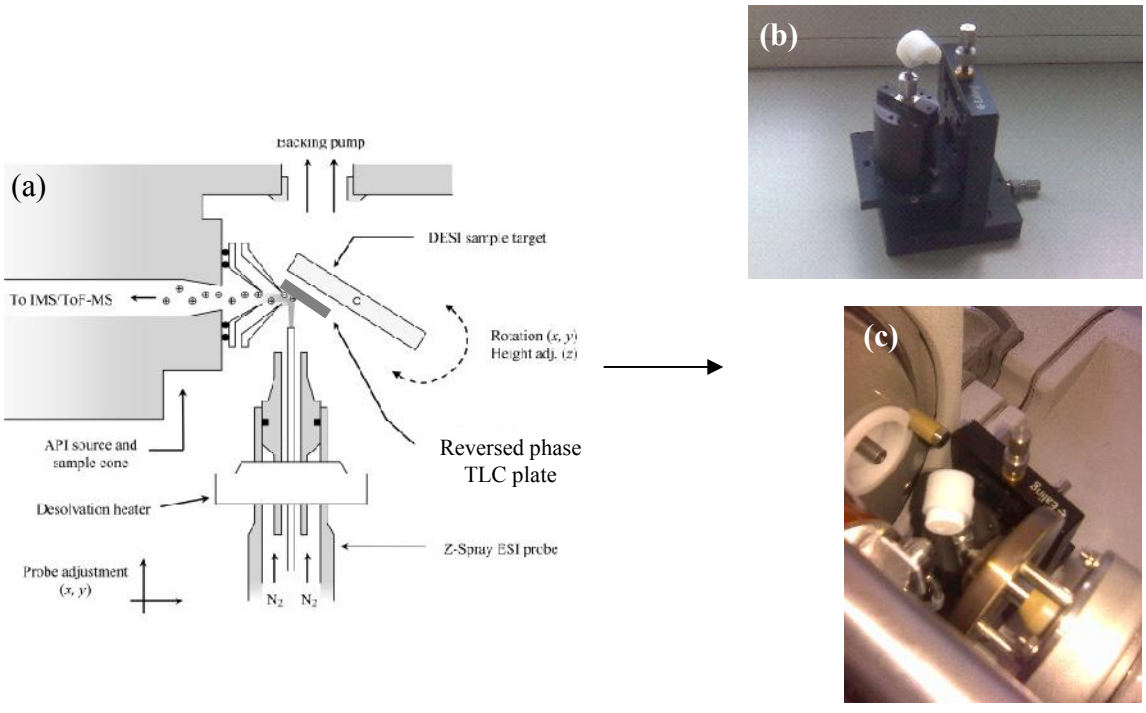

Figure 2.1. (a) Schematic diagram of DESI source and mass spectrometer interface, (b) photograph of the DESI sample stage (c) photograph of the DESI ion source region.

DESI was performed by attaching half a broken Imodium Plus tablet, (with internal portion of tablet exposed to DESI spray to overcome problems associated with the tablet coating), to the plate on the x,y manipulator which was placed in the atmospheric pressure ionisation region of the mass spectrometer at an approximate 45° angle relative to the spray tip and cone. The area of sample desorbed when the ESI probe and sample position were optimised was 1mm diameter (3.14 mm^2), which corresponds to the incident DESI solvent spray at the sample surface.

Ions from the DESI source were directed into the trap region at the head of the ion mobility drift cell. The instrument was operated in positive ion mode with the ESI capillary voltage set to 3.1 kV; cone voltage 60 V; source temperature 120 °C; desolvation gas, N_2 gas flow 250 L/hr; desolvation gas temperature, 180 °C. The quadrupole was operated in wide band pass mode (*m/z* 50-1000) and the collision cell operated without any collision gas. The IM-Q-ToFMS was operated in positive ion mode with the ESI capillary voltage set to 3.5 kV; cone voltage 40 V; source temperature 120 °C; desolvation gas, N_2 gas flow 250 L/hr; desolvation gas temperature, 180 °C. Ions from the DESI source were directed into the trap region at the head of the ion mobility drift cell and periodically gated into the drift cell, which was operated in the pressure region of 1.0 to 3.0 Torr N_2, using a gate electrode pulse (3.50 V, 200 μs pulse width and 15ms pulse period). The IM drift tube consisted of a multi-plate ion guide (15.2 cm in length) to which a voltage gradient (14.24 V/cm and a supplement RF voltage 3.8 V) were applied. Ions passing through the drift region were then directed through the quadrupole and collision cell into the reflectron TOF mass analyser. The quadrupole was operated in wide band pass mode (*m/z* 50-1000)

and the collision cell without any collision gas. Ion mobility spectra were acquired by collecting data from 200 ToF pushes (45 μs per bin) and plotting drift time (scan number) against mass-to-charge ratio (*m/z*). IM-MS data were typically accumulated for 5 s, with a 2 s interscan delay. Acquired data were presented as a plot of time against ion intensity; total ion mobility response or selected ion mobility responses. Masslynx version 4.1 (Waters Corporation, Manchester, UK) was used to control the IM-MS instrument and for data acquisition and processing.

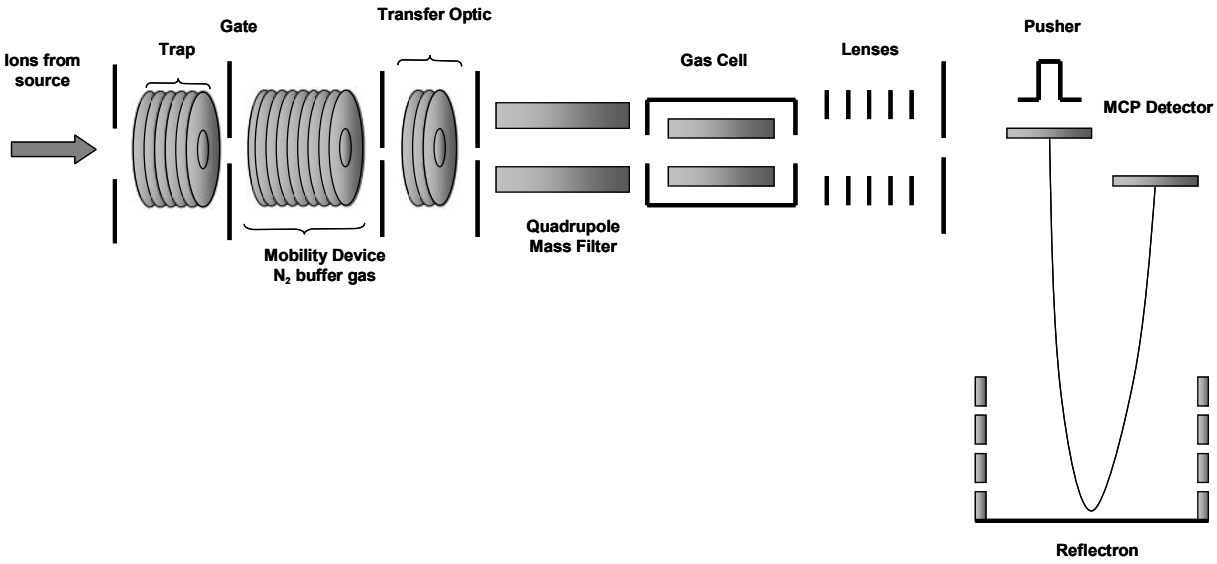

Figure 2.2 Schematic of prototype IMS-Q-ToF

2.3.3 Sample preparation for the desorption electrospray ionisation/ ion mobility-mass spectrometry analysis combined with reversed-phase thin layer chromatography.

Tablets were crushed and extracted in water (2 mL) and filtered (Whatman filter paper, qualitative). The extracted solution was manually spotted onto the reversed-phase hydrocarbon impregnated silica gel TLC plates (Analtech Uniplates, Newark, USA; 10 x 20 cm, 250 microns) in 1 μL aliquots up to 6 μL in total volume. The plates were developed in a saturated chamber with 50/50 (v/v) methanol-water. A saturated chamber containing iodine crystals was used to develop the TLC plates.

2.3.4 Desorption electrospray ionisation/ ion mobility-mass spectrometry analysis combined with reversed-phase thin layer chromatography

The DESI/IM-MS ion source region is shown in Figure 2.1. All experiments were carried out employing the prototype IM-quadrupole time-of-flight mass spectrometer (Waters Corporation, Manchester) Figure 2.2. A split was employed to reduce the solvent flow rate to the DESI probe (typically 25 μL/min) from the higher flow through the LC system (200 μL/min). The area of sample desorbed when the DESI probe and sample position were optimised was approximately 1 mm in diameter. Variable solvent composition experiments were carried out in which the TLC plate was analysed using three different solution compositions using the following step gradient: 10% A (0-1.5 min), increased to 50% A (1.5-3.0 min) and then to 90% A (3.0-4.5 min), where A = 0.1% aqueous formic acid and B = 0.1% formic acid in

acetonitrile. At each gradient step change the DESI source was moved in the vertical plane ensuring that an area of the TLC plate under interrogation had not previously been exposed or desorbed. Solvent and gas flow directed at the ionisation surface also creates a washing effect. The vertical movement of the sample stage ensured that that the solvent plume from the previous row was not interrogated.

The IM-Q-ToFMS was operated with the same parameters as in section 2.3.2 page 74.

2.4 RESULTS AND DISCUSSION

2.4.1 DESI/IM-MS of tablet formulations

Imodium is a tablet formulation prescribed for stomach upset and diarrhoea. The active pharmaceutical ingredients are, Loperamide (2 mg) and Simeticone (containing an equivalent to 125 mg of poly (dimethyl siloxane (PDMS)). The tablet was analysed after being broken in half, with the non-coated portion of the tablet being interrogated by the DESI solvent plume allowing direct analysis without sample pre-treatment. The resulting DESI spectrum displayed the oligomers of PDMS including the Na^+ adducts and the active ingredient Loperamide (Figures 2.3 to 2.6). However, the mass spectra obtained were dominated by ions from the oligomers of PDMS as shown in the *m/z* vs drift time (bins) plot (Figure 2.3). A significant increase in the relative intensity of the protonated Loperamide was obtained by combining only the bins corresponding to the selected ion mobility response for Loperamide (*m/z* 477.23, bins 57 to 65) (Figure 2.4 (b)) compared to the mass spectrum obtained by combining all 200 bins (Figure 2.4 (c)). Figure 2.4 (c) corresponds to mass spectral analysis in the absence of IM separation. The DESI technique required minimum sample

preparation and the IM separation allowed the acquisition of MS nested data sets to be acquired in the IM timescale. The use of data mining methods can be employed to improve visualisation of the data and to serve as a powerful aid to extract information on specific analytes, allowing only relevant information to be extracted. The data mining method employed in these investigations was the Driftscope ^{TM} mobility environment software (Waters Corporation). Driftscope ^{TM} software displays the drift time vs the *m/z* for each ion present in the data. The bands of colour in the drift time vs *m/z* plots (Figure 2.3) represent the intensity of the ion, with red indicating regions of highest intensity. Regions of interest may be selected and interrogation of the corresponding mass spectra carried out. The Additional dimension of IM and data mining improved selectivity for the active ingredient, Loperamide. These results indicate that by employing direct DESI/IM-MS for the analysis of solid pharmaceutical formulations, significant improvement in selectivity using IMS compared to MS alone can be achieved.

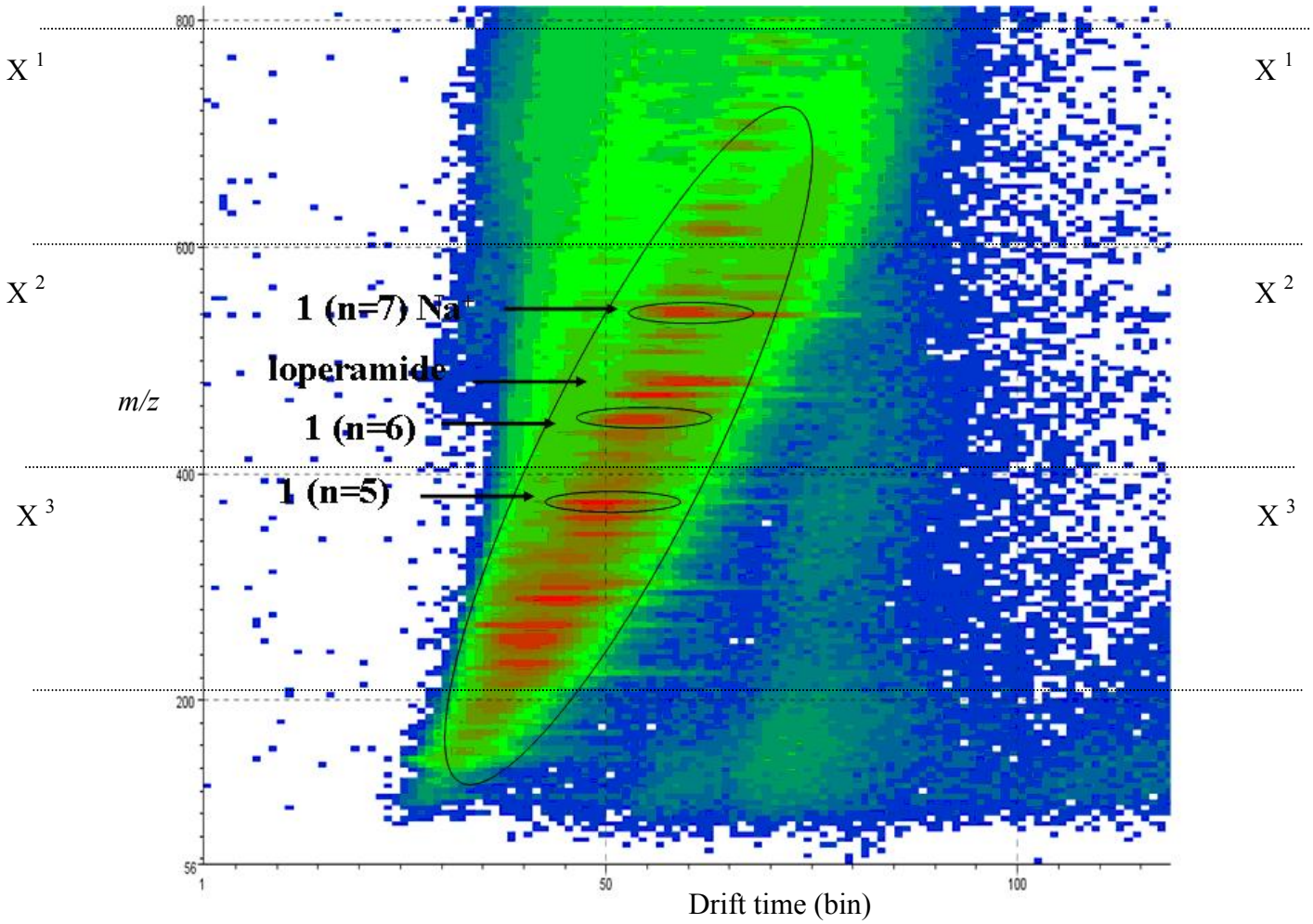

Figure 2.3 Drift time (bins) vs. *m/z* plot of DESI/IM-MS analysis of Imodium plus caplets

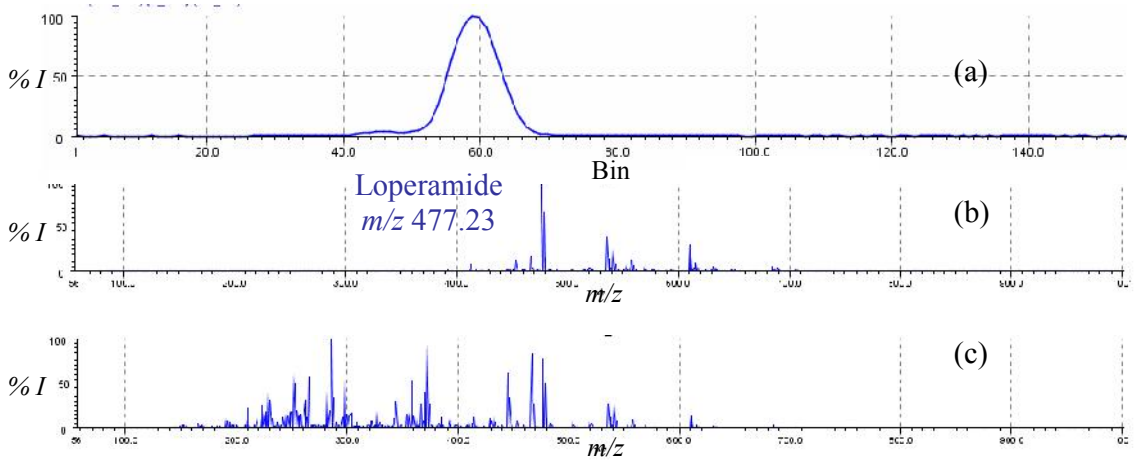

Figure. 2.4 Spectra corresponding to selected ion mobility response for Loperamide (*m/z* 477.23) from Figure 2.3. (a) Selected ion mobility spectrum (*m/z* 477.23) and (b) mass spectrum obtained by combining bins 57 to 65 for *m/z* 477.13 (c) mass spectrum obtained by combining all 200 bins.

The data can be manipulated to extract mass and ion mobility spectra from selected regions from the drift time vs *m/z* plots, Figure 2.3. Three sections were selected from Figure 2.3 and averaged together to give a mobility spectrum and corresponding mass spectrum of each section. Figure 2.5, (a), (b) and (c) displays the three regions corresponding to Figure 2.3, X^1, X^2 and X^3.

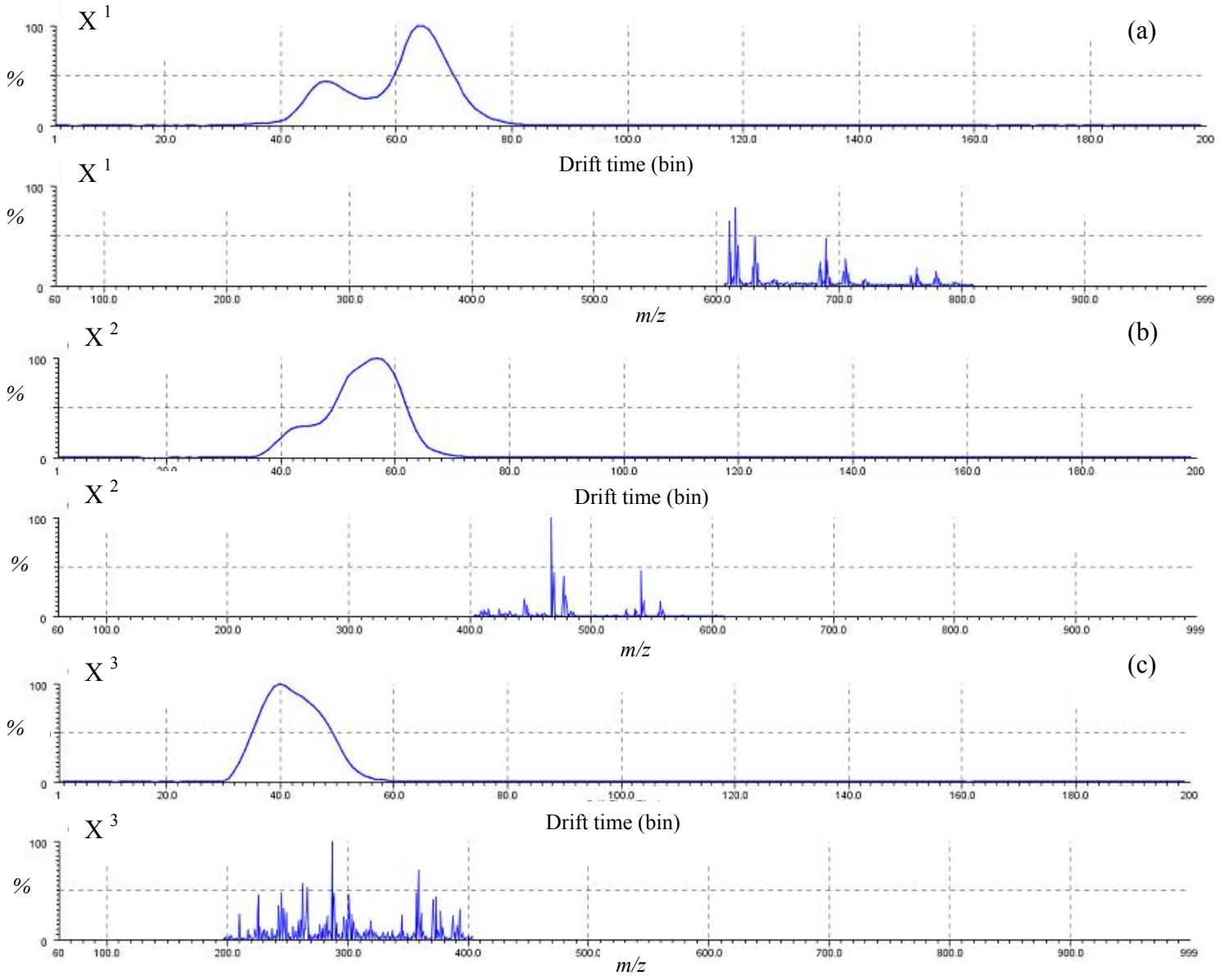

Figure 2.5 DESI/IM-MS analysis of Imodium. Ion mobility spectra and corresponding mass spectra for selected regions of Figure 2.3. (a) selected region X^1 (b) selected region X^2 (c) selected region X^3.

Data mining of Figure 2.3 therefore allows spectra to be enhanced and thus provides a means to reduce the complexity of the full data plot.

Figure 2.6 displays the ion mobility responses for the main PDMS polymers present in the Imodium tablet. Electrospray ionisation mass spectrometry (ESI-MS) and DESI-MS have previously been employed to characterise PDMS. However, IM was employed during this study to increase the selectivity of the analysis. The results show that as the *m/z* of the oligomers increases, the drift time also increases (Figure 2.6). An increase in drift time is consistent with an increase in size of the polymer and in turn the collision cross section, Ω. Comparison of the PDMS drift times (Figure 2.6 and Table 2.1) suggests that the n= 5 and 6 oligomers can be distinguished from each other by drift time within the precision of the measurement (± 0.045 ms). Calculated drift times are presented in Table 2.1 along with tentative assignments, *m/z* and corresponding empirical formulas for the oligomers of PDMS and Loperamide. Comparison of drift times between the protonated PDMS oligomers and the Na^+ adducts shows an increase in 0.09 ms for both the n=5 and n=6, however an increase of 0.04 ms was observed for the n= 7 oligomer.

PDMS investigations

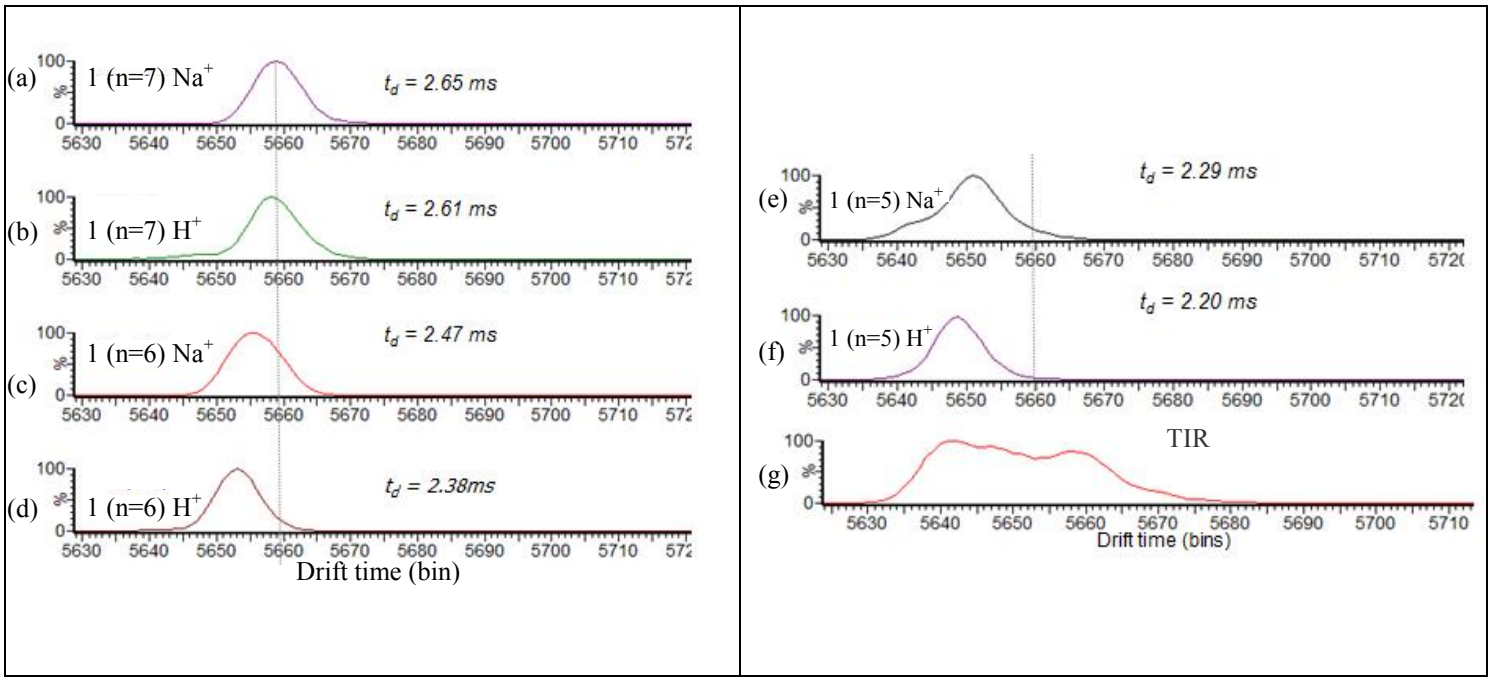

Figure 2.6 DESI/IM-MS analysis of Imodium tablet. Selected ion mobility responses of PDMS excipients (a) 1 (n=7) Na^+, (b) 1 (n=7), (c) 1 (n=6) Na^+, (d) 1 (n=6), (e) 1 (n=5) Na^+, (f) 1 (n=5), (g) Total ion response.

Table 2.1 Proposed assignment of PDMS excipients, including calculated drift times for each of the assigned oligomers.

Assignment	*m/z*	Drift time (ms)	Empirical formula
1 (n=5) H^+	371.1	2.20	$C_{10}H_{31}Si_5O_5$
1 (n=5) Na^+	393.1	2.29	$C_{10}H_{30}Si_5O_5Na$
1 (n=6) H^+	445.1	2.38	$C_{12}H_{37}Si_6O_6$
1 (n=6) Na^+	467.1	2.47	$C_{12}H_{36}Si_6O_6Na$
1 (n=7) H^+	519.1	2.61	$C_{14}H_{43}Si_7O_7$
1 (n=7) Na^+	541.1	2.65	$C_{14}H_{42}Si_7O_7Na$
Loperamide	477.23	2.70	$C_{29}H_{34}ClN_2O_2$

.

2.4.2 DESI/IM-MS analysis of non-bonded RP-TLC plates

Pharmaceutical formulations containing paracetamol, caffeine, codeine and ephedrine were analysed by DESI/IM-MS directly from the surface of non-bonded RP-TLC plates, generating mass-to-charge and mobility data for the desorbed ions. Optimisation of the positioning of the sample relative to the atmospheric pressure ionisation region of the mass spectrometer, including the spray tip and cone (Figure 2.1) was found to be a critical parameter influencing analyte signal intensity. The optimum position was determined by manipulation of the sample in the horizontal, vertical and rotational planes with the maximum analyte response observed at an angle of 45° relative to the spray tip and cone. A further parameter found to effect analyte responses significantly was the DESI solvent flow rate. An increase in flow correlated with an increase in analyte signal response and the amount of analyte desorbed from the RP-TLC plate surface. The signal intensity for the active ingredients paracetamol and codeine showed a nine-fold increase when the DESI solvent flow rate was increased from 2 μL/min to 5 μL/min. A further increase in ion intensity was observed up to a flow rate of 50 μL/min, but only a small increase in signal response was observed at flow rate above an optimised flow of 25 μL/min. The TLC plates showed a clear "wetting effect", with a solvent layer forming on the surface under interrogation by the incident electrospray, which facilitates the extraction of analytes from the surface into the thin liquid layer.

High noise levels were observed in the resulting DESI mass spectra, presumably as a result of interferences present on the plate or ablation of the hydrocarbon stationary phase, which was a non-bonded phase and could not, therefore, be washed prior to sample loading. IM-MS data were acquired by scanning of nested data sets, with mass

spectra (45 μs/scan) and IM spectra (~13 ms) scanned repetitively throughout the run. Spectra were accumulated to yield 200 mass spectra and one ion mobility spectrum every 7 s. The ion mobility drift time is plotted as 'bins', where each bin corresponds to an acquired mass spectrum. The nested data acquisition of IM and MS data results in an analysis incorporating a gas-phase electrophoretic separation of the ESI generated ions on the basis of charge state and collision cross section (i.e. size and shape), between the mass analysis, all within the timescale of the MS run.

Total ion and selected ion mobility responses for the active pharmaceutical ingredients extracted from a generic cold and flu tablet, including ephedrine, paracetamol and caffeine, deposited on the TLC plate without solvent development, are displayed in Figure 2.7 Selected ion responses for protonated ephedrine (*m/z* 168; Figure 2.8 (a)), paracetamol (*m/z* 152; Figure 2.8 (b)), and caffeine (*m/z* 195; Figure 2.8 (c)) showed drift times of 0.90 ms (bin 20), 0.95 ms (bin 21) and 1.04 ms (bin 23) respectively. The selected ion responses are much cleaner and sharper then the total ion mobility spectrum with peak widths at half height of 5 bins (ephedrine), 3 bins (paracetamol) and 4 bins (caffeine) compared to 11 bins for the total ion mobility spectrum.

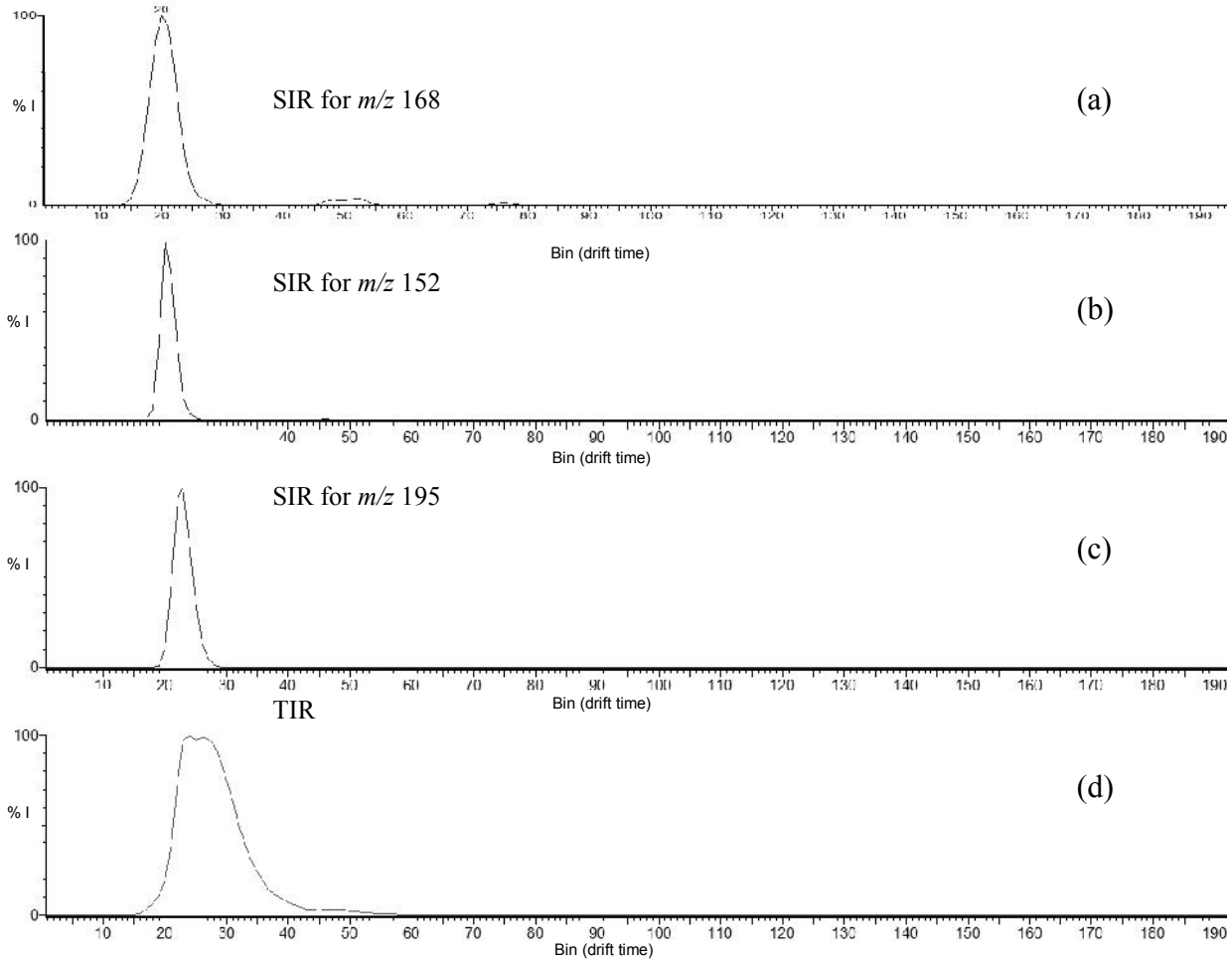

Figure 2.7 Ion mobility spectrum and selected ion mobility responses for the DESI/IM-MS analysis of a generic cold and flu tablet obtained from a RP-TLC plate without development, using DESI with a solvent composition of 50:50 (v/v) acetonitrile:water with 0.1% formic acid at a flow rate of 25 µL/min. (a) *m/z* 168 (ephedrine), (b) *m/z* 152 (paracetamol), (c) *m/z* 195 (caffeine), and (d) total ion mobility spectrum.

The corresponding mass spectra are shown in Figure 2.8. The mass spectrum obtained by combining all 200 bins (Figure 2.8 (d)) corresponds to the mass spectrum expected in the absence of IM separation and contains a large number of desorbed ions across the whole mass range. In contrast, when the mass spectra obtained by combining bins at the drift times (bins 15-24, 18-23 and 21-25; Figure 2.8) of the active ingredient peaks (Figures 2.8(a), (b) and (c)) are compared to the mass spectrum from the combined total ion mobility response, the enhanced selectivity for the actives is observed. The resulting mass spectra show fewer ions and, in the case of paracetamol (*m/z* 152) and caffeine (*m/z* 195), the $[M+H]^+$ ion is the base peak. Paracetamol was the most abundant component in the cold and flu tablet (250 mg per tablet); however, caffeine (25 mg per tablet) showed the highest IM-MS response, as a result of higher DESI ionisation efficiency from the TLC plate. On the basis of the amount of active ingredient spotted on the plate the limit of detection (LOD) (3:1 signal-to-noise) was estimated to be 16 $\mu g/cm^2$, 34 $\mu g/cm^2$ and 239 $\mu g/cm^2$ for caffeine, ephedrine and paracetamol respectively. The amount spotted on the plate was determined by the original concentration of the active ingredient in relation to the spot diameter.

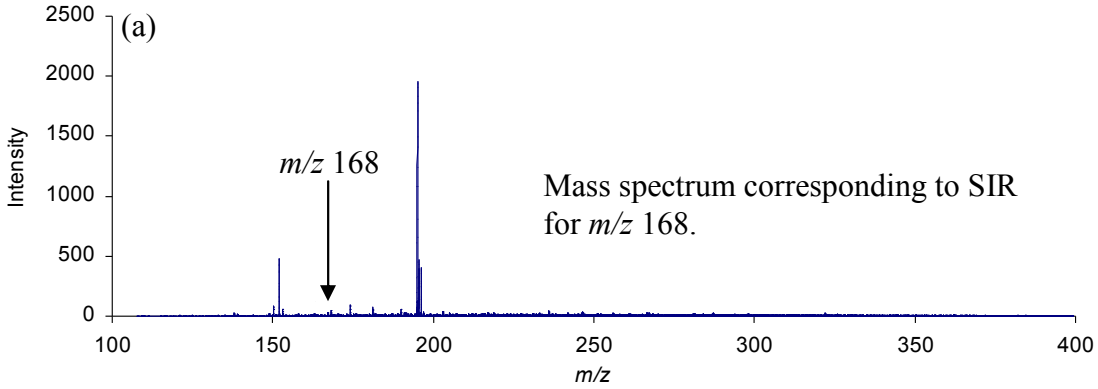
(a)
Intensity
m/z 168
Mass spectrum corresponding to SIR for m/z 168.
m/z

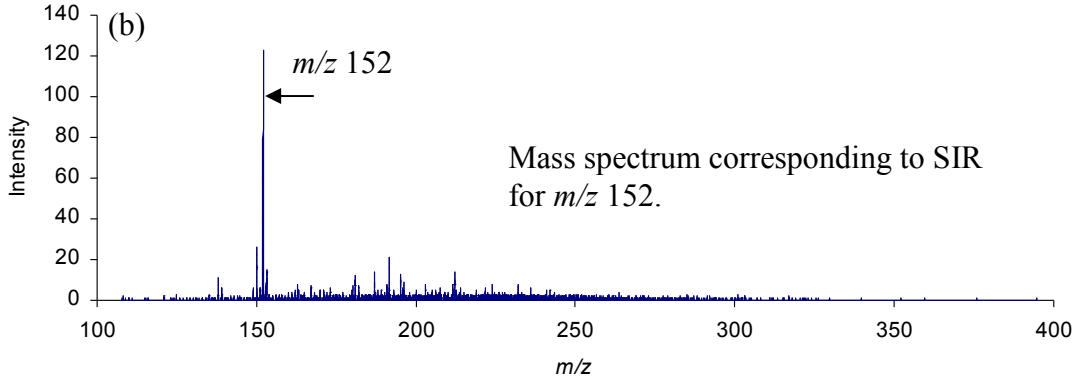
(b)
Intensity
m/z 152
Mass spectrum corresponding to SIR for m/z 152.
m/z

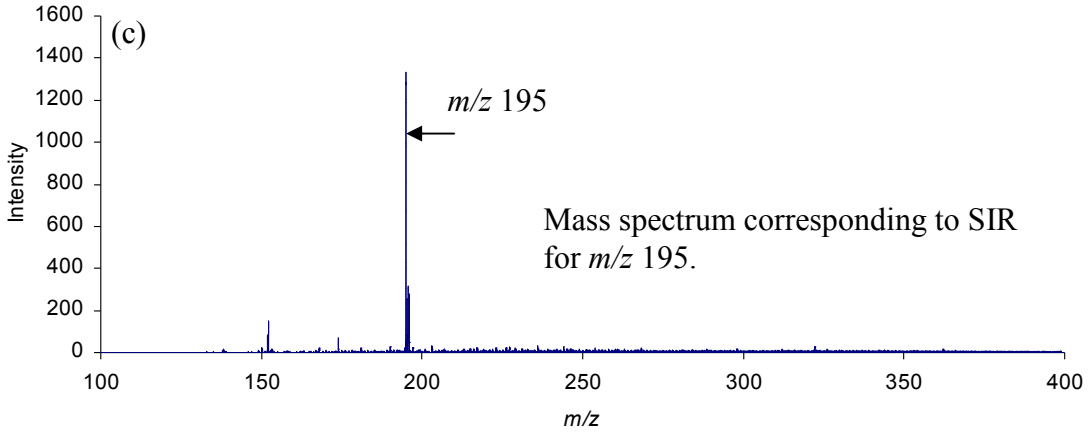
(c)
Intensity
m/z 195
Mass spectrum corresponding to SIR for m/z 195.
m/z

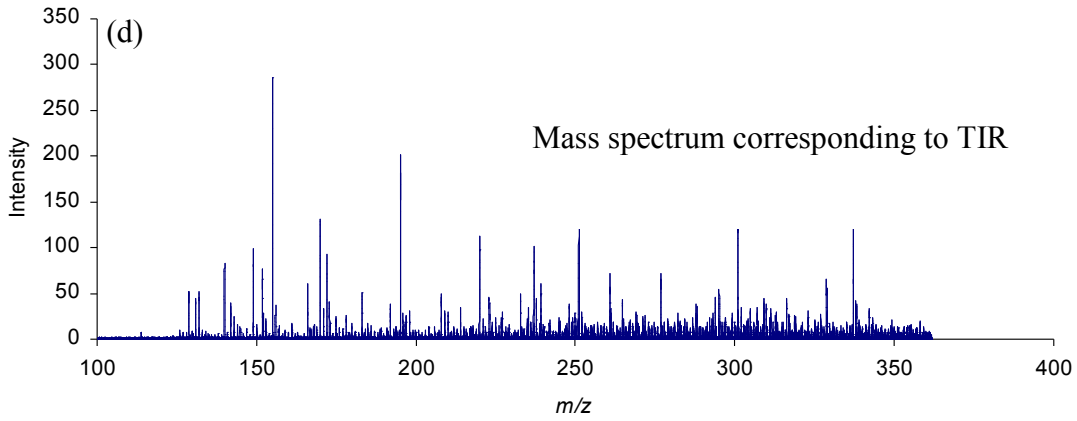
(d)
Intensity
Mass spectrum corresponding to TIR
m/z

Figure 2.8 Mass spectra corresponding to selected ion mobility responses for the DESI/IM-MS analysis of a generic cold and flu tablet obtained from a RP-TLC plate without development (a) bins 15-24 (ephedrine), (b) bins 18-23 (paracetamol), (c) bins 21-25 (caffeine), and, (d) mass spectrum obtained by combining all 200 bins acquired during the ion mobility separation.

The total ion and selected ion mobility responses obtained from the DESI/IM-MS analysis of paracetamol and codeine extracted from a generic Co-codamol tablet, following separation by TLC, are displayed in Figures 2.9 and 2.10, together with an image of the developed reversed-phase plate. The LODs were again estimated on the basis of the amount spotted for both the active ingredients within the co-codamol tablet. Paracetamol was found to have a LOD of 225 $\mu g/cm^2$ and codeine 9 $\mu g/cm^2$. The similar lower limit of detection for paracetamol following chromatographic separation indicates that there is no significant ion suppression due to the presence of excipient components in the undeveloped spot. The drift time for paracetamol (Figure 2.8a)) was 0.90 ms (bin 20) showing good IM reproducibility for the RP-TLC/DESI/IM-MS analysis of paracetamol (Figure 2.7b)). The sharp peak observed in the *m/z* 152 selected ion response for paracetamol (Figure 2.9a)) contrasts with the broad total ion mobility response when all 200 bins were averaged, shown in Figure 2.9b). The mass spectrum obtained by averaging the spectra in the range bin 19-23 (Figure 2.9(c)) has *m/z* 152 as the base peak. Comparing this spectrum with that shown in Figure 2.9d), which is equivalent to the DESI-MS analysis without mobility selection, demonstrates the effectiveness of the orthogonal IM and MS analysis in simplifying and improving spectral quality.

Analysis of the developed codeine spot also shows an increased selectivity for the active ingredient. Figure 2.10 displays the total ion response and the selected ion response for *m/z* 300, assigned to protonated codeine with a drift time of 2.3 ms. The corresponding mass spectra are shown in Figure 2.10(c) and (d). A comparison of the mass spectrum corresponding to the codeine selected ion response with the total ion response shows that the additional separation of ion mobility improves selectivity for codeine.

It should be noted that the paracetamol (Figure 2.9(a)), and codeine (Figure 2.10(a)), selected ion mobility responses were fully resolved by the ion mobility separation.

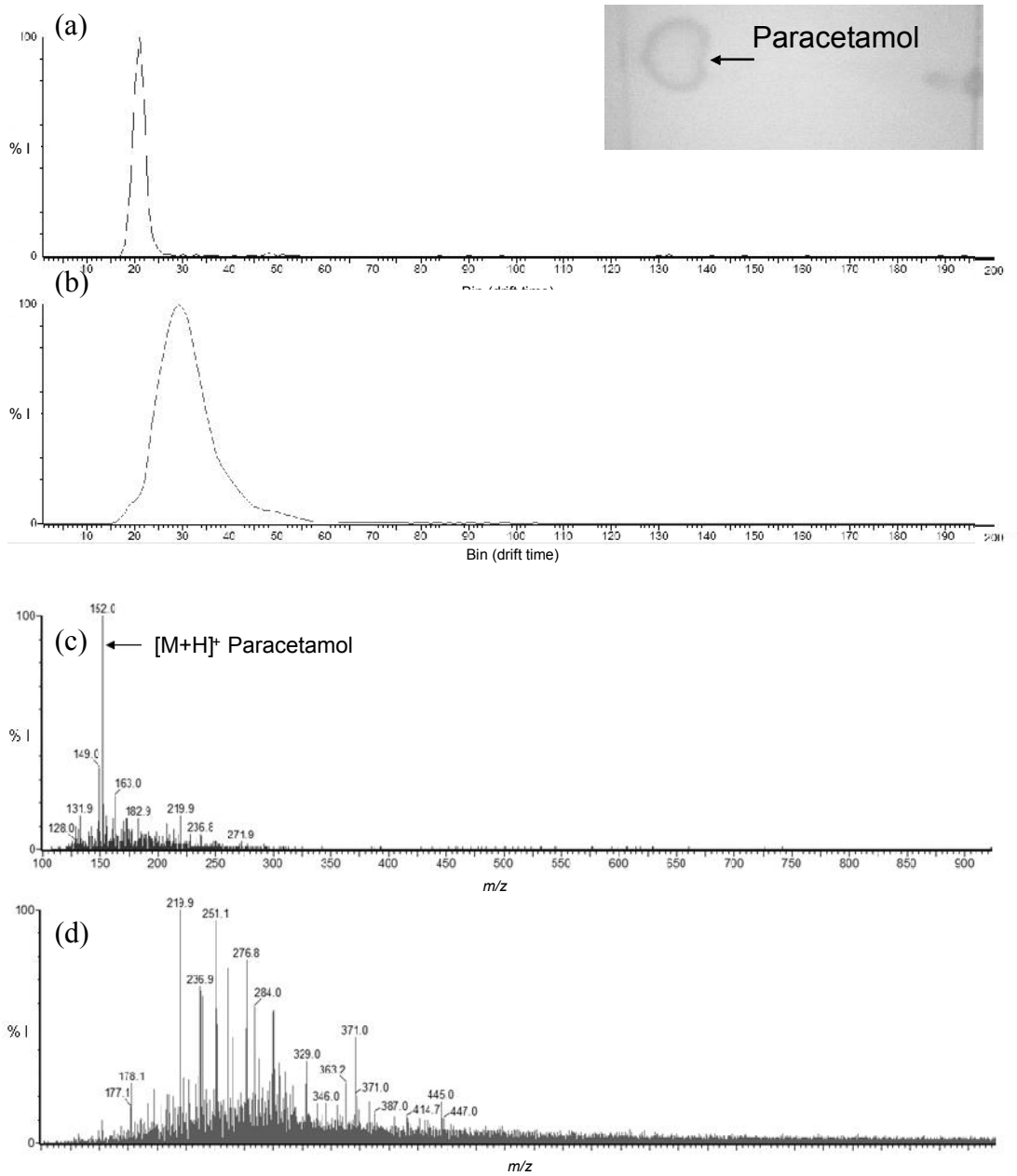

Figure 2.9. Ion mobility spectrum and selected ion mobility response for the DESI/IM-MS analysis of a generic Co-codamol tablet obtained from a RP-TLC plate following chromatographic development, using DESI with a solvent composition of 50:50 (v/v) acetonitrile:water with 0.1% formic acid at a flow rate of 20 µL/min. (a) selected ion response for *m/z* 152 (paracetamol), (b) total ion mobility spectrum, (c) mass spectrum corresponding to the selected ion response for *m/z* 152 (bins 19-23), (d) mass spectrum obtained by combining all 200 bins acquired during the ion mobility separation

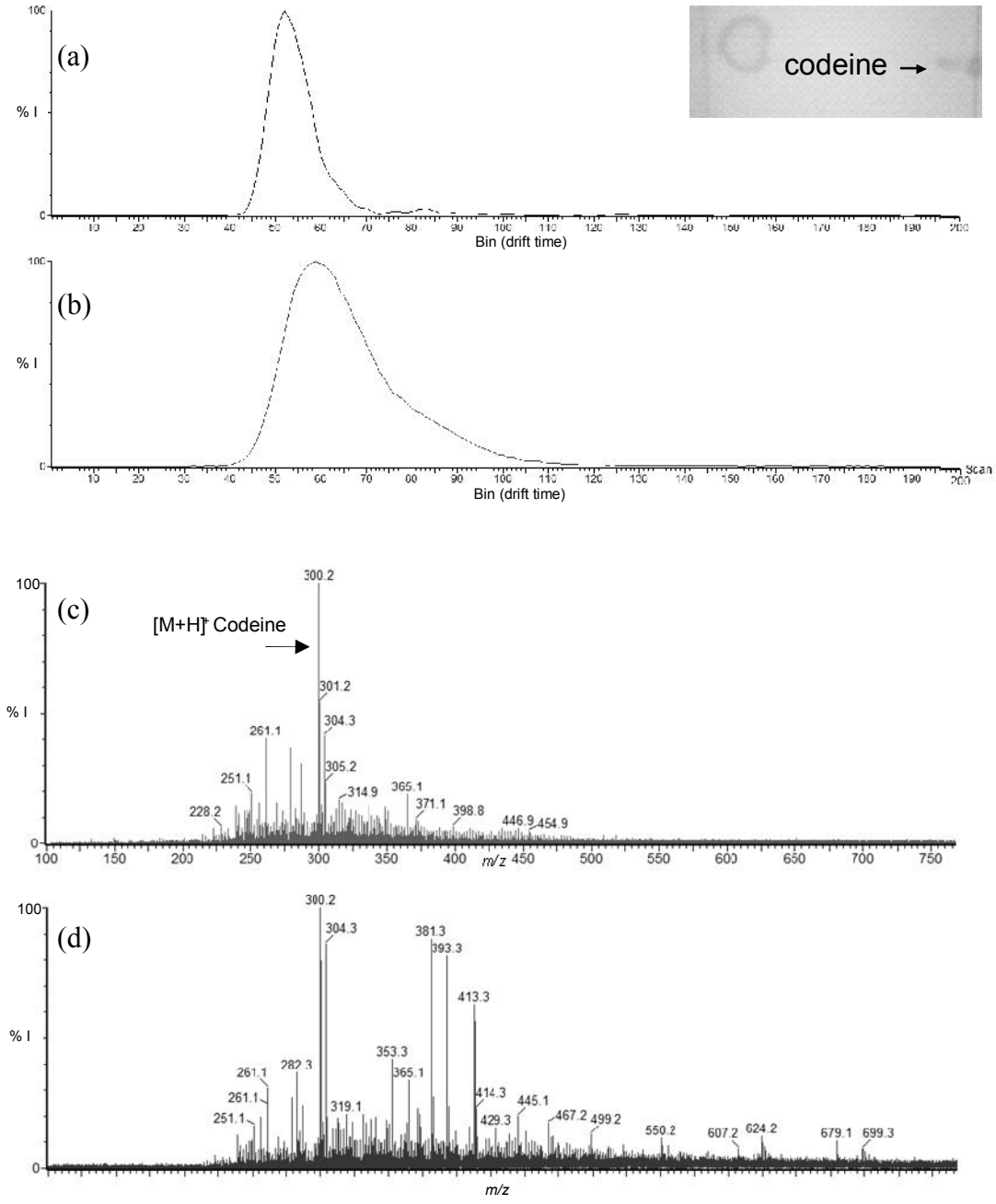

Figure 2.10. Ion mobility spectrum and selected ion mobility response for the DESI/IM-MS analysis of a generic Co-codamol tablet (conditions as Figure 2.4), (a) selected ion response for *m/z* 300 (codeine), (b) total ion mobility spectrum, (c) mass spectrum corresponding to the selected ion response for *m/z* 300 (bins 48-59), (d) mass spectra corresponding to the total ion response.

Method development experiments, although essential are often time consuming and relatively expensive. In this work, the solvent composition of the DESI spray was varied by employing a step gradient to determine the optimum solvent for desorption. Extracted Co-codamol was spotted onto the TLC plate, which was analysed sequentially using three different solvent compositions (90:10, 50:50, 10:90, acetonitrile:water with 0.1% formic acid).

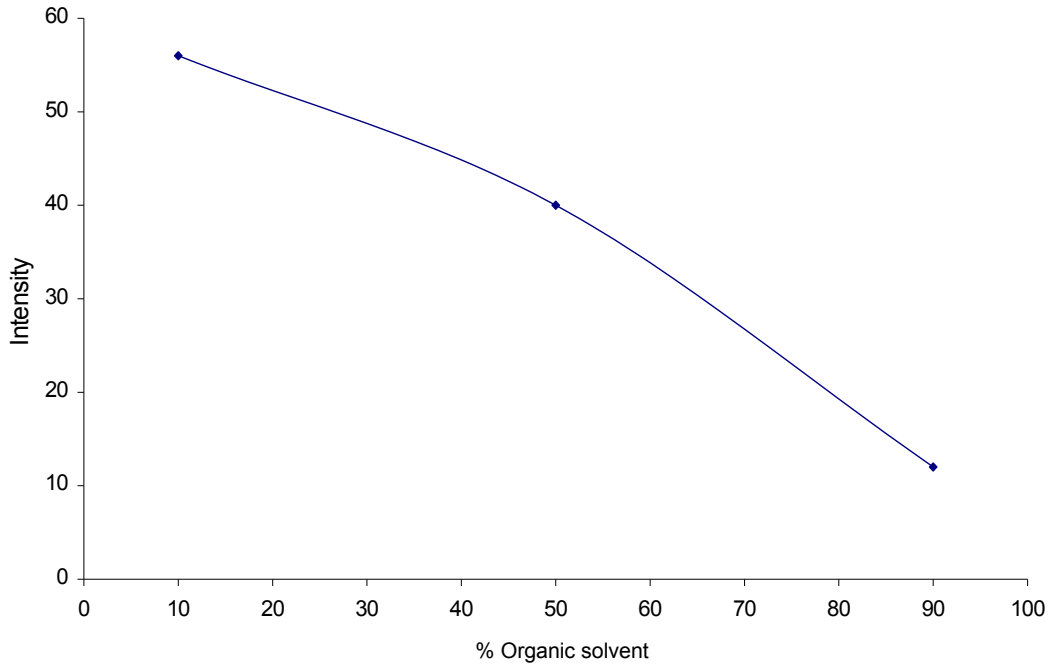

Figure 2.11. RP-TLC/DESI/IM-MS analysis of an extracted Co-codamol tablet employing a step gradient for the DESI analysis (90:10, 50:50, 10:90, acetonitrile:water with 0.1% formic acid): signal response versus % organic solvent for *m/z* 300 (codeine).

Figure 2.11 shows signal response (*m/z* 300) versus % organic solvent. Signal responses were determined from the mass spectra corresponding to the selected ion mobility response for codeine by combining bins across the peak at half height. It can be seen that the signal response for codeine increased signal response as the organic component of the spray was reduced, which correlates with the high aqueous solubility of codeine (1 g in 0.7 mL at 25 °C). A greater % of water would facilitate extraction of codeine from the surface of the TLC plate into the wetted surface layer.

Chemical imaging of the developed codeine spot was carried out by rastering across the spot to obtain a 1-D image. The DESI sampling stage was moved in increments of 0.5 mm in the vertical plane to move the DESI plume across the spot and IM-MS spectra were acquired and accumulated at each point. Ion mobility spectra, consisting of 200 mass spectra (bins), were averaged and the selected ion mobility response for *m/z* 300 extracted from the data.

The image obtained for the mass spectral ion intensity of *m/z* 300 at the drift time for codeine, is displayed in Figure 2.12. The codeine response for the TLC spot shows a maximum intensity at 16 mm corresponding to the R_f of codeine (R_f = 0.16). The 1-D image allows peak areas to be calculated for quantitative analysis by DESI.

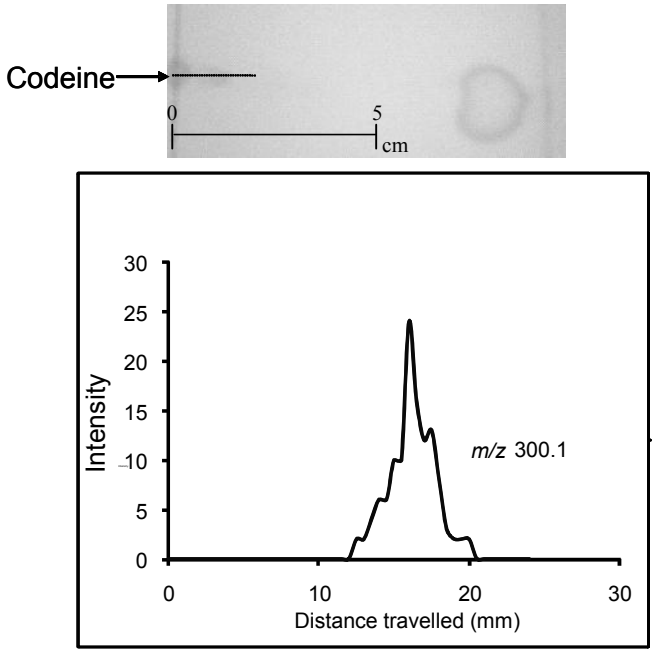

Figure 2.12 RP-TLC/DESI/IM-MS selected ion response for scanned 1-D image, showing signal distribution along a lane of the codeine TLC spot (*m/z* 300 and bin 53). Line represents scan direction.

An alternative to a step gradient is a continuous gradient, Figure 2.13 displays an online continuous gradient DESI-IM-MS analysis of paracetamol and diphenhydramine spotted together on a non-bonded RP-TLC plate. A three minute fast gradient was employed going from 0 to 100% methanol over 3 minutes. The DESI sampling stage was moved in increments of 0.5 mm in the vertical plane to move the DESI plume across the spot, ensuring that the analytes were not depleted during the experiment. It can be seen that the two analytes desorb at different parts of the gradient with the signal intensity for protonated paracetamol decreasing as the percentage of organic increases and the protonated diphenhydramine molecule, intensity increasing with the percentage of methanol (55-70% methanol). The

potential to enhance separation whilst reducing analysis and method development times is shown. The additional elution dimension of gradient DESI coupled to IM-MS enhances the overall separation whilst overcoming the possibility of carry over of the analytes normally associated with conventional LC systems.

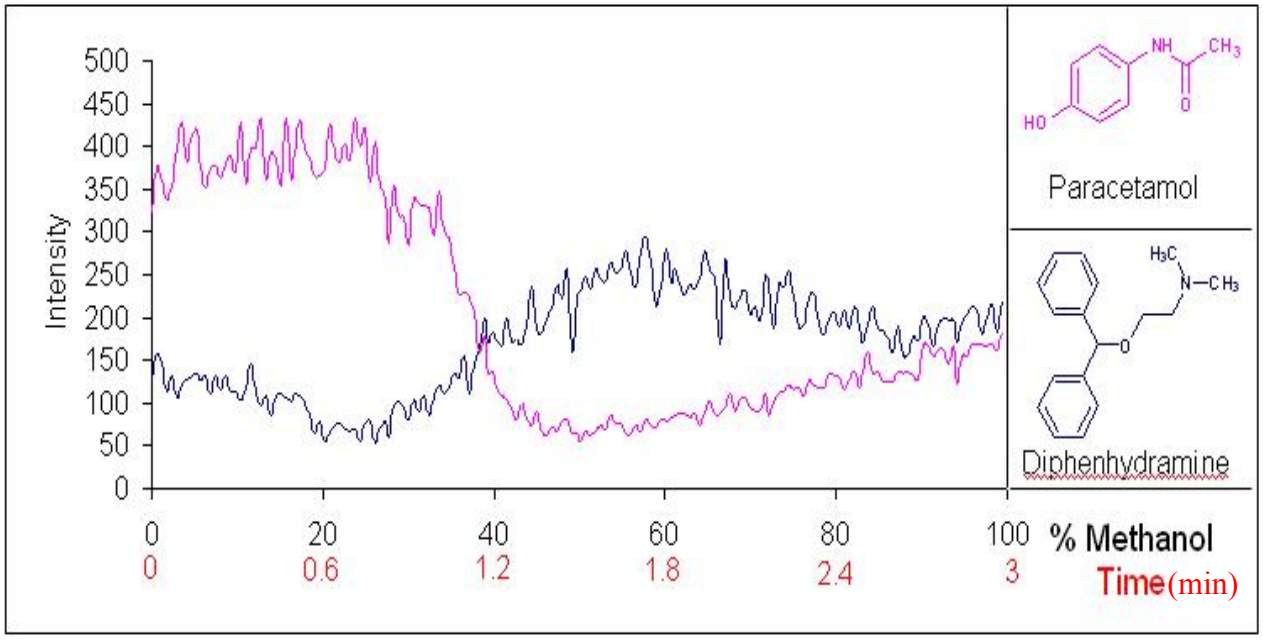

Figure 2.13. RP-TLC/DESI-IM-MS analysis of extracted paracetamol from a co-codamol tablet and diphenhydramine from a generic sleepeaze tablet employing a gradient for the DESI analysis. Signal response versus % organic solvent for *m/z* 152 (paracetamol) and *m/z* 255 (diphenhydramine).

2.5 CONCLUSION

Direct DESI/IM-MS analysis of pharmaceutical drug formulations has shown that this approach may be rapidly employed to characterise and separate analytes of interest from complex samples with little or no sample preparation. Ion mobility provided an increase in selectivity for the active ingredient Loperamide in a tablet formulation by improving spectral quality. IM investigations also demonstrated the ability to separate PDMS oligomers based upon their collision cross sections.

This study has further demonstrated that active pharmaceutical ingredients can be desorbed by DESI directly from non-bonded RP-TLC plates, with or without separation from the excipient components. Variation of the solvent composition of the DESI spray using a step gradient allows the optimisation of the method for analytes can be achieved with reduced development times. Continuous gradient RP-TLC/DESI/IM-MS analysis shows the potential to further enhance separation whilst reducing analysis and method development times. The combined RP-TLC/DESI/IM-MS approach has been shown to have potential to enhance selectivity for analytes compared to DESI/MS alone. Improved mass spectral quality was observed in all cases when IM separation was used in conjunction with mass spectrometry as a result of the orthogonal mobility and mass-to-charge separation.

2.6 REFERENCES

1. Wilson I.D. *J. Chromatogr. A*. 1999; **856**: 429-422.
2. Van Berkel G.J, Ford M.J & Deibel. *Anal. Chem*. 2005; **77**: 1207-1215.
3. Pasilis S.P, Kertesz V, Van Berkel G.J, Schulz M & Schorcht S. *Anal Bioanal Chem*. 2008; **391**: 317-324.
4. Pasilis S.P, Kertesz V & Van Berkel G.J. *Anal. Chem*. 2007; **79**: 5956-5962.
5. Kertesz V & Van Berkel GJ. *Rapid Commun. Mass Spectrom* . 2008; **22**: 2639-2644.
6. Van Berkel G.J, Tomkins B.A & Kertesz V. *Anal. Chem*. 2007; **79**: 2778-2789.
7. Pasilis S.P, Kertesz V, Van Berkel G.J, Schulz M, & Schorcht S. *J. Mass Spectrom*. 2008; **43**: 1627-1635.
8. Lin S.Y, Huang M.Z, Chang H.C & Shiea J. *Anal. Chem*. 2007; **79**: 8789-8795.
9. Van Berkel G.J & Kertesz V. *Anal. Chem*. 2006; **78**: 4938-4944.
10. Ford M.J & Van Berkel G.J. *Rapid Commun. Mass Spectrom*. 2004; **18**: 1303-1309.
11. Ford M.J, Kertesz V & Van Berkel G.J. *J. Mass Spectrom*. 2005; **40**: 866-875.
12. Janecki D.J, Novonty A.L, Woodward S.D, Wiseman J.M & Nurok D. *Journal of Planar Chromatography*. 2008; **21**: 11-14.

CHAPTER 3

The application of liquid chromatography-ion mobility-mass spectrometry for the metabonomic screening of rat urine.

3.1 INTRODUCTION

IM is a separation technique that until recently has not been used in bioanalytical applications, but preliminary studies have shown that using IM can aid the analysis of small molecules in complex systems[1] and IM-MS has proved to be a valuable tool for proteomic research.[2,3,4] The application of IM-MS using an atmospheric pressure drift tube to the analysis of metabolic mixtures has recently been reported for extracts of bacterial cell cultures (*E. coli*) infused directly into the ESI ion source of the spectrometer.[5] IM-MS analysis of the human glycourinome using pre-fractionated urine has also been reported.[6] These studies suggest that LC hyphenated with IM-MS, may have potential for enhancing metabonomic studies without the requirement for additional sample clean-up. This chapter describes a preliminary evaluation of the potential of LC-IM-MS using a low pressure IM drift cell for the analysis of the urinary metabolome without prior extraction. Fast gradient reversed-phase liquid chromatography was used for the rapid elution of endogonous metabolites, prior to electrophoretic separation and *m/z* measurement by IM-MS.

FAIMS technology separates gas-phase ions at atmospheric pressure on the basis of differences in their mobility under high field and low field conditions. This chapter also describes the combination of FAIMS with ion trap mass spectrometry, using electrospray ionisation (ESI), to afford gas-phase analyte characterisation based on mass-to-charge (*m/z*) ratio and differential mobility (characteristic compensation voltages (CV)). Selectivity offered by FAIMS-MS is exploited in this study for the metabonomic analysis of rat urine using a cylindrical FAIMS configuration (Thermo Fisher Scientific) combined with linear ion trap mass spectrometry. To overcome the problems of coupling liquid chromatography (LC) to FAIMS resulting from the slow

CV scan speed of the cylindrical FAIMS device, six compensation voltages in the range -12V to -22 V were chosen to cover the range of metabolite differential mobility. Metabonomics provides rich datasets for systems biology necessitating the use of bioinformatics. In this study sample data sets were analysed using a stepwise artificial neural network (ANNs) analysis to give rank orders of ions of interest for each characteristic CV. Principal component analysis was also carried out to test reproducibility using quality control samples.

3.2 CHAPTER THREE AIMS AND OBJECTIVES

The purpose of the work presented in this chapter was to explore novel methods for the metabonomic study of urine employing drift tube ion mobility and FAIMS as an additional separation technique to afford additional selectivity for analytes of interest. The specific objectives were:

- To investigate the potential of drift tube IM combined with fast liquid chromatography and mass spectrometry for the analysis of metabonomic samples.

- To investigate the potential of FAIMS combined with fast liquid chromatography and mass spectrometry for the analysis of metabonomic samples.

- To carry out a full metabonomic investigation to distinguish age groups of rats via the analysis of urinary profiles obtained by LC-FAIMS-MS.

3.3. EXPERIMENTAL

3.3.1 Chemicals

Methanol (HPLC grade), acetonitrile (HPLC gradient grade) and formic acid (99.5% Puriss grade) were purchased from Thermo Fisher Scientific (Loughborough, UK). Distilled and deionised water was obtained in-house using a Triple red water purification system (Triple red, Long Crendon, UK).

3.3.2 IM-MS and LC-IM-MS analysis

All experiments were carried out employing a prototype IM-Q-TOF-MS (Waters Corporation, Manchester), which is shown schematically in Figure 2.2 (Chapter 2) Ions from the ESI source were directed into the trap region at the head of the ion mobility drift cell, which was operated in the pressure region of 1.0 to 3.0 Torr N_2. Ions were gated into the drift cell using a gate electrode pulse (3.50 V, 200 µs pulse width and 15 ms pulse period). The IM drift tube consisted of a multi-plate ion guide (15.2 cm in length) to which a voltage gradient (14.24 V/cm and a supplement RF voltage 3.8 V) were applied to facilitate separation of ion species by relative mobility. Ions passing through the drift region were then directed into the reflectron TOF mass analyses. Ion mobility spectra were acquired by collecting data from 200 TOF pushes (65 µs per bin) and plotting drift time (scan) against mass-to-charge ratio (*m/z*). IM-MS data were typically accumulated for 5 s, with a 2 s interscan delay. Initial studies using direct introduction of urine samples into the IM-Q-TOF-MS spectrometer

without chromatographic separation were performed by infusing the aliquots of the prepared urine into the ESI ion source at 10 µl/min using the integrated syringe pump.

Liquid chromatography was performed on a Waters Alliance 2790 chromatograph (Waters Corporation, Manchester, UK) fitted with a Symmetry® (Waters Corporation, Manchester, UK) C18 column (2.1 x 50 mm, 5 µm). The LC system was coupled to the ESI ion source of the IM-Q-TOF-MS spectrometer. Urine samples (50 µl injected) were eluted with the following gradient: 100% A (0-2 min), increased to 100% B (2-5 min) and then to 100% A (5-8 min), where A = 0.1% aqueous formic acid and B = 0.1% formic acid in acetonitrile. The mobile phase flow rate was set to 0.2 mL/min. Electrospray ionization conditions for the MS, with the ion source operated in positive ion mode were: capillary voltage, 3.5 kV; cone voltage 60 V; source temperature 120°C; desolvation gas, N_2 gas flow 250 l/hr; desolvation gas temperature, 180°C. Masslynx version 4.1 (Waters Corporation, Manchester, UK) was used to control the LC and IM-MS instrument and for data acquisition. Data mining was carried out using DriftScope version 1.0 (Waters Corporation, Manchester, UK).

3.3.3 LC-FAIMS-MS analysis

The FAIMS interface (Thermo Fisher Scientific, USA. Figure 1.3 (Chapter 1)) was located between the ESI source and the linear ion trap mass spectrometer, LTQ (Thermo Fischer Scientific, USA). The FAIMS interface consists of inner and outer cylindrical electrodes to which dispersion and compensation voltages are applied, is shown schematically in Figure 1.4 and 1.5 (Chapter 1).

Liquid chromatography was performed on a Thermo Surveyor Liquid chromatography system (Thermo Fisher Scientific, USA.) fitted with an Atlantis® T3 5 µm (2.5 x 50 mm) column (Waters Corporation, Manchester, UK). The LC system was coupled to the ESI ion source of the FAIMS/LTQ spectrometer. Urine samples (20 µl injected) were eluted with the following fast gradient: 5% B increased to 20% B (0- 0.5 min), held at 20% B (0.5-3.00 min), increased to 70% B (3.00-6.00), held at 70% B (6.00-8.00). Where A = 0.1% aqueous formic acid and B = 0.1% formic acid in acetonitrile. Heated electrospray ionization conditions for the MS, with the ion source operated in positive ion mode were: spray voltage: 5.5 kV, vaporizer temperature 400 °C, sheath gas pressure (N_2): 12 units, capillary voltage 25 kV, capillary temperature 270 °C. The FAIMS experimental conditions after optimisation were dispersion voltage -5000 V, drift gas 50:50 mix of He and N_2 at a flow rate of 3.75 L/min, outer bias voltage 25 V, inner electrode temperature 70 °C, outer electrode temperature 90 °C. The compensation voltage was cycled between the following values of, -12, -14, -16, -18, -20 and -22 V was selected. FAIMS parameters and heated ESI source parameters are summarised in Table 3.1. Xcalibur

2.0.7 (Thermo Fisher Scientific, USA) was used to control the LC, FAIMS and MS system. Excel (2003, Microsoft corporation) was employed to construct mass-to-charge tables for principal component analysis (PCA) and artifical neural network analysis (ANNs). Spectra in each run were combined with the plotting style set to stick, data was then converted to centroid data to provide spectra lists consisting of *m/z* and ion intensity values. PCA and ANNs analysis was carried out by Andrew Barnett and Professor Graham Ball of the Nottingham Trent University, Nottingham, UK using Statistica version 8 (Statsoft).

Table 3.1 FAIMS and heated ESI source parameters including defined mass parameters of the mass spectrometer.

FAIMS parameters	**Heated ESI probe**	**Define mass parameters**
Outer bias voltage: 25 V	heater temp : 20 °C	mass range : normal
Dispersion voltage :-5000 V	sheath gas flow rate : 12 L/min	scan rate : normal
Inner electrode temperature: 70 °C	aux gas flow rate : 5 L/min	scan type : full
	sweep gas flow rate : 0 L/min	microscans : 1 s
	spary volt : 5.5 kV	max inject time :10 s
	capillary temp : 270 °C	source fragmentation : off
	capillary voltage : 25 kV	first mass : 150 *m/z*
	tube lens : 100 V	last mass : 2000 *m/z*

3.3.3.1 Sample preparation

Urine samples from a group of rats (n=45) male Wistar-derived rats provided by AstraZeneca (Alderley Park, Macclesfield, UK) were centrifuged at 13 000 rpm for 5 minutes to remove particulates and then frozen to -80°C prior to analysis. Aliquots of each urine sample were combined to provide a pooled sample which was further split to provide a multi-sample QC set. QC preparation consisted of firstly centrifuging the urine samples, a 50 µL aliquot from each sample was then taken and pooled to give a total volume of 3.45mL of quality control sample (50 uL x 69 = 3.45 mL).

Table 3.2 Urine sample information

** AP rats = Alderly Park (wistar-derived))*

Number of samples	Date Taken	Rat Type	Age
6	18:09:09	AP Rats *	4wks
6	19:09:09	AP Rats	4wks
6	02:10:09	AP Rats	6wks
6	16:10:09	AP Rats	8wks
6	30:10:09	AP Rats	10wks
5	13:11:09	AP Rats	12wks
5	27:11:09	AP Rats	14wks
5	11:02:09	AP Rats	16wks

3.3.3.2 Sample run order and treatment

All samples were run in a random order with quality control samples (QC) to provide a means of monitoring overall system and experimental performance. QC samples where run at the beginning, end and randomly throughout the experiment (randomise via Excel, 2003 Microsoft corporation). System conditioning consisted of 5 injections prior to the first QC run as the first several runs have previously shown most variance due to column and FAIMS equilibration. The sample run order was as shown in Table 3.3

Table 3.3 Randomisation and sample run order including; QC's, blanks and conditioning runs

Sample number	Date taken	Age	Gender
Calibration check			
Blank			
conditioning			
conditioning			
conditioning			
Conditioning			
Conditioning			
QC 1			
25	30:10:09	10 wks	M
30	30:10:09	10 wks	M
22	16:10:09	8 wks	M
45	11:02:09	16 wks	M
35	13:11:09	12 wks	M
12	19:09:09	4 wks	M
Blank			
QC 2			
21	16:10:09	8 wks	M
19	16:10:09	8 wks	M

9	19:09:09	4 wks	M
5	18:09:09	4 wks	M
41	11:02:09	16 wks	M
16	02:10:09	6 wks	M
Blank			
QC 3			
32	13:11:09	12 wks	M
36	27:11:09	14 wks	M
17	02:10:09	6 wks	M
4	18:09:09	4 wks	M
24	16:10:09	8 wks	M
3	18:09:09	4 wks	M
Blank			
QC 5			
1	18:09:09	4 wks	M
40	27:11:09	14 wks	M
37	27:11:09	14 wks	M
6	18:09:09	4 wks	M
29	30:10:09	10 wks	M
15	02:10:09	6 wks	M
Blank			
QC 6			
31	13:11:09	12 wks	M
39	27:11:09	14 wks	M
7	19:09:09	4 wks	M
28	30:10:09	10 wks	M
18	02:10:09	6 wks	M
33	13:11:09	12 wks	M
Blank			
QC 7			
42	11:02:09	16 wks	M
23	16:10:09	8 wks	M
27	30:10:09	10 wks	M
20	16:10:09	8 wks	M
8	19:09:09	4 wks	M
43	11:02:09	16 wks	M
Blank			
QC 8			
44	11:02:09	16 wks	M
11	19:09:09	4 wks	M
2	18:09:09	4 wks	M
26	30:10:09	10 wks	M
14	02:10:09	6 wks	M
13	02:10:09	6 wks	M

Blank			
QC 9			
34	13:11:09	12 wks	M
10	19:09:09	4 wks	M
38	27:11:09	14 wks	M

3.4 RESULTS AND DISCUSSION

3.4.1 An approach to enhancing coverage of the urinary metabonome using liquid chromatography-ion mobility-mass spectrometry

Initial experiments were carried out by directly infusing aliquots of urine into the ESI-IM-Q-TOF-MS spectrometer as described in the experimental section, pages 104-105. However, the salt component of the urine caused significant ion suppression in the electrospray ion source (data not shown) and hence liquid chromatography was employed to reduce these suppression effects. The urinary metabolic profile is composed mainly of relatively polar/ionic substances, which must be retained on the LC column whilst the salts elute prior to mass spectrometry analysis. In order to obtain the best possible retention of these polar metabolites, we therefore used a gradient separation where the initial segment (0-2 min) was entirely aqueous formic acid, followed by a rapid increase (over 5 min) to 100% acetonitrile. The effectiveness of the LC column for improving spectral quality is shown in the LC-ESI-IM-MS data for a pooled urine sample obtained from the Wistar-derived rats, shown in Figure 3.1. The peaks in the LC chromatogram correspond to the IM spectra accumulated during the LC run (Figure 3.1(a)). The salt component was eluted in less than 1 minute (Figure 3.1 (a)) showing ion suppression effects and an increased noise in the mass spectrum (Figure 3.1 (b)), leaving the metabolites and other components of the urine to be eluted in the region 3-8 minutes, free from salt interferences (Figure 3.1(c)).

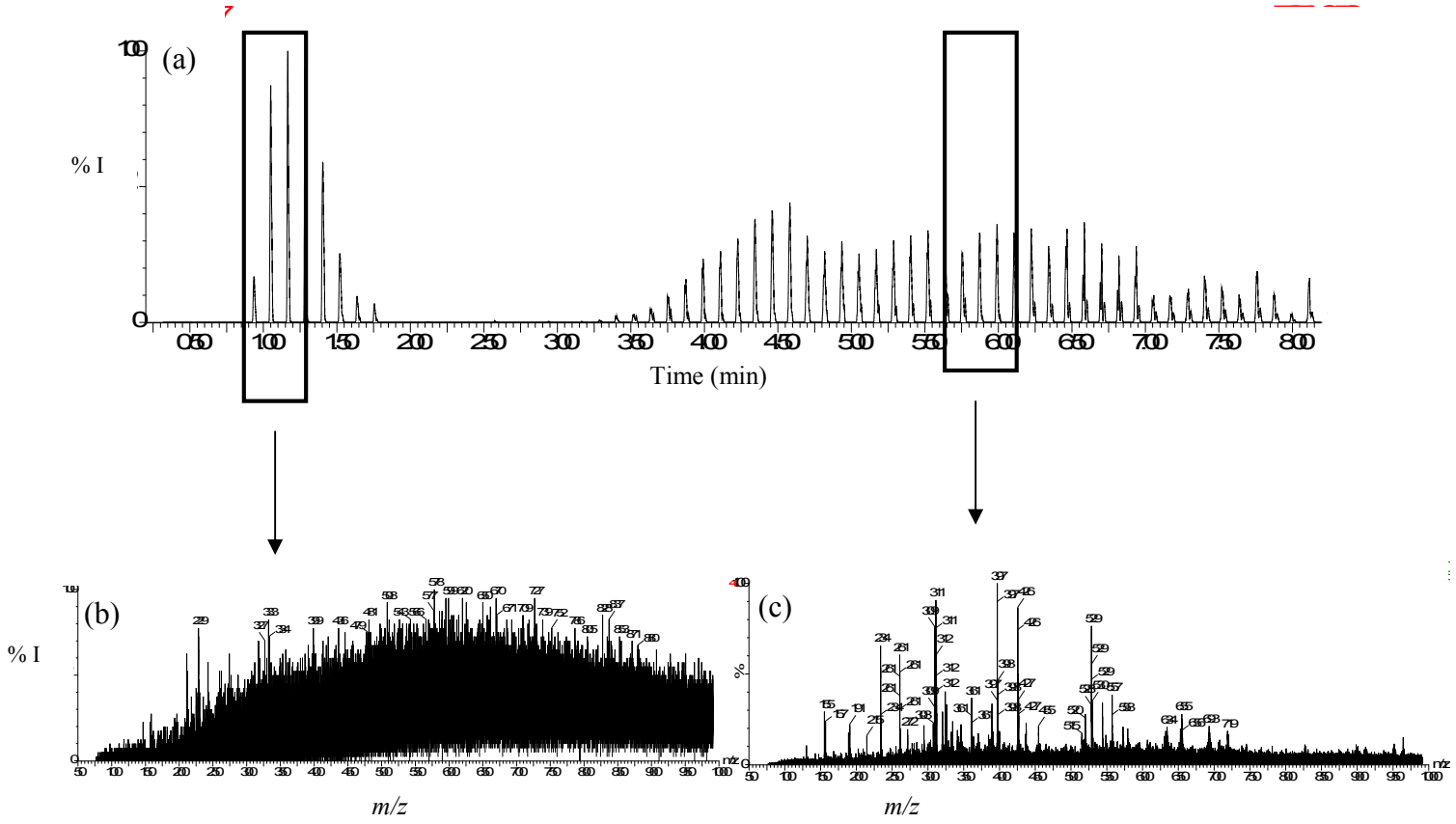

Figure 3.1 (a) LC chromatogram showing accumulated IM spectra derived from the LC-IM-MS analysis of urine obtained from male Wistar-derived rats, (b) mass spectrum corresponding to retention time window 1.0 – 1.3 min, (c) mass spectrum corresponding to retention window 5.5 – 6.0 min.

The effect of introducing an IM separation in tandem with LC and MS analysis of urinary metabolites is shown in Figure 3.2. In this experiment, data were acquired as nested data sets, with mass spectra (65 μs/scan) and IM spectra (~13 ms) scanned repetitively throughout the LC run. Spectra were accumulated to yield 200 mass spectra and one ion mobility spectrum every 7 s. The ion mobility drift time is plotted

as ‘bins’, where each bin corresponds to an acquired mass spectrum. The nested data acquisition of IM and MS data results in an analysis incorporating a gas-phase electrophoretic separation of the ESI generated ions on the basis of charge state and collision cross section (i.e. size and shape), between the reversed-phase chromatography and mass analysis, all within the timescale of the LC-MS run (Figure 3.2(a)). IM has a relatively poor resolving power, with a typical full width at half height (FWHH) resolution of 10, corresponding to ~500 theoretical plates in total. However, peak capacity is increased in LC-IM-MS, because the IM separation is orthogonal to that of LC retention and mass-to-charge ratio.

The mass spectrum shown in Figure 3.2(b) was generated by summing all 200 mass spectra in each IM scan and is therefore equivalent to the mass spectrum for LC-MS analysis without IM separation. Figure 3.2(c) shows the IM spectrum summed over all *m/z* values and corresponds to LC-IM analysis without mass separation. The enhanced separation afforded by the combined IM-MS analysis is shown in the 2-D plot of ion drift time (bins) vs *m/z*, which is presented in Figure 3.2(d) for data averaged over the whole LC run (0-7 min). The bands of colour reflect the intensity of the ions with red representing the highest intensity and blue/white the lowest intensity.

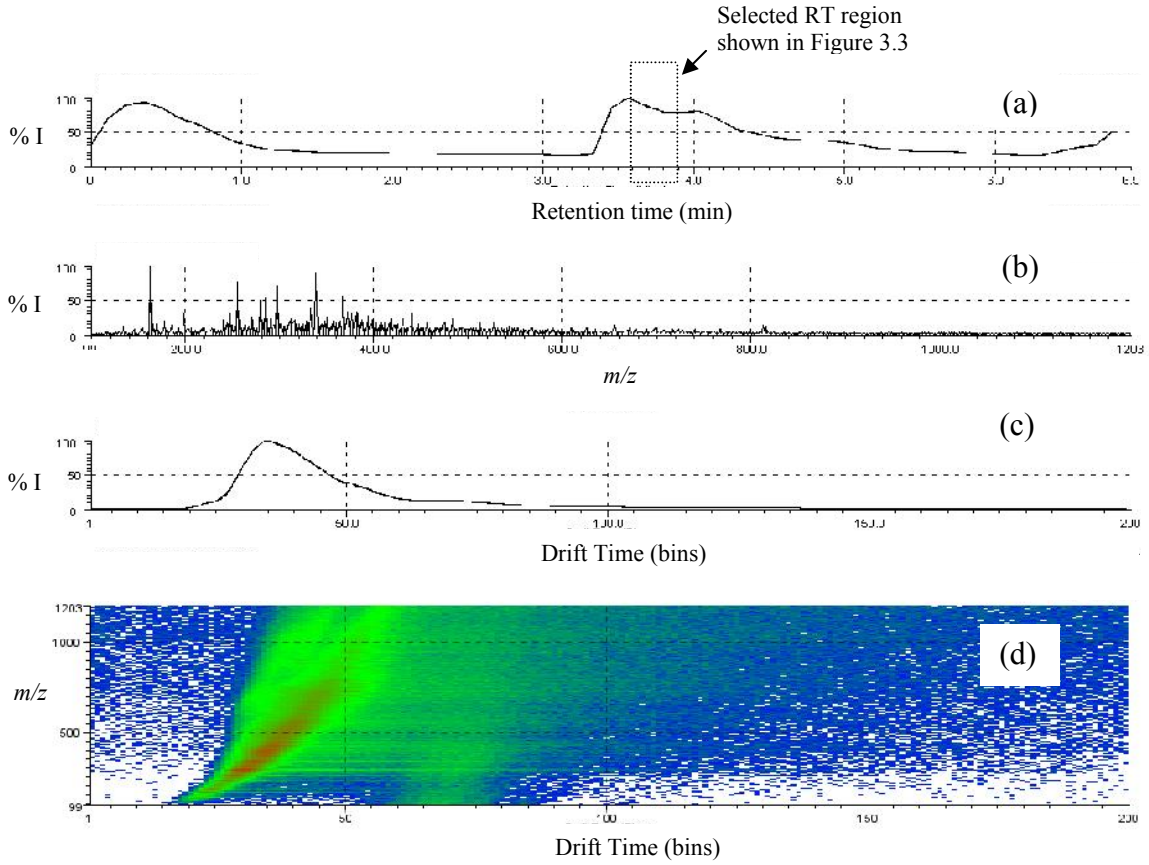

Figure 3.2 LC-IM-MS analysis of urine obtained from male Wistar-derived rats, (a) LC chromatogram, (b) the mass spectrum generated by summing all 200 mass spectra in each IM scan during the LC run, (c) total ion mobility spectrum summed over all *m/*z values, (d) 2D plot of drift time (bins) versus *m/z* plot for the full data set.

Analysing these multidimensional LC-IM-MS data sets presents a challenge for multivariate statistical techniques commonly used in comparative metabonomics, since conventional statistical theory requires at least twice as many sample replicates

as the number of dimensions in the data. Advanced bioinformatic techniques are required, such as artificial neural networks, which are capable of handling complex, multidimensional and non-linear data sets.[7] An alternative approach is to reduce the complexity of the data by selecting retention time or drift time windows for analysis, or by other pre-treatment strategies.[8] A retention time region (3.6 – 3.9 min) from the LC run was selected because of the many metabolites eluting in this time window and Figure 3.3 shows the IM-MS data associated with this region.

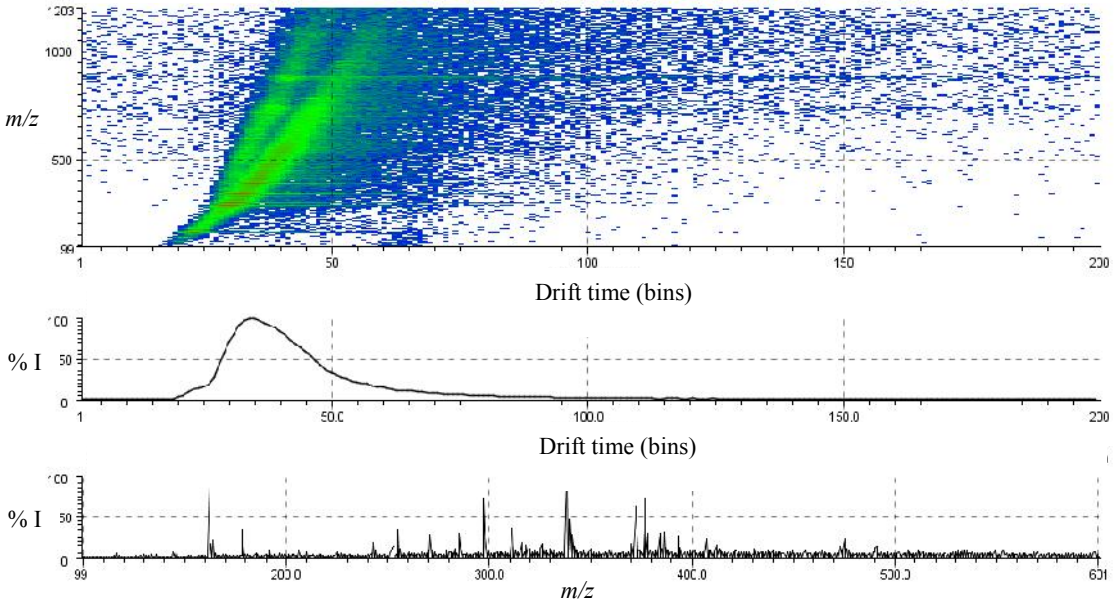

Figure 3.3 (a) Drift time (bins) versus *m/z* plot of selected retention window 3.6-3.9 minutes derived from the LC-IM-MS analysis of rat urine, (b) total ion mobility spectrum corresponding to retention time window 3.6-3.9 minutes, (c) mass spectrum corresponding to total ion mobility spectrum of retention time window 3.6-3.9 minutes.

There is a significant reduction in background noise (indicated by an increase in blue/white shading) and an overall simplification of the drift time vs *m/z* analytical space. The IM and MS spectra shown in Figure 3.3(b) and 3.3(c) were obtained by averaging the drift time and *m/z* data shown in Figure 3.3(a). The resulting spectra (Figure 3.3(b) and 3.3(c)) therefore correspond to those expected for LC-IM (Figure 3.3 (b)) and LC-MS (Figure 3.3(c)) separations respectively.

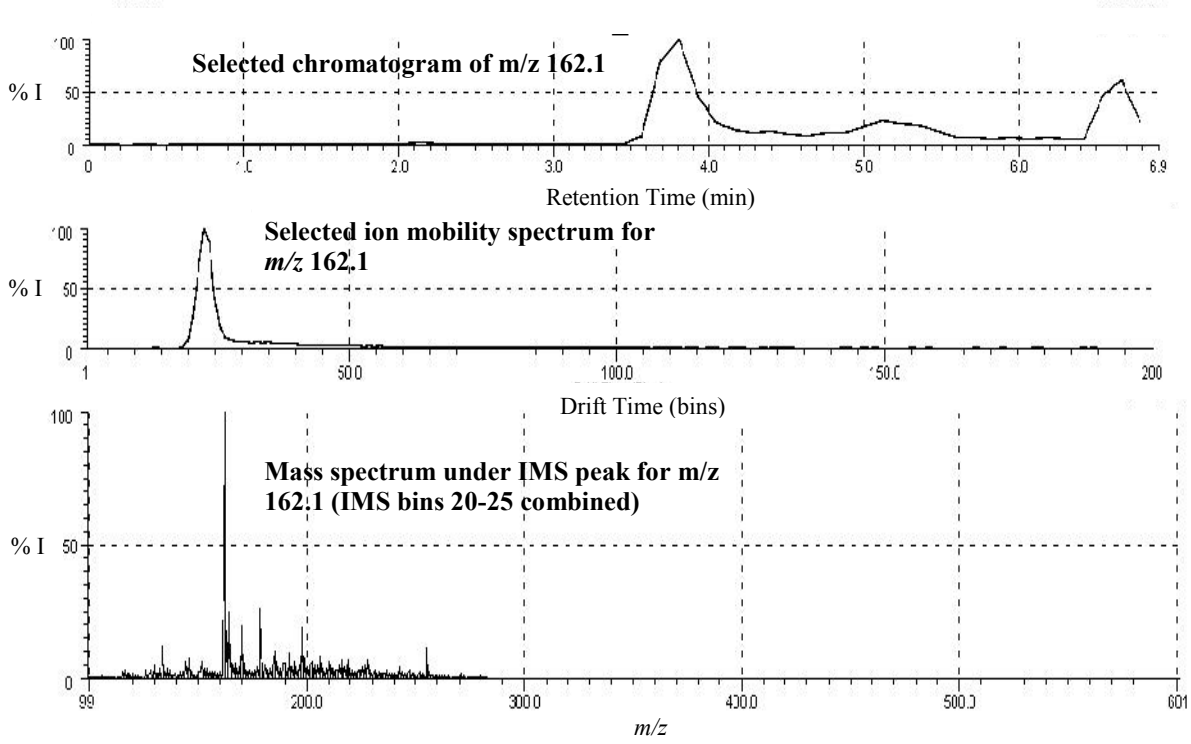

Figure 3.4 (a) Extracted ion chromatogram (XIC) for *m/z* 162.1 obtained from the LC-IM-MS analysis of male Wistar-derived rat urine, (b) selected ion mobility spectrum of *m/z* 162.1, corresponding to the selected retention time window 3.6-3.9 min, (c) mass spectrum corresponding to selected ion mobility spectrum for *m/z* 162.1 (IM bins 20-25 combined).

It is possible to enhance selectivity for target analytes by utilising the orthogonal separation of the LC, IM and MS dimensions. This is illustrated in Figure 3.4 for the *m/z* 162.1 ion, assigned to the endogenous metabolite carnitine ($C_7H_{15}NO_3$)[9]. The extracted ion chromatogram for this ion is shown in Figure 3.4(a). The ion intensity reaches a maximum at a retention time of 3.8 min and the selected ion mobility response for the *m/z* 162.1 ion in the ion mobility spectra acquired in the retention time window 3.6 – 3.9 min is shown in Figure 3.4(b). The sharp peak observed in the drift time region corresponding to bins 20-25 contrasts with broad total ion mobility response observed in the same retention time window when all 200 bins were averaged, seen in Figure 3.3(b). The mass spectrum obtained by averaging the spectra in the region 20-25 bins (Figure 3.4(c)) has *m/z* 162 as the base peak. Comparing this spectrum with that shown in Figure 3.3(c), which is equivalent to the LC-MS analysis without mobility selection, demonstrates the effectiveness of the orthogonal LC, IM and MS analysis in simplifying and improving spectral quality. Confidence in the assignment of targeted or unknown species is increased by the presence of an ion of the correct *m/z* at the expected IM drift time and the LC retention time associated with a metabolite.

3.4.2 Metabonomic screening of rat urine using high field asymmetric waveform ion mobility spectrometry combined with liquid chromatography-linear ion trap mass spectrometry

Optimisation of the FAIMS system was initially carried out to ensure that the filtering effect of the FAIMS was utilised allowing the removal of interferences, whilst maintaining optimum ion transmission of the analytes of interest. Due to the slow CV scan speed of the FAIMS separation it was not possible to scan the FAIMS spectrum (> 1min for full CV range) within the time scale of a typical chromatography peak. Experiments therefore, consisted of injections of urine through the LC-FAIMS-MS system at fixed CV values. The CV range where most urinary analytes where transmitted to the MS was found to be -12 to -22 V. Six fixed CV values were chosen; -12.0, -14.0, -16.0, -18.0, -20.0 and -22.0 and the FAIMS device was set to cycle between these values throughout the experiment ensuring all separations were conducted within the time limit of a single chromatography peak. Further experiments were carried out to determine the experimental conditions for the both the FAIMS and MS system to ensure optimum signal intensity and transmission. Validation experiments consisted of six urine injections (after column and system conditioning) with four ions selected across the *m/z* range (*m/z* 104.1, 118.2, 175.2, 309.3). Ion intensities for these ions over the six runs were recorded and compared. A decrease in ion intensity was observed as the FAIMS front plate became increasingly contaminated, but an increase in the desolvation flow rate significantly improved the stability of the ion intensities. % Relative standard deviations of the ion intensities *m/z* 104.1, 118.2, 175.2, 309.3 were 112.5, 37.5, 62.5 and 35 % respectively showing reasonable reproducibility. A FAIMS acceptance test was carried out before the start

of experiments ensuring the FAIMS device was producing acceptable CV values for known ions, Caffeine, *m/z* 195 (CV range -5 to -10), ultramark, *m/z* 524 (CV range -20 to -28) and MRFA, *m/z* 1522 (CV range -10 to -16) recorded CV values of -8.47, -21.71, and -11.87 respectively.

In order to obtain the best possible retention of polar metabolites, a gradient separation was employed where the initial segment (0-2 min) was entirely aqueous formic acid, followed by a rapid increase (over 5min) to 100% acetonitrile. The effectiveness of the LC column for improving spectral quality was previously shown in Figure 3.1. The LC separation further enhances the overall analysis by reducing the number of coeluting analytes entering the FAIMS -mass spectrometer ion source, hence reducing ion suppression. Sample responses can depend on the sample run order, as the source of the mass spectrometer becomes contaminated over time leading to sensitivity changes. Randomisation of the sample run order was used to ensure that all the experimental samples and subsequent statistical analysis of the data did not show systematic bias. All experimental samples were randomised throughout and the sample run order is displayed in (Table 3.2.) A further challenge as discussed above is the potential for the analytical system to change with time. A number of approaches have been suggested to ensure that the results obtained are valid and, in this study, the use of quality control samples (QCs) was employed. The QCs consisted of a pooled urine sample prepared, by taking aliquots of the samples to be analysed as previously discussed, section 3.3.3.1.

The fractionation of the rat urinary metabonome afforded by FAIMS can be seen in Figure 3.5. Different ions are detected at the different CV values showing the potential to increase the available analytical space via FAIMS analytes of separation. Three of the six CV values are displayed (-12, -18 and -22). In each mass spectrum a different base peak and overall ion compliment is seen, with base peaks of *m/z* 76, 231 and 187 for CVs -22, -18 and -12 respectively.

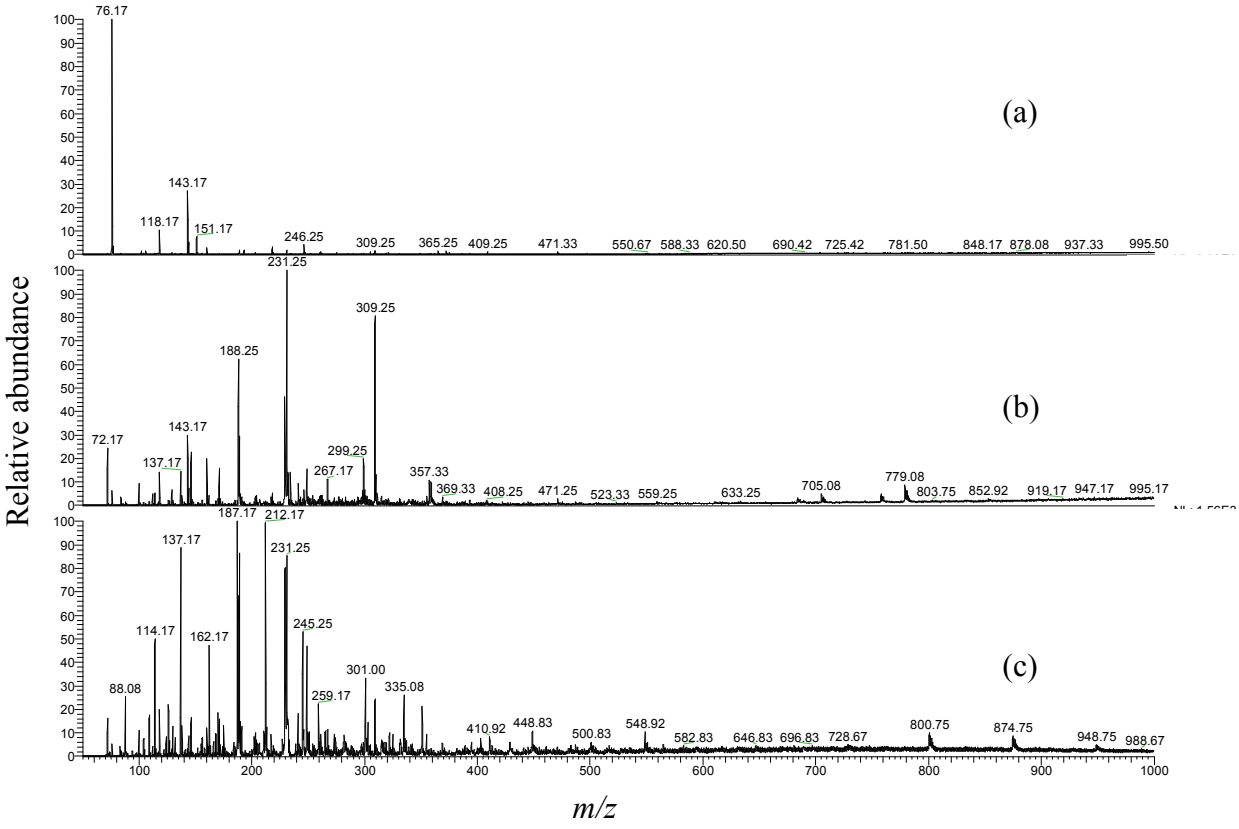

Figure 3.5 LC-FAIMS-MS analysis of rat urine. Mass spectra showing three selected compensation voltage values (a) -22 (b) -18 and (C) -12.

It is possible to enhance selectivity for target analytes by utilizing the orthogonal separation of the LC, IM and MS dimesions. This is shown in Figure 3.6 for the *m/z* 309 ion. The total FAIMS mass spectrum obtained by combining mass spectral data from all six CV scans in the FAIMS run is displayed in Figure 3.6(a), which is equivalent to the LC/MS analysis without FAIMS selection and shows a large number of ions. In contrast, when the mass spectrum obtained by selecting a retention time 3.56 min and CV value of -16V (Figure 3.6 (b)) is compared with the total FAIMS spectrum, enhanced selectivity for *m/z* 309 is achieved with the selected *m/z* 309 as the base peak. Overall the spectral simplification and reduction in background noise demonstrated the effectiveness of the orthogonal LC, FAIMS and MS analysis for improving spectral quality for targeted analytes.

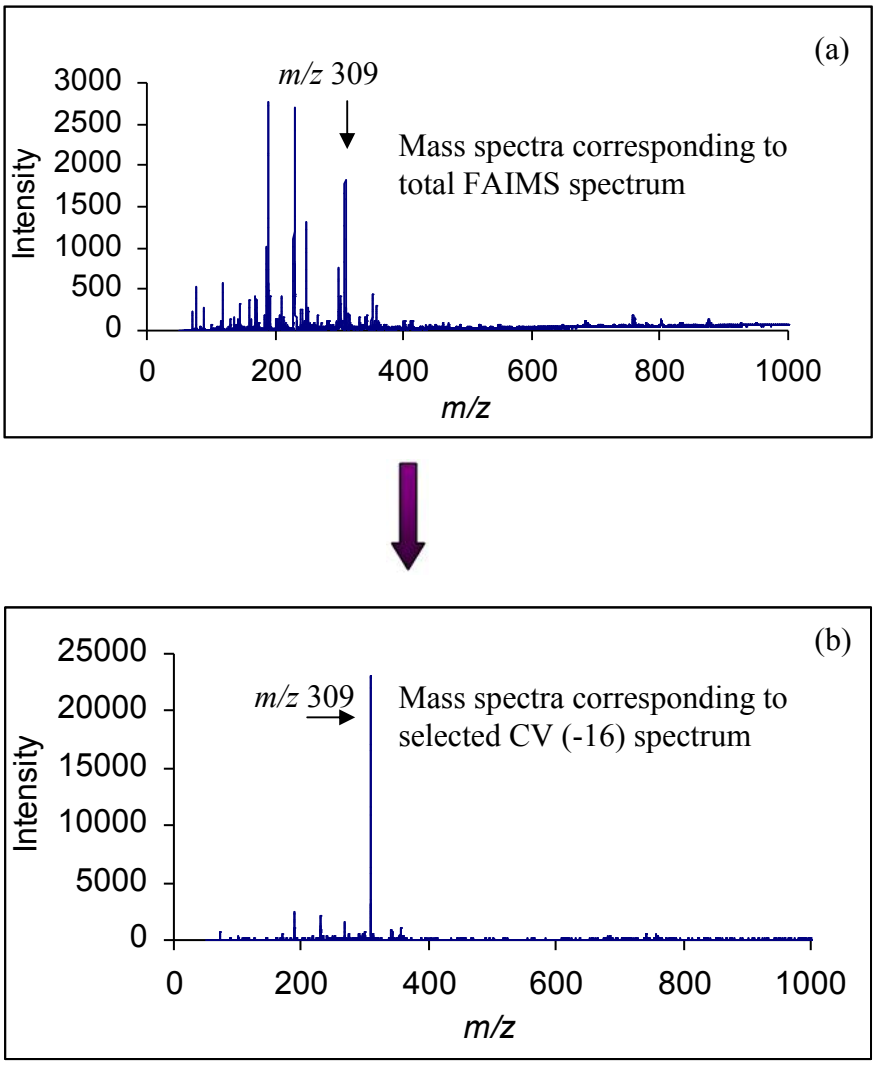

Figure 3.6 (a) Mass spectra corresponding to total FAIMS spectrum derived from the analysis of rat urine employing LC-FAIMS-MS generated by combining all cv values and (b) mass spectrum corresponding to selected CV value of -16V and a retention time 3.54 min.

The study of metabonomics depends on the generation of global metabolite profiles and by recording changes in the concentrations of low molecular weight metabolites. Such investigations generate large volumes of data. Data mining methods are therefore required to obtain insights into biological processes such as ageing. During this metabonomic study of rat urine, Statistica version 8 (Statsoft) was employed for data analysis.

The ability to demonstrate that metabonomic data is of high quality is crucial if studies are to provide biological insights into the processes of development, disease and toxicity. Demonstrating that variability of metabonomic data generated is within acceptable limits is essential, the use of quality control samples to define the reproducibility of data with quality control measures was required at all stages of the analytical process. To test reproducibility, preliminary statistical analysis of a biological QC sample data set by principal component analysis (PCA) was employed to assess the stability of the analytical method. If all QC samples group then the system is stable. QC samples were generated as described in section 3.3.3.1 to provide a representative mean sample containing all the analytes that will be encountered during the analysis.

Figure 3.7 shows the PCA results with QC samples 1 to 4 indicating good reproducibility. However, QC 5-6 did not show characteristic clustering compared to QC 1 to 4. The instrumental response appears to have drifted towards the end of the experiment with QC samples 5 and 6 showing drift away from the other QCs, indicating that as the experiment progresses the reproducibility decreases. A possible explanation is the effect of contamination of the FAIMS device over time reducing

the signal intensity and the compliment of ions transferred into the FAIMS device. The clustering of the main group of QCs suggests the majority of the data is valid and worth further study. Artificial neural networks (ANNs) was employed for data analysis. Both the PCA and ANN analysis was carried out by Andrew Barnett and Professor Graham Ball of the Nottingham Trent University, UK. Artificial neural networks are a form of machine learning from the field of artificial intelligence with proven pattern recognition capabilities and have been utilized in many areas of bioinformatics. This is due to their ability to cope with highly dimensional complex datasets such as those developed by protein mass spectrometry and DNA microarray experiments. As such, neural networks have been applied to problems such as disease classification and identification of biomarkers[10].

.

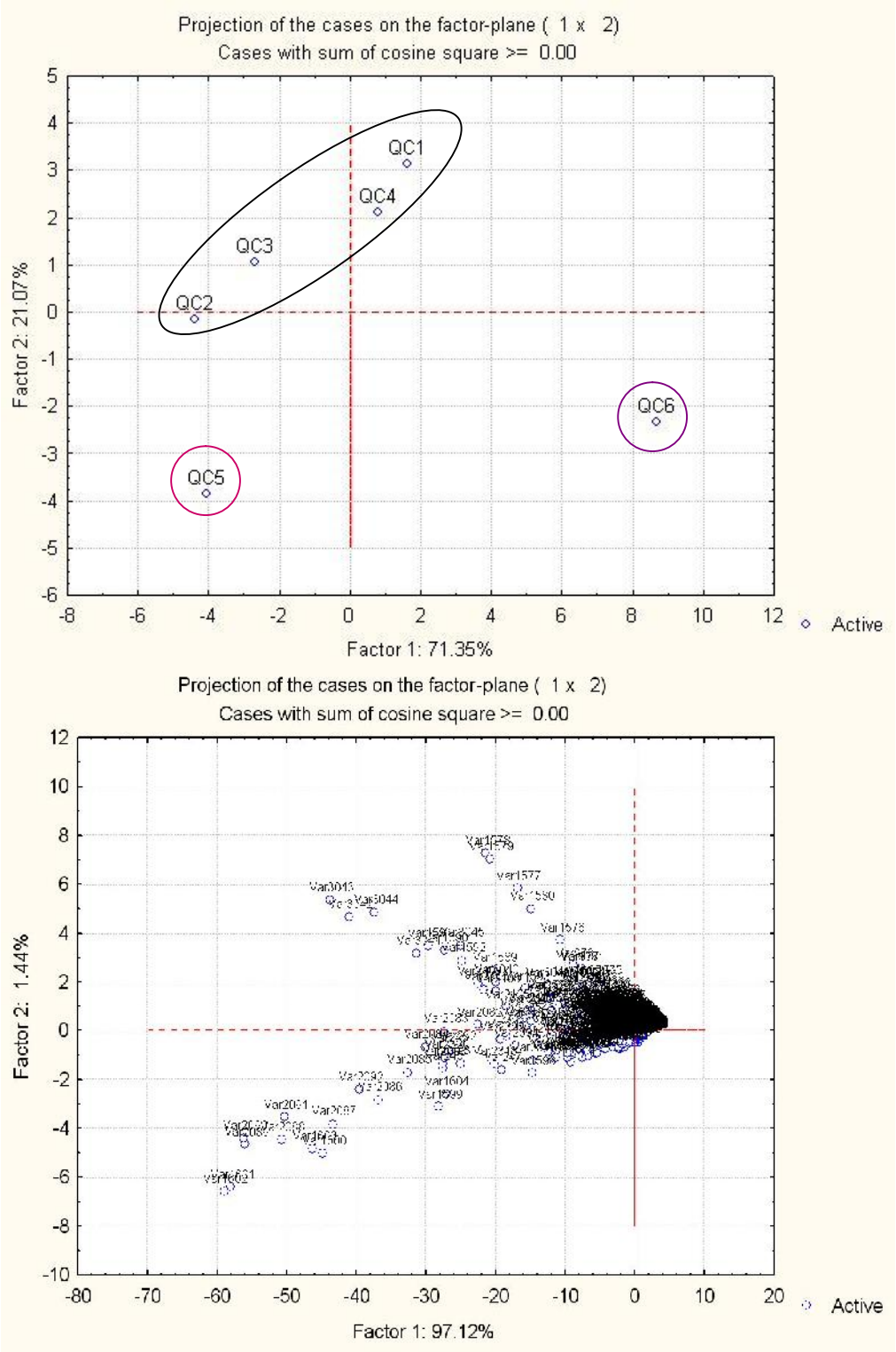

Figure 3.7 Principal Component Analysis of the quality control samples (a) PCA score plot of PC1 vs. PC2 and (b) plot of variance for the PCA analysis.

Due to the volume and complexity of the data generated, statistical analysis was carried out employing an ANNs, a step-wise approach to produce a rank order of ions for each compensation value. In most cases, ANN is an adaptive system that changes its structure based on external or internal information that flows through the network during the learning phase. Modern neural networks are non-linear statistical data modeling tools. They are usually used to model complex relationships between inputs and outputs or to find patterns in data[11]. In this study the ANNs was employed to distinguish between young and old rats based on their urinary profile and to determine which compensation value is most discriminatory and which ions provide the discrimination to determine age groups from urinary profiles.

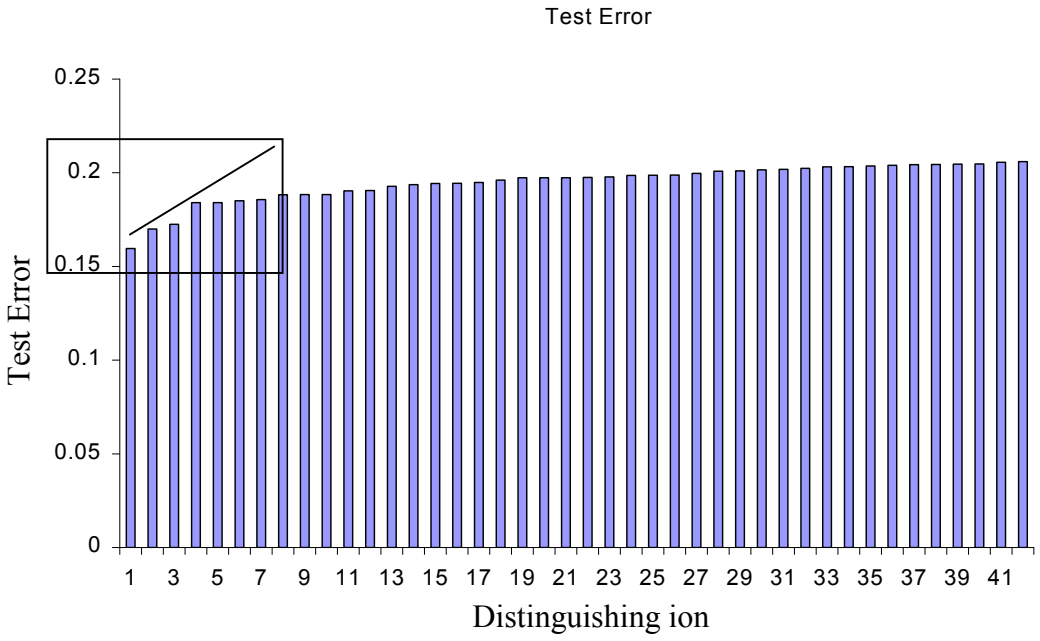

Figure 3.8. ANN statistical analysis of LC-FAIMS-MS analysis of rat urine: Plot of averaged error for each compensation voltage

A plot of test error vs distinguishing ion is shown in Figure 3.8. The steepness of the line show in Figure 3.8 determines how many distinguishing ions are present to distinguish old from young rats based upon their urinary profiles and the level to which they distinguish, the steeper the range within the test error the more distinction is possible. It can be seen that 4 predominate ions are identified in Figure 3.8 to provide a distinction between old and young rats from their urinary profiles. Further analysis searched for commonalities in adjacent compensation values. It can be seen that four predominant ions are identified in Figure 3.8, which provide a distinction between old and young rats from their urinary profiles. The highest ranked ion had an RMS error of 0.162. This model predicted 83.8% of cases correctly. The most discriminatory CV and *m/z* values for distinguishing age based on urinary profiles were -18 V and *m/z* 278 respectively.

3.5. CONCLUSION

This study demonstrates that nested LC-IM-MS data may be acquired on directly injected urine samples within the timescale of an LC-MS experiment. The combined LC-IM-MS approach has the potential to enhance the metabonomic coverage by the introduction of a gas-phase electrophoretic separation that is orthogonal to the reversed-phase LC and mass-to-charge MS separations. Data mining for the detection of a targeted analyte is also demonstrated yielding improved spectral quality and confidence in assignment.

This study has further demonstrated that the combined LC-FAIMS-MS approach has the potential to enhance selectivity and improve mass spectral quality for analytes of interest compared to LC-MS alone. Preliminary statistical analysis of data from a LC-FAIMS-MS analysis of rat urine samples has shown the use of QC data analysis with rank ordering of ions allowing 84% of young and old rats to be distinguished from each other.

3.6 REFERENCES

1. Weston D.J, Bateman R, Wilson I.D, Wood T.R & Creaser C.S. *Anal. Chem*. 2005; **77**: 7572-7580.
2. Sowell R.A, Hersberger K.E, Kaufman T.C & Clemmer D.E. *Journal of Proteome Research*. 2007; **6**: 3637-3647.
3. Liu X, Valentine S.J, Plasencia M.D, Trimpin S, Naylor S & Clemmer D.E. *J Am Soc Mass Spectrom*. 2007; **7**: 1249-1264.
4. Matz L.M, Dion H.M & Hill H.H. *J. Chromatogr. A*. 2002; **946**: 59-68.
5. Dwivedi P, Wu P, Klopsch S.J, Puzon G.J, Xun L & Hill H.H. *Metabolomics*. 2008; **4**: 63-80.
6. Vakhrushev S.Y, Langridge J, Campuzano I, Hughes C & Peter-Katalinic J. *Anal. Chem*. 2008; DOI10.1021/ac7023443 CCC.
7. Bishop, C., *Neural networks for pattern recognition*. 1995: Oxford University Press.
8. Arneberg R, Rajalahti T, Flikka K, Berven F.S, Kroksveen A.C, Berle M. Myhr K.M, Vedeler C.A, Ulvik R.J.A & Kvalheim O.M. *Anal. Chem*. 2007; **79**: 7014-7026.
9. Williams R.E, Lenz E.M, Rantalainen M & Wilson I.D. *Mol. BioSyst.*, 2006; **2**: 193-202.
10. Lancashire L, Lemetre C & Ball G.R. *Briefings in Bioinformatics*. 2009; **10**: 315-329.
11. http://www.spirit-technology.com/neuro-artificial/artificial-neural-network.html. Date accessed 03.12.10.

CHAPTER FOUR

Real-time reaction monitoring using ion mobility-mass spectrometry

4.1 INTRODUCTION

Process understanding and validation is an essential requirement for process control, to assure quality and purity in the manufacture of chemicals and pharmaceuticals. The Food and Drug Administration (FDA) has recognised that process knowledge is key to quality and, through better understanding, to building a cause and effect model that improves process control[1]. The pharmaceutical industry also requires quick, efficient, sensitive and high throughput methods for both quality control and quality assurance of drug products. Real-time reaction monitoring can provide detailed information about the course of a reaction and in turn aid process understanding. Current techniques employed for real-time reaction monitoring include, liquid chromatography (LC)[2], mass spectrometry,[3] infrared spectroscopy,[4] nuclear magnetic resonance spectroscopy[5] and near infrared spectrometry[6] However, there is a need to develop new approaches for real-time reaction monitoring that provide enhanced quantitative and structural information on reaction intermediates and products.

The combination of ion mobility spectrometry with mass spectrometry (IM-MS) allows gas-phase ions generated in an electrospray ion source to be separated first by their ion mobility in a drift cell and then by mass-to-charge ratio in the mass analyser. The technique also lends itself to the acquisition of nested data sets, in which MS spectra are acquired at regular intervals (45-60 μs) during each IM separation (~15 ms), thereby reducing analysis times whilst having the potential to improve selectivity and data quality compared to MS analysis alone.[7]

IM has evolved into a technique for sensitive detection of many trace compounds and a wide range of chemical species such as chemical warfare agents,[8] biomolecules,[9] drugs of abuse[10] and inorganic substances.[11] IM has also been reported for the online monitoring of monomer concentrations in (semi-) batch emulsion polymerisation reactors,[12] the monitoring of yeast fermentation,[13] part per billion level process monitoring of ammonia in process streams[14] thus indicating the potential of IM as a rapid and precise measurement device for the monitoring of processes. More recently IM has been reported in pharmaceutical applications ranging from cleaning verification of manufacturing equipment,[15] direct formulation analysis[16] and protection of pharmaceutical workers health and safety.[17] These studies suggest that IM combined with MS, may have potential for enhancing pharmaceutical process understanding and process control.

.

4.2 CHAPTER FOUR AIMS AND OBJECTIVES

In this chapter, demonstrating proof of principle for the use of IM-MS for reaction monitoring applied to the direct, real-time analysis of the products formed when 7-fluoro-6-hydroxy-2-methylindole is deprotonated by sodium hydroxide was shown. The use of orthogonal IM and MS analysis yields data comparable to mass spectrometry alone, but with the addition of an ion mobility dimension.

The specific objectives were:

- To investigate the potential of IM-MS for reaction monitoring studies to increase selectivity and separate analytes of interest with little or no sample preparation.
- Improve understanding of reaction monitoring processes to aid pharmaceutical development.
- The comparison of IM-MS and MS for reaction monitoring studies and to evaluate the potential of IM as a pre-separation technique for gas phase ions.

4.3 EXPERIMENTAL

4.3.1 Chemicals

Acetonitrile (HPLC gradient grade) and water (HPLC grade) were purchased from Thermo Fisher Scientific (Loughborough, UK) Mass spectrometry grade (puriss, p.a) formic acid and sodium hydroxide (ACS reagent, ≥ 97.0%) pellets were purchased from Sigma-Aldrich (Gillingham, UK). 7-fluoro-6-hydroxy-2-methylindole was provided by AstraZeneca (Macclesfield, UK).

4.3.2 Sample preparation and real time monitoring

Stock solutions of 7-fluoro-6-hydroxy-2-methylindole were prepared at concentrations of 0.1, 1, 3, 5, 10, 15, 20 and 50 μg/mL in 49.5/49.5/1 (v/v/v) acetonitrile/water/formic acid for calibration procedures.

7-fluoro-6-hydroxy-2-methylindole (125 μg/mL) was prepared in acetonitrile and stirred for 10 minutes on ice. Aqueous sodium hydroxide (40 m moles) was prepared in deionized water and added to the indole reaction vessel over a two minute period to initiate the deprotonation reaction. The reaction vessel was maintained at a temperature between -5 and 0 °C for the first six hours of the reaction, after which the reaction vessel was left overnight to warm to room temperature. Aliquots (20 μl) of the reaction mixture were removed from the reaction vessel and diluted to a concentration within the linear dynamic range of the analysis in 49.5/49.5/1 (v/v/v) acetonitrile/water/formic acid to quench the reaction for IM-MS analysis and infused into the ESI source at 5 μl min^{-1}. For real-time reaction monitoring, spectra were

recorded at regular intervals during the deprotonation of the indole. Thus, a time zero spectrum was acquired before the addition of the sodium hydroxide and further spectra were acquired at 60, 80, 160, 220 minutes and 24 hr and 7 days after addition of the sodium hydroxide.

4.3.3 Instrumentation

Direct infusion IM–MS experiments were performed on a Synapt HDMS spectrometer (Waters Corporation, Manchester, UK), operated in positive ion mode with the ESI capillary voltage set to 3 kV and the cone voltage to 27 V. The nitrogen desolvation and cone gas flow rates were set to 500 and 30 L h^{-1} respectively, with a source temperature of 120 °C and desolvation gas temperature set to 300 °C. The ion mobility region contains three (trap, IM, and transfer) travelling wave stacked ion guides (TWIGS). The trap ion guide was used to accumulate ions and periodically then release an ion packet into the IM ion guide for mobility separation. A full description of the mode of operation of stacked ring ion guides with travelling waves is given elsewhere.[18] The travelling wave velocity was set to 300 ms^{-1} with a pulse height of 12 V in all acquisitions. Ions were injected into the IM TWIG from the trap TWIG for 200 μs in every ion mobility separation. Each ion mobility spectrum consists of 200 sequential ToF mass spectra (acquisition time typically less than 15 ms). The quadrupole was operated in wide band pass mode (*m/z* 50-1000) and the collision cell contained no collision gas. IM–MS data were obtained by combining the ion mobility spectra acquired in a 120 s infusion. Acquired data were presented as a

plot of time against ion signal intensity; total ion mobility response or selected ion mobility responses. Masslynx version 4.1 software (Waters corporation, Manchester, UK) was used to control the IM-MS instrument and for data acquisition. Data mining was carried out using DriftScope version 2 (Waters corporation, Manchester, UK).

4.4 RESULTS AND DISCUSSION

7-fluoro-6-hydroxy-2-methylindole (I) is converted to the O-linked indole product, 4-[(4-fluoro-2-methyl-1H-indol-5-yl)oxy]-2-methyl-1H-indol-5-ol (II), in the presence of air and sunlight, and through the addition of aqueous sodium hydroxide. Further deprotonation of II by the sodium hydroxide leads to the formation of higher O-linked polymeric products, resulting in an increase in sample complexity over time. Improved understanding of these processes is required for pharmaceutical development. Reaction monitoring was carried out by IM-MS and MS with electrospray ionization, to follow the rate of polymerization of the indole I to II and other O-linked products (Figure 4.1), generating mass-to-charge and mobility data for the analyte ions present in the reaction mixture.

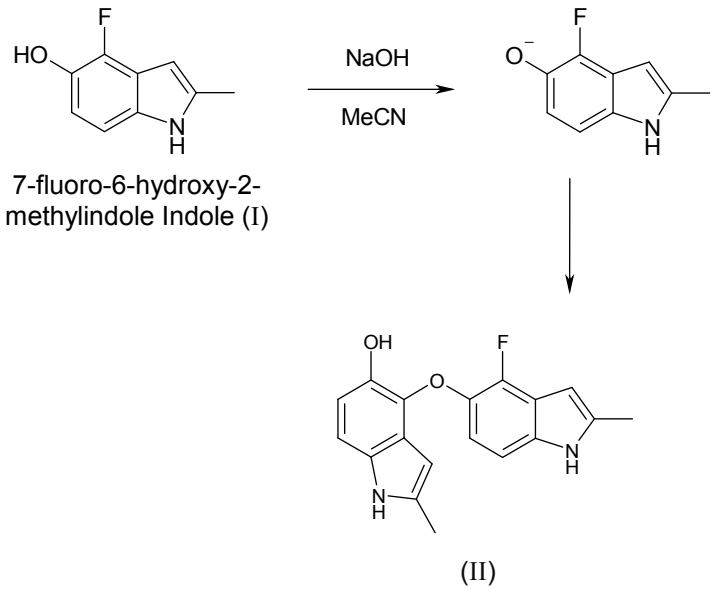

Figure 4.1 Schematic representation of the polymerization of indole I to II and other O-linked products.

Initial investigations were directed at the optimization of the composition of the solvent system used to quench the aliquots of reaction mixture extracted from the reaction vessel for analysis. Three solvent systems were investigated: 100 % acetonitrile (ACN), 50/50 (v/v) ACN/water and 49.5/49.5/1 (v/v/v) ACN/water/formic acid. Experiments carried out in 100 % ACN, gave a low signal response for all ions, with a total ion mobility response ion count approximately an order of magnitude less than the 50/50 (v/v) ACN/water and ~30 times less than the 49.5/49.5/1 (v/v/v) ACN/water/formic acid solvent system, for an initial indole concentration of 2.5 µg/mL. The presence of formic acid quenches the base catalysed reaction and enhances ionization efficiency, so 49.5/49.5/1 (v/v/v) ACN/water/formic acid was used for reaction monitoring with spectral acquisition carried out immediately after sample dilution.

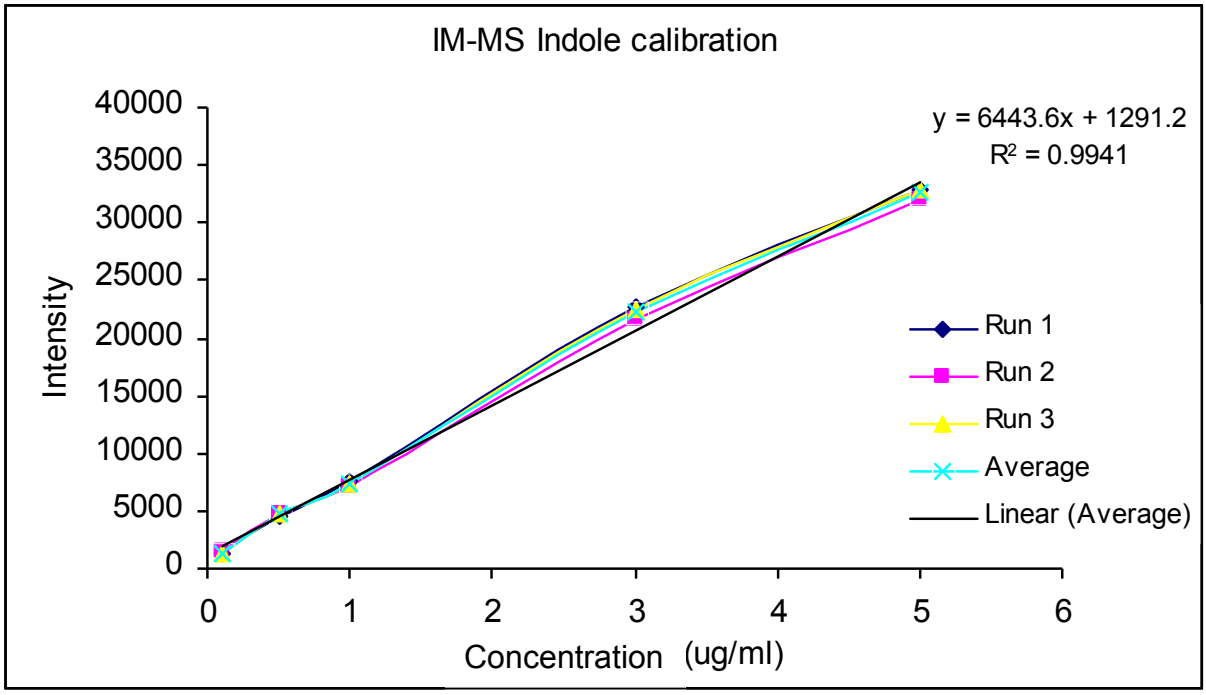

Figure 4.2. Calibration curve for the IM-MS analysis of indole.

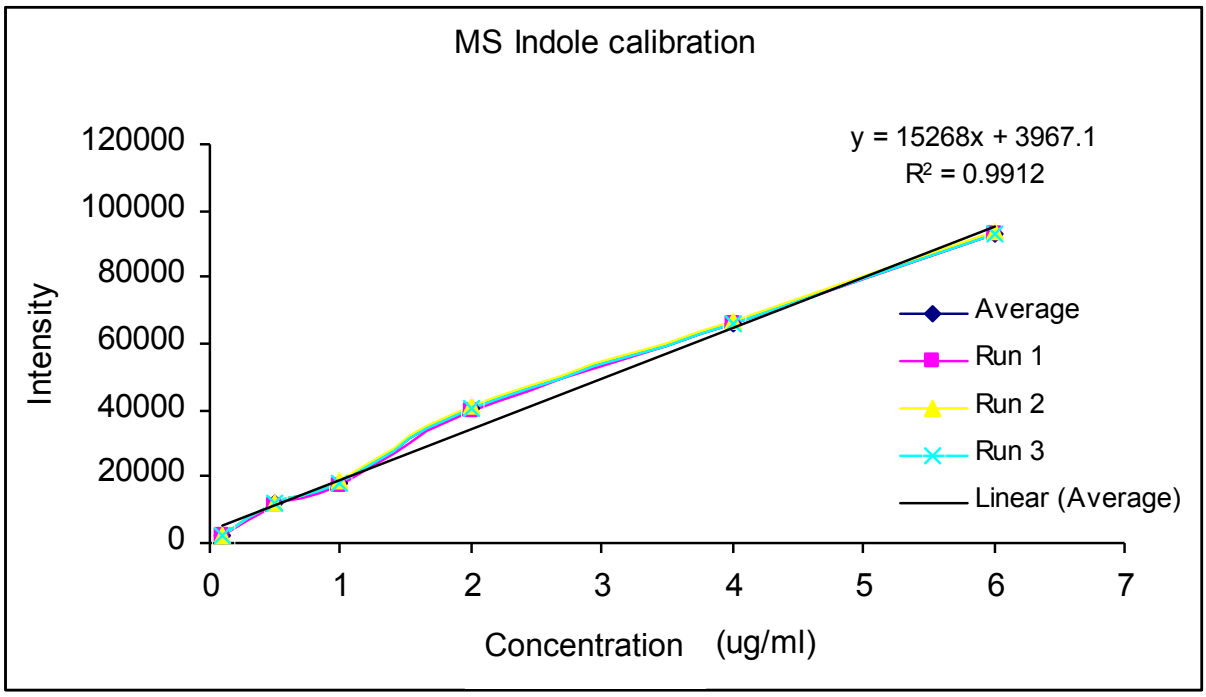

Figure 4.3. Calibration curve for the MS analysis of indole

Calibration curves were created from the indole standards for both IM-MS (Figure 4.2) and MS analysis (Figure 4.3). IM-MS analysis has a lower linear dynamic range than MS because of detector saturation, but the analysis of the calibration standards showed a linear response in the concentration range 0.1 - 5 µg/mL for the indole, with an R^2 value of 0.9941. The MS analysis showed a linear response in the concentration range 0.1-6 µg/mL for the indole, with an R^2 value of 0.9912. To ensure experiments were carried out within the linear dynamic range of the instrument, sample aliquots removed from the reaction vessel were diluted to a concentration within the linear dynamic range for the analysis. IM-MS data were acquired by repetitive scanning of nested data sets, with mass spectra (45 µs/scan) and IM spectra (~13 ms) scanned repetitively throughout, spectra were accumulated to yield 200

mass spectra and one IM spectrum every 7 seconds. The IM drift time is plotted as 'bins', where each bin corresponds to an acquired mass spectrum.

The total ion and selected ion mobility responses for the IM-MS analysis of the indole reaction mixture one hour after addition of aqueous sodium hydroxide are displayed in Figure 4.4.

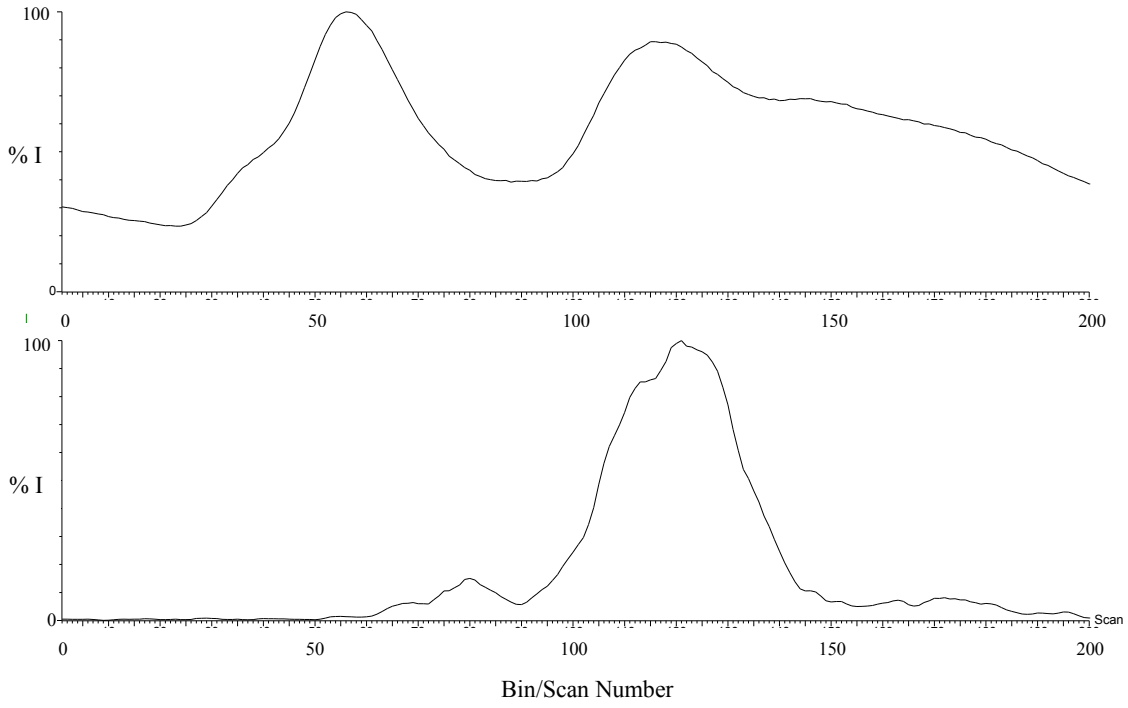

Figure 4.4 Ion mobility spectra for the IM-MS analysis of 7-fluoro-6-hydroxy-2-methylindole reaction mixture: (a) total ion mobility spectrum, (b) selected ion mobility response for *m/z* 311 (protonated indole II)

The selected ion response for the protonated indole, II (*m/z* 311.13; Figure. 4.4(b)), shows a sharp peak, compared to the total ion mobility response, which is centered at a drift time of 5.72 ms and has a peak width at half height of 25 bins. The corresponding mass spectra are shown in Figure 4.5.

The mass spectrum obtained by combining all 200 bins (Figure 4.5(a)) corresponds to the spectrum expected in the absence of IM separation and contains a large number of ions across the whole mass range. In contrast, when the mass spectrum obtained in IM-MS mode by combining bins 128-130 (drift time range 5.7-5.8 ms; Figure. 4.5(b)) is compared with the mass spectrum in the absence of ion mobility separation, the relative intensity of the $[M+H]^+$ ion for II (*m/z* 311.13) has been enhanced selectively and is observed as the base peak in the ion mobility-selected mass spectrum.

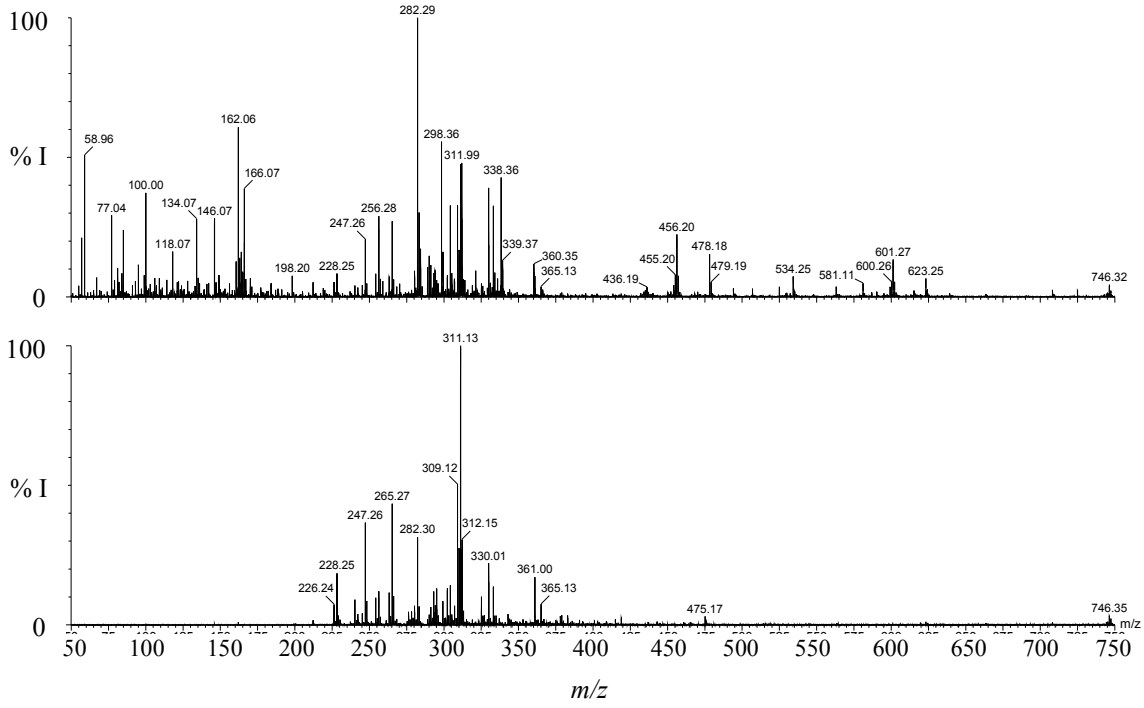

Figure 4.5 Mass spectra for the IM-MS analysis of 7-fluoro-6-hydroxy-2-methylindole reaction mixture: (a) mass spectrum obtained by combining all 200 bins acquired during the ion mobility separation and (b) mass spectrum corresponding to the mobility-selected ion response for *m/z* 311 (bins 128-130; drift time range 5.7-5.8 ms)

The complexity of the reaction mixture one hour after addition of sodium hydroxide is illustrated in Figure 4.6, which shows the *m/z* versus ion drift time (bins) space, averaged over the whole IM-MS analysis, allowing good visualisation of the full IM-MS analysis data. The protonated monomer (I), O-linked product (II) and O-linked trimer ions are highlighted showing that these ions are resolved on the basis of mass-to-charge and drift time.

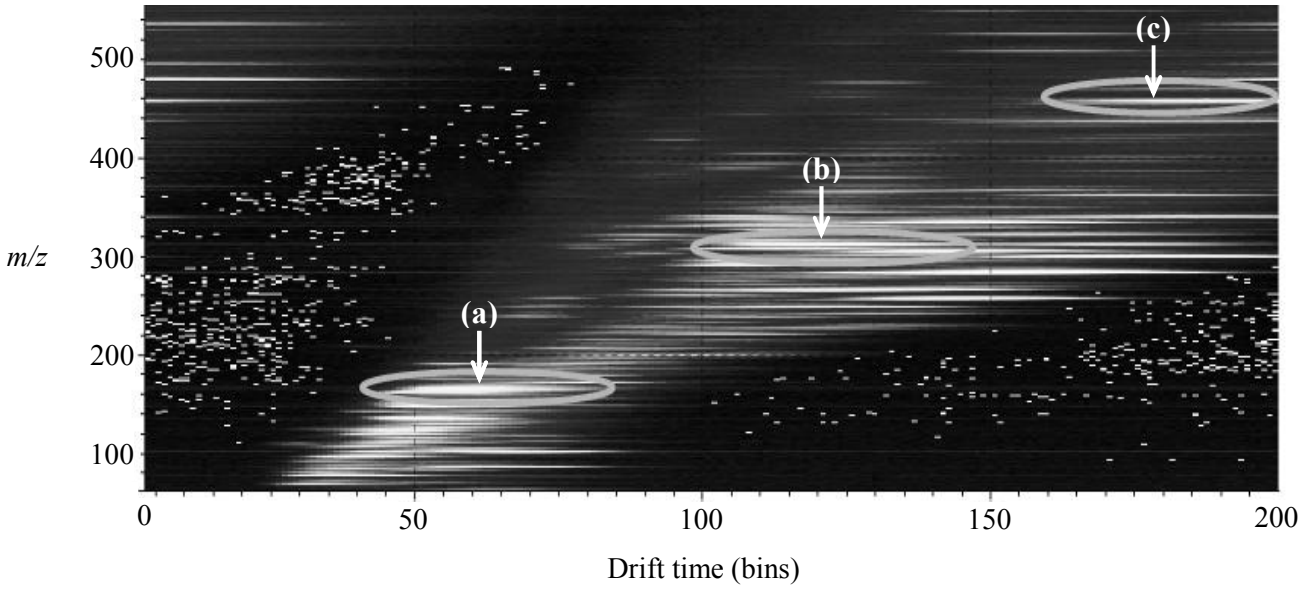

Figure 4.6 2D plot of drift time (bins) vs *m/z* for full data set of IM-MS analysis of indole reaction mixture, one hour after addition of aqueous sodium hydroxide, (a) indole monomer (*m/z* 166, I), (b) O-linked dimer (*m/z* 311, II) and (c) O-linked trimer (*m/z* 456).

The drift time of an ion may be used to determine the collision cross section which may be correlated with modelled or predicted structures[19,20,21] so IM-MS data has the potential for the structural analysis of mass-selected transient intermediates and products in complex reaction mixtures for enhanced process understanding.

The indole reaction mixture was monitored by MS and IM-MS over a period of seven days. The reaction of indole monomer (I, *m/z* 166) to O-linked dimer (II, *m/z* 311) following addition of aqueous sodium hydroxide was fast, indicated by the reaction mixture rapidly turning from a straw coloured to a dark brown solution. The reaction continues via further addition of indole phenolate, with elimination of fluorine, to produce higher polymeric products.

Figure 4.7 displays the time dependent ion intensities for the protonated ions derived from the reactant and products under MS and IM-MS analysis: *m/z* 166 (monomer, I), *m/z* 311 (O-linked dimer, II), *m/z* 456 (O-linked trimer), *m/z* 601 (O-linked tetramer), *m/z* 746 (O-linked pentamer) and *m/z* 891 (O-linked hexamer).

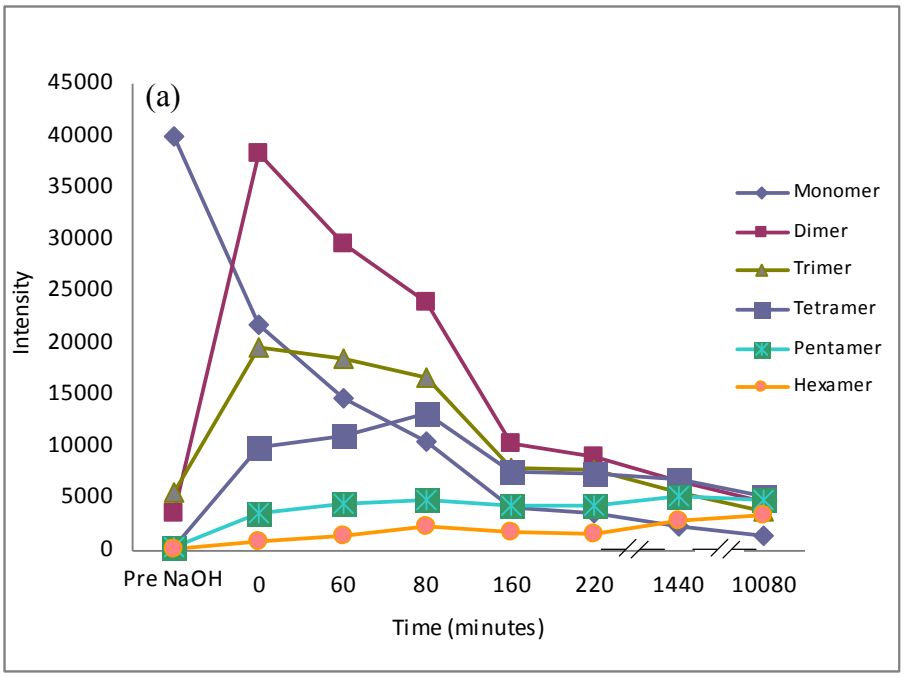

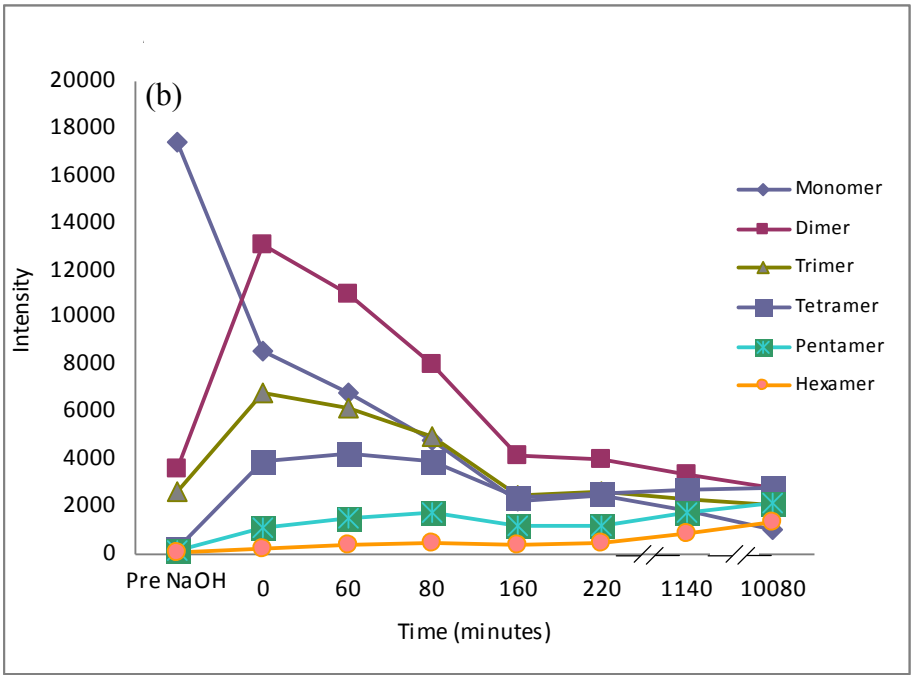

Figure 4.7 MS and IM-MS analysis of the reaction of 7-fluoro-6-hydroxy-2-methylindole following the addition of aqueous sodium hydroxide. (a) signal response versus time in minutes for m/z 166 (monomer, I), m/z 311 (O-linked dimer, II), m/z 456 (O-linked trimer), m/z 601 (O-linked tetramer), m/z 746 (O-linked pentamer) and m/z 891 (O-linked hexamer) using (a) MS and (b) IM-MS.

Products and reactants ions were observed under both MS and IM-MS conditions. The ion intensities were lower in IM-MS mode, because of the transmission efficiency through the IM drift cell, but the instrumental sensitivity was sufficient for monitoring reactant and products throughout the course of the reaction. Ion counts were generated by combining selected bins (mass spectra) from the ion responses for each ion of interest at half height across the mobility peak. The O-linked dimer formation quickly reached a maximum intensity after the addition of sodium hydroxide and decreased thereafter as seen in Figure 4.7. The decrease in dimer ion intensity was associated with further polymerisation to form higher multimers. The formation of O-linked trimer reached a maximum at the same time as the dimer, but ion intensity showed only a slow decline during the first 80 minutes, followed thereafter by a sharper decline. The O-linked tetramer, pentamer and hexamer ion intensities rose more slowly, with the tetramer reaching an ion count maximum after 60-80 minutes in both the MS and IM-MS modes. The total ion current for all ions summed falls with time reflecting the difference in mass spectrometric response between the O-linked multimers and the monomer. These data suggest that the monomer was progressively converted to the higher oligomers over time. The close similarity of the ion intensity trends observed in both the MS and IM-MS modes demonstrates that no loss of information is observed in IM-MS mode, whilst the greater selectivity and potential for structural analysis that IM measurement brings to the analysis has the potential to enhance ion assignments and process understanding.

4.5 CONCLUSION

This study has demonstrated that ion mobility-mass spectrometry can be employed as a rapid means to analyse a model chemical reaction mixture, offering the potential for real time reaction monitoring. The IM-MS approach has been shown to have potential to enhance visualization of the data selectivity for analytes compared with MS alone, as a direct result of the orthogonal mobility and mass-to-charge separation.

4.6 REFERENCES

1. US Food and Drug Administration, Process Validation: General Principles and Practices, Draft Guidance 2008.
2. Radhakrishna T, Sreenivas Rao & Reddy. *Journal of Pharmaceutical and Biomedical Analysis*. 2001; **26**: 617–628.
3. Rudaz S, Souverain S, Schelling C, Deleers M, Klompb A, Norris A, Vu T.L, Ariano B & Veuthey J.L. *Analytica Chimica Acta.* 2003; **492**: 271–282.
4. Tewari J, Dixit V & Malik K. *Sensors and Actuators B.* 2010; **144**:104–111.
5. Bakeev K. Process Analytical Technology, Spectroscopic Tools and Implementation Strategies for the Chemical and Pharmaceutical Industries. JohnWiley & Sons, 1st edn., 2005, pp159.
6. Hammond J, Kellam B, Moffata A.C & Jee R.D, *Anal. Commun*. 1999; **36**:127-129.
7. Harry E.L, Weston D.J, Bristow A.W.T, Wilson I.D & Creaser C.S. *J. Chromatogr. B*, 2008; **871**: 357-361.
8. Steiner W.E, Klopsch S.J, English W.A, Clowers B.H & Hill H.H, *Anal. Chem*. 2005; **77**: 4792–4799.
9. Bohrer B.C, Merenbloom S.I, Koeniger S.L, Hilderbrand A.E & Clemmer D.E. *Annual Review of Analytical Chemistry*. 2008; **1**: 293-327.
10. Keller T, Mikib A, Regenschetic P, Dirnhofer R, Schneider A & Tsuchihashib H. *Forensic science international*. 1998; **94**: 55-63.
11. Eiceman G.A, Leasure C.S & Vandiver V.J. *Anal. Chem*. 1986; **58**: 76–80.
12. Vautz W, Mauntz W, Engell S & Baumbach J.I. *Macromol. React, Eng*. 2009; **3**: 85-90.
13. Kolehmainen M, Rönkkö P & Raatikainen O. *Analytica Chimica Acta*. 2003; **484**: 93-100.
14. Bacon T & Webber K. Acid and Halogen Gas Monitoring Utilizing Ion Mobility Spectroscopy (IMS), Technical Note, *Molecular Analytics*. 2005.
15. Debono R, Stefanou S, Davis M & Walia G. *Pharmaceutical technology*. 2002; **72**: 78.
16. Weston D.J, Bateman R, Wilson I.D, Wood T.R & Creaser C.S. *Anal. Chem*. 2005; **77**: 7572-7580.

17. O'Donnell R.M, Sun X & Harrington P.B. *Trends in Analytical Chemistry*. 2008; **27**: 44-53.

18. Giles K, Wildgoose J.L, Langridge D.J & Campuzano I. *Int. J. Mass Spectrom*. 2010; **298**: 10-16.

19. Knapman T.W, Berryman J.T, Campuzano I, Harris S.A & Ashcroft A.E. *Int. J. Mass Spectrom*. 2010; **298**: 17-23.

20. Mesleh M.F, Hunter J.M, Shvartsburg A.A, Schatz G.C & Jarrold M.F. *J. Phys. Chem.* 1996; **100**: 16082-16086.

21. Wyttenbach T, Helden von G, Batka J.J, Carlat D & Bowers M.T. *J. Am. Soc. Mass Spectrom*. 1997; **8**: 275-282.

CHAPTER FIVE

Conclusions & Further Work

5.1 CONCLUSIONS TO THESIS & FURTHER WORK

The research presented in this thesis describes the development of IMS in combination with other analytical techniques for the high-throughput analysis of complex samples. The combination of ion mobility spectrometry with mass spectrometry (IM-MS), allows gas-phase ions generated in either the ESI or DESI ion source to be separated first by their mobility in a drift cell and then by mass-to-charge ratio in the mass analyser, providing a multidimensional separation with improved selectivity for the analytes of interest**.**

Chapter 2 describes the direct, rapid analysis of pharmaceutical drug formulations and active ingredients employing DESI-IM-MS. The direct analysis of Imodium plus caplets, containing active ingredients loperamide (2 mg) and simethicone (containing an equivalent to 125 mg of poly(dimethyl siloxane) (PDMS) was investigated. Ion mobility provided an increase in selectivity for the active ingredient Loperamide in a tablet formulation. IM investigations also demonstrated the ability to separate PDMS oligomers based upon their collision cross sections.

Further studies investigated the direct analysis of pharmaceutical formulations and active ingredients from non-bonded reversed-phase thin layer chromatography (RP-TLC) plates by desorption electrospray ionisation (DESI) combined with IM-MS. The analysis of formulations containing analgesic (paracetamol), decongestant (ephedrine), opiate (codeine) and stimulant (caffeine) active pharmaceutical ingredients was carried out with, and without, chromatographic development to separate the active ingredients from the excipient formulation. Spectral quality was enhanced by combining ion mobility and mass spectrometry. Variation of the solvent composition of the DESI spray using a step gradient allows the optimisation of the

conditions for analytes with reduced method development times. The use of a continuous DESI solvent gradient in the RP-TLC/DESI/IM-MS analysis allows selective desorption of active pharmaceutical ingredients from the surface of the TLC plate,whilst reducing analysis times. The combined RP-TLC/DESI/IM-MS approach has potential as a rapid and selective technique for pharmaceutical analysis by orthogonal gas-phase electrophoretic and mass-to-charge separation. Further work to investigate the potential of on-line variation of the DESI solvent spray could be explored to provide direct pre-fractionation of complex samples, or matrix clean-up, equivalent to an SPE procedure with minimum sample preparation for a variety of analytes. The application of RP-TLC/DESI/IM-MS could be employed to desalt complex from biological samples, such as urine, without the need for liquid chromatography separation. The potential for DESI imaging has been demonstrated and further investigations could be directed towards the fast metabonomic analysis of intact tissue samples.

Chapter 3 shows the potential of drift tube ion mobility (IM) spectrometry in combination with high performance liquid chromatography (LC) and mass spectrometry (MS) for the metabonomic analysis of rat urine. The combined LC-IM-MS approach using quadrupole/time-of-flight mass spectrometry with electrospray ionisation, uses gas-phase analyte characterisation based on both *m/z* and relative gas-phase mobility following LC separation. The technique allowed the acquisition of nested data sets, with mass spectra acquired at regular intervals (65 μs) during each IMS separation (~13 ms) and several IMS spectra acquired during the elution of a single LC peak, without increasing the overall analysis time compared to LC-MS. Results indicate that spectral quality is improved when using LC-IM-MS, compared

to direct injection IM-MS, for which significant ion suppression effects were observed in the electrospray ion source. The use of reversed-phase LC employing fast gradient elution reduced sample preparation to a minimum, whilst maintaining the potential for high throughput analysis. Data mining allowed information on specific analytes to be extracted from the complex metabonomic data set. LC-IM-MS based approaches may have a useful role in metabonomic analyses by introducing an additional discriminatory dimension of ion mobility (drift time). The combination of liquid chromatography with with field asymmetric waveform ion mobility spectrometry (FAIMS) and mass spectrometry, using electrospray ionisation (ESI), was used for gas-phase analyte separation based on mass-to-charge (*m/z*) ratio and characteristic compensation voltages (CV). The selectivity by FAIMS/MS was exploited for the metabonomic analysis of rat urine using a cylindrical FAIMS device coupled to a linear ion trap mass spectrometer to attain LC-FAIMS-MS urinary profiles.

Urine samples from a groups of young and old Wistar rats were analysed by gradient reversed phase HPLC, following centrifugation. Aliquots of a pooled sample were used to form a multi–replicate QC set to test and condition the IM-MS system.. Six compensation voltages were selected to cover the range for metabolite detection and the FAIMS selected fractions analysed by ion trap mass spectrometry. This study further demonstrated that the combined LC-FAIMS-MS approach has the potential to enhance selectivity and improve mass spectral quality for analytes of interest compared to LC-MS alone. Statistical analysis of data from the LC-FAIMS-MS analysis of rat urine samples using artificial neural networks, with rank ordering of ions, allowed the young and old rats to be distinguished with an RMS of less than 0.162% Future investigation using negative ion mode data could be investigated and

may yield improved performance and show greater discrimination of the urinary profiles. Tandem mass spectrometry and metabolite identification could also be performed. Future studies could also look at the potential of IM-MS and FAIMS-MS for the detection of novel and established biomarkers of disease states from urinary profiles.

Chapter 4 demonstrates proof of principle for the use of IM-MS for reaction monitoring applied to the direct, real-time analysis of the products formed when 7-fluoro-6-hydroxy-2-methylindole is deprotonated by sodium hydroxide. The use of orthogonal IM and MS analysis yields data comparable to mass spectrometry alone, but with the addition of an ion mobility dimension. Ion mobility-mass spectrometry can be employed as a rapid means to analyse a model chemical reaction mixture, offering the potential for real-time reaction monitoring. The IM-MS approach has been shown to have potential to enhance visualization of the data selectivity for analytes compared with MS alone, as a direct result of the orthogonal mobility and mass-to-charge separation. Further work could be undertaken to investigate the potential of on-line monitoring of genotoxic impurities within pharmaceutical formulations employing DESI. These further studies will give an indication of the potential to employ IM for on-line monitoring without the need for sample preparation.

APPENDICES

APPENDIX 1 – PUBLICATIONS AND PRESENTATIONS

PUBLICATIONS

An approach to enhancing coverage of the urinary metabonome using liquid chromatography-ion mobility-mass spectrometry. E.L. Harry, D.J. Weston, A.W. Bristow, I.D. Wilson & C.S. Creaser. *J Chromatogr B*. 2008; 871:357-361.

Direct analysis of pharmaceutical drug formulations from reversed-phase thin-layer chromatography plates by desorption electrospray ionisation ion mobility mass spectrometry. E.L. Harry, J.C. Reynolds, A.W.T. Bristow, I.D. Wilson & C.S. Creaser. *Rapid Commun. Mass Spectrom*. 2009; 23: 2597-2604.

Detection of Volatile Organic Compounds in Breath Using Thermal Desorption Electrospray Ionization-Ion Mobility-Mass Spectrometry. J. C. Reynolds, G. J. Blackburn, C. Guallar-Hoyas, V. H. Moll, V. Bocos-Bintintan, G. Kaur-Atwal, M. D. Howdle, E. L. Harry, L. J. Brown, C. S. Creaser and C. L. P. Thomas. *Anal. Chem*. 2010; 82: 2139-2144.

Real-time reaction monitoring using ion mobility-mass spectrometry. Emma L. Harry, Anthony W. T. Bristow, Ian D. Wilson and Colin S. Creaser. *Analyst*. 2011; 136: 1728-1732.

PRESENTATIONS

Applications of ion mobility/mass spectrometry in pharmaceutical analysis. C.S. Creaser, E.L. Harry, M.D. Howdle, N. Budimir, D.J. Weston, C. Eckers, A. Laures, A.W.T. Bristow & I.D. Wilson. Proceedings of the 55th American Society of Mass Spectrometry, conference on mass spectrometry and allied topics, Indianapolis, 2007. (oral)

Metabonomic screening of rat urine using ion mobility spectrometry combined with time-of-flight mass spectrometry. E.L. Harry, D.J. Weston, N. Budimir, A.W.T. Bristow, I.D. Wilson, C.S. Creaser. Presented at the Royal Society of Chemistry Analytical Research Forum, Strathclyde, 2007. (poster)

Metabonomic screening of rat urine using ion mobility spectrometry & high-field asymmetric waveform ion mobility spectrometry combined with time-of-flight mass spectrometry. E.L. Harry, D.J. Weston, N. Budimir, A.W.T. Bristow, I.D. Wilson, C.S. Creaser. Presented at the 42nd Annual meeting of the British Mass Spectrometry Society, Edinburgh, 2007. (poster)

Direct analysis of pharmaceutical drug formulations employing Ion Mobility-Mass Spectrometry combined with Desorption Electrospray Ionisation. E.L. Harry, A.W.T. Bristow, I.D. Wilson & C.S. Creaser. Presented at the Royal Society of Chemistry Analytical Research Forum, Hull, 2008. (poster)

Direct analysis of pharmaceutical drug formulations employing Desorption Electrospray Ionisation- Ion Mobility-Mass Spectrometry combined with Reversed-Phase Thin-Layer Chromatography. E.L. Harry, A.W.T. Bristow, I.D. Wilson & C.S. Creaser. Presented at the 43rd Annual meeting of the British Mass Spectrometry Society 3 day meeting, York, 2008. (oral)

Metabonomic approach employing LC-FAIMS-MS to study the effects of age on the profile of endogenous metabolites in rat urine. E.L. Harry, J.C. Reynolds, A.W.T. Bristow, I.D. Wilson & C.S. Creaser. Presented at the Royal Society of Chemistry Analytical Research Forum, Canterbury, 2009. (poster)

DESI-IM-MS combined with RP-TLC for the direct analysis of pharmaceutical drug formulations. Presented at the 18th International Mass Spectrometry Society Conference, Bremen, 2009. (poster)

APPENDIX 2:

An approach to enhancing coverage of the urinary metabonome using liquid chromatography-ion mobility-mass spectrometry

***J Chromatogr B*. 2008, 871:357.**

Emma L. Harry[a], Daniel J. Weston[b], Anthony W. T. Bristow[c], Ian D. Wilson[d], Colin S. Creaser [a]*

[a] *Department of Chemistry, Loughborough University, Loughborough, Leicestershire, LE11 3TU.*

[b] *AstraZeneca R&D Charnwood, Clinical Pharmacology and DMPK, Bakewell Road, Loughborough, Leicestershire, LE11 5RH, UK.*

[c] *AstraZeneca, Charter Way, Silk Road Business Park, Macclesfield, Cheshire, SK10 2NA, UK.*

[d] *AstraZeneca, Alderley Park, Macclesfield, Cheshire, SK10 4TF, UK.*

* Corresponding author:

Email. c.s.creaser@lboro.ac.uk

Tel. +44 (0)1509 222552

Fax. +44 (0)1509 223925

Abstract

The potential of drift tube ion mobility (IM) spectrometry in combination with high performance liquid chromatography (LC) and mass spectrometry (MS) for the metabonomic analysis of rat urine is reported. The combined LC-IMMS approach using quadrupole/time-of-flight mass spectrometry with electrospray ionisation, uses gas-phase analyte characterisation based on both mass-to-charge (*m/z*) ratio and relative gas-phase mobility (drift time) following LC separation. The technique allowed the acquisition of nested data sets, with mass spectra acquired at regular intervals (65 μs) during each IMS separation (~13 ms) and several IMS spectra acquired during the elution of a single LC peak, without increasing the overall analysis time compared to LC-MS. Preliminary results indicate that spectral quality is improved when using LC-IMMS, compared to direct injection IMMS, for which significant ion suppression effects were observed in the electrospray ion source. The use of reversed-phase LC employing fast gradient elution reduced sample preparation to a minimum, whilst maintaining the potential for high throughput analysis. Data mining allowed information on specific analytes to be extracted from the complex metabonomic data set. LC-IMMS based approaches may have a useful role in metabonomic analyses by introducing an additional discriminatory dimension of ion mobility (drift time).

Keywords:

Ion mobility-mass spectrometry; reversed phase HPLC; metabonomics; urinary metabolome.

1. Introduction

A number of analytical methods have been employed to produce metabolic signatures of biomaterials. The main techniques currently used in metabonomic studies are high resolution nuclear magnetic resonance (NMR) spectroscopy [1-3], gas chromatography-mass spectrometry (GC-MS) [4-6], liquid chromatography-mass spectrometry (LC-MS) [4, 7-9], including ultra performance liquid chromatography (UPLC) [10], and capillary electrophoresis-mass spectrometry (CE-MS) [11] (for a recent review of analytical strategies in this area see [12]). All these techniques result in complex multivariate data sets, which in turn require bioinformatic methods for visualisation and interpretation. There are various advantages in employing NMR in metabonomic/metabolomic studies because the technique is non-destructive and applicable to the direct analysis of biofluid samples and intact biomaterials, with minimal or no sample preparation, for example the direct analysis of tissue employing magic angle spinning NMR [13]. NMR spectroscopy also has good potential for structure determination. However, there are limitations for NMR-based metabonomic studies including issues around sensitivity (>1 nmol metabolite for ^{1}H-NMR detection) and the inability to detect some nuclei (e.g. O and S). MS is inherently more sensitive than NMR (though sensitivity is compound dependant) and also has the potential for molecular identification using tandem MS fragmentation or accurate mass determination.

Ion mobility (IM) spectrometry is a gas-phase electrophoretic technique which allows ionized analytes to be characterised on the basis of their ion mobility (K), defined by the reduced mass (μ), charge (e) and collision cross section (Ω) (*i.e.,* size and shape) of the ion (eqn 1) [14].

$$K = \left(\frac{3ze}{16N}\right)\left(\frac{2\pi}{\mu k_B T}\right)^{1/2}\left(\frac{1}{\Omega_D}\right) \qquad \text{equation 1}$$

where N is the number density of the buffer gas, k_B is the Boltzmann constant and T is the temperature. The time (t_d) taken for an analyte ion to traverse a drift cell (of length l), under the influence of a weak electric field (E) and in the presence of a buffer gas is determined by the mobility of the ion, so mixtures of analyte ions may be separated on the basis of their relative drift times.

$$t_d = l/\mathrm{K.E} \qquad \text{equation 2}$$

The principles and applications of IM have been the subject of several recent reviews [15-17].

The combination of ion mobility spectrometry with mass spectrometry (IM-MS), as shown in Fig. 1, allows ions generated in the ion source to be separated initially by their mobility in the low pressure drift cell and then by mass-to-charge ratio in the fast scanning time-of-flight (TOF) mass analyser. The coupling of these complementary techniques therefore provides a multidimensional separation of gas-phase ions.

IM is a separation technique that has not until recently been used in bioanalytical applications, but preliminary studies have shown that using IM can aid the analysis of small molecules in complex systems [18] and IM-MS has proved to be a valuable tool for proteomic research [19-21]. The application of IM-MS using an atmospheric pressure drift tube to the analysis of metabolic mixtures has recently been reported for

extracts of bacterial cell cultures (*E. coli*) infused directly into the ESI ion source of the spectrometer [22]. IM-MS analysis of the human glycourinome using pre-fractionated urine has also been reported [23]. These studies suggest that LC hyphenated with IM-MS, may have potential for enhancing metabonomic studies without the requirement for additional sample clean-up. In this communication, we describe a preliminary evaluation of the potential of LC-IM-MS using a low pressure IM drift cell for the analysis of the urinary metabolome without prior extraction. Fast gradient reversed-phase liquid chromatography was used for the rapid elution of endogonous metabolites, prior to electrophoretic separation and *m/z* measurement by IM-MS.

2. Experimental

2.1. Chemicals

Methanol (HPLC grade), acetonitrile (HPLC gradient grade) and formic acid (99.5% Puriss grade) were purchased from Thermo Fisher Scientific (Loughborough, UK). Distilled and deionised water was obtained in-house using a Triple red water purification system (Triple red, Long Crendon, UK).

2.2 IM-MS and LC-IM-MS method

All experiments were carried out employing a prototype IM-Q-TOF-MS (Waters Corporation, Manchester), which is shown schematically in Fig. 1 and has been described in detail elsewhere [14]. Ions from the ESI source were directed into the

trap region at the head of the ion mobility drift cell, which was operated in the pressure region of 1.0 to 3.0 Torr N_2. Ions were gated into the drift cell using a gate electrode pulse (3.50 V, 200 μs pulse width and 15ms pulse period). The IM drift tube consisted of a multi-plate ion guide (15.2 cm in length) to which a voltage gradient (14.24 V/cm and a supplement RF voltage 3.8 V) were applied to facilitate separation of ion species by relative mobility. Ions passing through the drift region were then directed into the reflectron TOF mass analyses. Ion mobility spectra were acquired by collecting data from 200 TOF pushes (65 μs per bin) and plotting drift time (scan) against mass-to-charge ratio (*m/z*). IM-MS data were typically accumulated for 5 s, with a 2 s interscan delay. Initial studies using direct introduction of urine samples into the IMS-Q-TOF-MS spectrometer without chromatographic separation were preformed by infusing the aliquots of the prepared urine into the ESI ion source at 10 μl/min using the integrated syringe pump.

Liquid chromatography was performed on a Waters Alliance 2790 chromatograph (Waters Corporation, Manchester, UK) fitted with a Symmetry® (Waters Corporation, Manchester, UK) C18 column (2.1 x 50 mm, 5 μm). The LC system was coupled to the ESI ion source of the IM-Q-TOF-MS spectrometer. Urine samples (50 μl injected) were eluted with the following gradient: 100% A (0-2 min), increased to 100% B (2-5 min) and then to 100% A (5-8 min), where A = 0.1% aqueous formic acid and B = 0.1% formic acid in acetonitrile. The mobile phase flow rate was set to 0.200 ml/min. Electrospray ionization conditions for the MS, with the ion source operated in positive ion mode were: capillary voltage, 3.5 kV; cone voltage 60 V; source temperature 120°C; desolvation gas, N_2 gas flow 250 l/hr; desolvation gas temperature, 180°C. Masslynx version 4.1 (Waters Corporation, Manchester, UK)

was used to control the LC and IM-MS instrument and for data acquisition. Data mining was carried out using DriftScope version 1.0 (Waters Corporation, Manchester, UK).

2.3 Urine sample preparation

Urine samples from male Wistar-derived rats were provided by AstraZeneca (Alderley Park, Macclesfield, UK). Aliquots of a pooled urine (n=4) were used for IM-MS and LC-IM-MS studies. The urine was centrifuged at 13,000 rpm for 5 minutes to remove particulates and then frozen to -80°C prior to analysis.

3. Results and discussion

Initial experiments were carried out by directly infusing aliquots of urine into the ESI-IM-Q-TOF-MS spectrometer as described in the experimental section. However, the salt component of the urine caused significant ion suppression in the electrospray ion source (data not shown) and hence liquid chromatography was employed to reduce these suppression effects. The urinary metabolic profile is composed mainly of relatively polar/ionic substances, which must be retained on the LC column whilst the salts elute prior to mass spectrometry analysis. In order to obtain the best possible retention of these polar metabolites, we therefore used a gradient separation where the initial segment (0-2 min) was entirely aqueous formic acid, followed by a rapid increase (over 5min) to 100% acetonitrile. The effectiveness of the LC column for improving spectral quality is shown in the LC-ESI-IM-MS data for a pooled urine sample obtained from the Wistar-derived rats, shown in Fig. 2. The peaks in the LC chromatogram correspond to the IM spectra accumulated during the LC run (Fig.

2(a)). The salt component was eluted in less than 1 minute (Fig. 2(a)) showing ion suppression effects and an increased noise in the mass spectrum (Fig. 2(b)), leaving the metabolites and other components of the urine to be eluted in the region 3-8 minutes, free from salt interferences (Fig. 2(c)).

The effect of introducing an IM separation in tandem with LC and MS analysis of urinary metabolites is shown in Fig. 3. In this experiment, data were acquired as nested data sets, with mass spectra (65 μs/scan) and IM spectra (~13 ms) scanned repetitively throughout the LC run. Spectra were accumulated to yield 200 mass spectra and one ion mobility spectrum every 7 s. The ion mobility drift time is plotted as 'bins', where each bin corresponds to an acquired mass spectrum. The nested data acquisition of IM and MS data results in an analysis incorporating a gas-phase electrophoretic separation of the ESI generated ions on the basis of charge state and collision cross section (i.e. size and shape), between the reversed-phase chromatography and mass analysis, all within the timescale of the LC-MS run (Fig. 3(a)). IM has a relatively poor resolving power, with a typical full width at half height (FWHH) resolution of 10, corresponding to ~500 theoretical plates in total. However, peak capacity is increased in LC-IM-MS, because the IM separation is orthogonal to that of LC retention and mass-to-charge ratio.

The mass spectrum shown in Fig. 3(b) was generated by summing all 200 mass spectra in each IM scan and is therefore equivalent to the mass spectrum for LC-MS analysis without IM separation. Fig. 3(c) shows the IM spectrum summed over all *m/z* values and corresponds to LC-IM analysis without mass separation. The enhanced separation afforded by the combined IM-MS analysis is shown in the 2-D plot of ion

drift time (bins) vs *m/z*, which is presented in Fig. 3(b) for data averaged over the whole LC run (0-7 min). The bands of colour reflect the intensity of the ions with red representing the highest intensity and blue/white the lowest intensity.

Analysing these multidimensional data sets presents a challenge for multivariate statistical techniques commonly used in comparative metabonomics, since conventional statistical theory requires at least twice as many sample replicates as the number of dimensions in the data. Advanced bioinformatic techniques are required, such as artificial neural networks, which are capable of handling complex, multidimensional and non-linear data sets [24]. An alternative approach is to reduce the complexity of the data by selecting retention time and drift time windows for analysis, or by other pre-treatment strategies [25].

A retention time region (3.6 – 3.9 min) from the LC run was selected because of the many metabolites eluting in this time window and Figure 4 shows the IM-MS data associated with this region. There is a significant reduction in background noise (indicated by an increase in blue/white shading) and an overall simplification of the drift time vs *m/z* analytical space. The IM and MS spectra shown in Fig. 4(b) and 4(c) were obtained by averaging the drift time and *m/z* data shown in Fig. 4(a). The resulting spectra (Fig. 4(b) and 4(c)) therefore correspond to those expected for LC-IM (Fig. 4(b)) and LC-MS (Fig. 4(c)) separations respectively.

It is possible to enhance selectivity for target analytes by utilising the orthogonal separation of the LC, IM and MS dimensions. This is illustrated in Fig. 5 for the *m/z* 162.1 ion, assigned to the endogenous metabolite carnitine ($C_7H_{15}NO_3$) [21]. The extracted ion chromatogram for this ion is shown in Fig. 5(a). The ion intensity

reaches a maximum at a retention time of 3.8 min and the selected ion mobility response for the *m/z* 162.1 ion in the ion mobility spectra acquired in the retention time window 3.6 – 3.9 min is shown in Fig. 5(b). The sharp peak observed in the drift time region corresponding to bins 20-25 contrasts with broad total ion mobility response observed in the same retention time window when all 200 bins were averaged, seen in Fig. 4(b). The mass spectrum obtained by averaging the spectra in the region 20-25 bins (Fig. 5(c)) has *m/z* 162 as the base peak. Comparing this spectrum with that shown in Fig. 4(c), which is equivalent to the LC-MS analysis without mobility selection, demonstrates the effectiveness of the orthogonal LC, IM and MS analysis in simplifying and improving spectral quality. Confidence in the assignment of targeted or unknown species is increased by the presence of an ion of the correct *m/z* at the expected IM drift time and the LC retention time associated with a metabolite.

4. Conclusions

This study demonstrates that nested LC-IM-MS data may be acquired on directly injected urine samples within the timescale of an LC-MS experiment. The combined LC-IM-MS approach has the potential to enhance the metabonomic coverage by the introduction of a gas-phase electrophoretic separation that is orthogonal to the reversed-phase LC and mass-to-charge MS separations. Data mining for the detection of a targeted analyte is also demonstrated yielding improved spectral quality and confidence in assignment.

Acknowledgements

We thank AstraZeneca UK for financial support and Waters Corporation, Manchester, for operational support for the IM-Q-TOF-MS.

References:

[1] J.K. Nicholson, J.C. Lindon, E. Holmes, Xenobiotica. 29 (1999) 1181

[2] M. Coen, E. Holmes, J.C. Lindon & J.K. Nicholson, Chem. Res Toxicol. 21 (2008) 9.

[3] E. Homes, H. Antti, Analyst. 127 (2002) 1549.

[4] R. Williams, E.M. Lenz, A.J. Wilson, J. Granger, I.D. Wilson, H. Major, C. Stumpf, R. Plumb, Mol. Biosyst. 2 (2006) 174.

[5] K. Yu, G. Sheng, J. Sheng, Y. Chen, W. Xu, X. Liu, H. Cao, H. Qu, Y. Cheng, L. Li, J. Proteome Res. 6 (2007) 2413.

[6] Q. Zhang, G. Wang, Y. Du, L. Zhu, A. Jiye, J. Chromatogr. B. 854 (2007) 20.

[7] R. Plumb, J. Granger, C. Stumpf, I.D. Wilson, J.A. Evans, E.M. Lenz, Analyst. 128 (2003) 819.

[8] I.D. Wilson, R. Plumb, J. Granger, H. Major, R. Williams, E.M. Lenz, J. Chromatogr. B. 817 (2004) 67.

[9] H. Lee, J. Liq. Chromatogr. Related Technol. 28 (2005) 1161.

[10] I.D. Wilson, J.K. Nicholson, Castro-Perez, J.H. Granger, K.A. Johnson, B.W. Smith, R.S. Plumb, J. Proteome Res. 4 (2005) 591.

[11] E.C. Soo, A.J. Aubry, S.M. Logan, P. Guerry, J.F. Kelly, N.M. Young, P. Thibault, Anal. Chem. 76 (2004) 619.

[12] E.M. Lenz, I.D. Wilson, J. Proteome Res. 6 (2007) 443.

[13] Y. Wang, O. Cloarec, H. Tang, J.C. Lindon, E. Holmes, S. Kochhar, J.K. Nicholson, Anal. Chem. 80 (2008) 1058.

[14] Ion Mobility Spectrometry, 2nd Edition, G Eiceman, Z Karpas, CRC Press, 2005.

[15] C.S. Creaser, J.R. Griffiths, C.J. Bramwell, S. Noreen, C.A. Hill, C.L.P. Thomas, Analyst. 129 (2004) 984.

[16] A B Kanu, P Dwivedi, M Tam, L Matz, H H Hill, J. Mass Spectrom. 43 (2008) 1.

[17] R M O'Donnell, X Sun, P de B Harrington, (2008) doi:10.1016/j.trac.2007.10.014.

[18] D.J. Weston, R. Bateman, I.D. Wilson, T.R. Wood, C.S. Creaser, Anal. Chem. 77 (2005) 7572.

[19] R.A. Sowell, K.E. Hersberger, T.C. Kaufman, D.E. Clemmer, Journal of Proteome Research. 6 (2007) 3637.

[20] X. Liu, S.J. Valentine, M.D. Plasencia, S. Trimpin, S. Naylor, D.E. Clemmer, J Am Soc Mass Spectrom. 7 (2007) 1249.

[21] L.M. Matz, H.M. Dion, H.H. Hill, J. Chromatogr. A. 946 (2002) 59.

[22] P. Dwivedi, P. Wu, S.J. Klopsch, G.J. Puzon, L. Xun, H.H. Hill, Metabolomics. 4 (2008) 63.

[23] S.Y. Vakhrushev, J. Langridge, I. Campuzano, C. Hughes, J. Peter-Katalinic, Anal. Chem. (2008) DOI10.1021/ac7023443 CCC.

[24] Bishop, C., Neural networks for pattern recognition. 1995: Oxford University Press.

[25] R. Arneberg, T. Rajalahti, K. Flikka, F.S. Berven, A.C. Kroksveen, M. Berle, K.M. Myhr, C.A. Vedeler, R.J.A Ulvik, O.M. Kvalheim, Anal Chem. 79 (2007) 7014.

[26] R.E. Williams, E.M. Lenz, J.S. Lowden, M. Rantalainen, I.D. Wilson, Mol. Biosyst. 1 (2005) 166.

Legends to Figures

Figure 1. Schematic diagram of the prototype IM-Q-TOF-MS spectrometer.

Figure 2. (a) LC chromatogram showing accumulated IM spectra derived from the LC-IM-MS analysis of urine obtained from male Wistar-derived rats, (b) mass spectrum corresponding to retention time window 1.0 – 1.3 min, (c) mass spectrum corresponding to retention window 5.5 – 6.0 min.

Figure 3. LC-IM-MS analysis of urine obtained from male Wistar-derived rats, (a) LC chromatogram, (b) the mass spectrum generated by summing all 200 mass spectra in each IMS scan during the LC run, (c) total ion mobility spectrum summed over all *m/z* values, (d) 2D plot of drift time (bins) versus *m/z* plot for the full data set.

Figure 4. (a) Drift time (bins) versus *m/z* plot of selected retention window 3.6-3.9 minutes derived from the LC-IM-MS analysis of rat urine, (b) total ion mobility spectrum corresponding to retention time window 3.6-3.9 minutes, (c) mass spectrum corresponding to total ion mobility spectrum of retention time window 3.6-3.9 minutes.

Figure 5. (a) Extracted ion chromatogram (XIC) for *m/z* 162.1 obtained from the LC-IM-MS analysis of male Wistar-derived rat urine, (b) selected ion mobility spectrum of *m/z* 162.1, corresponding to the selected retention time window 3.6-3.9 min, (c) mass spectrum corresponding to selected ion mobility spectrum for *m/z* 162.1 (IM bins 20-25 combined).

Figures

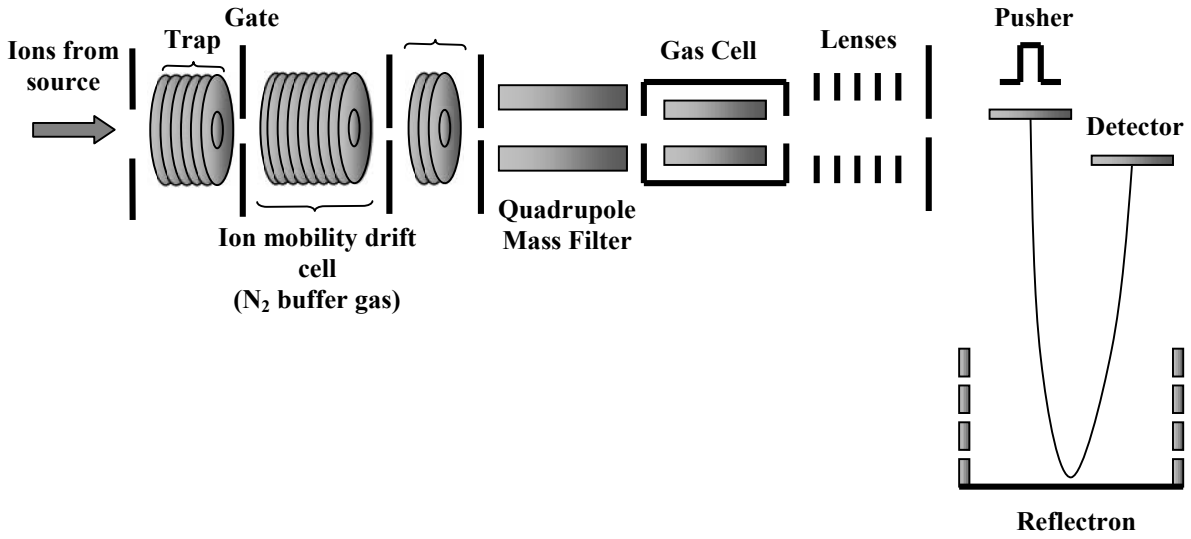

Figure 1

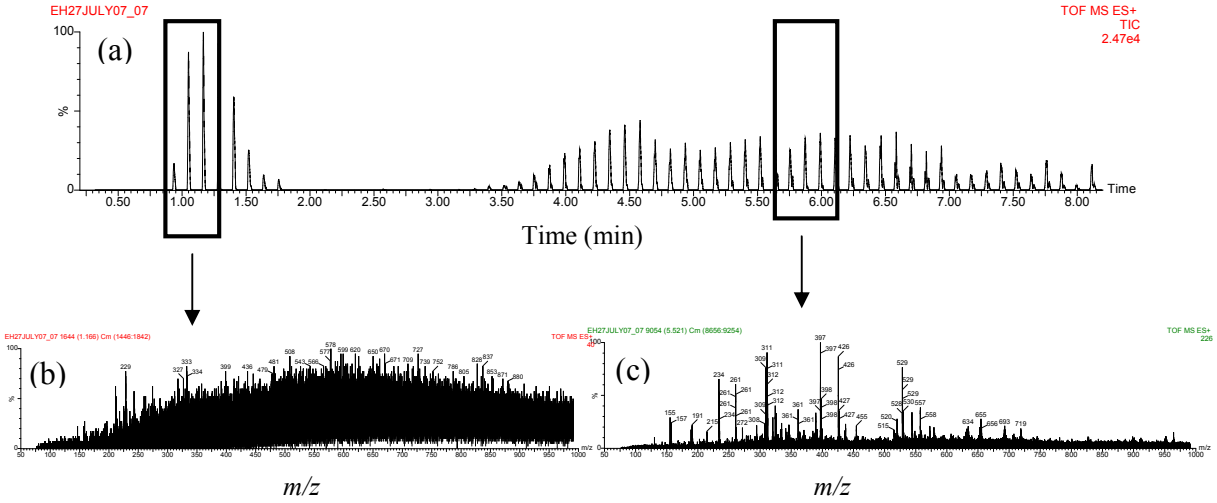
EH27JULY07_07
TOF MS ES+
TIC
2.47e4
(a)
100
%
0
0.50
1.00
1.50
2.00
2.50
3.00
3.50
4.00
4.50
5.00
5.50
6.00
6.50
7.00
7.50
8.00
Time
Time (min)
(b)
(c)
m/z
m/z

Figure 2

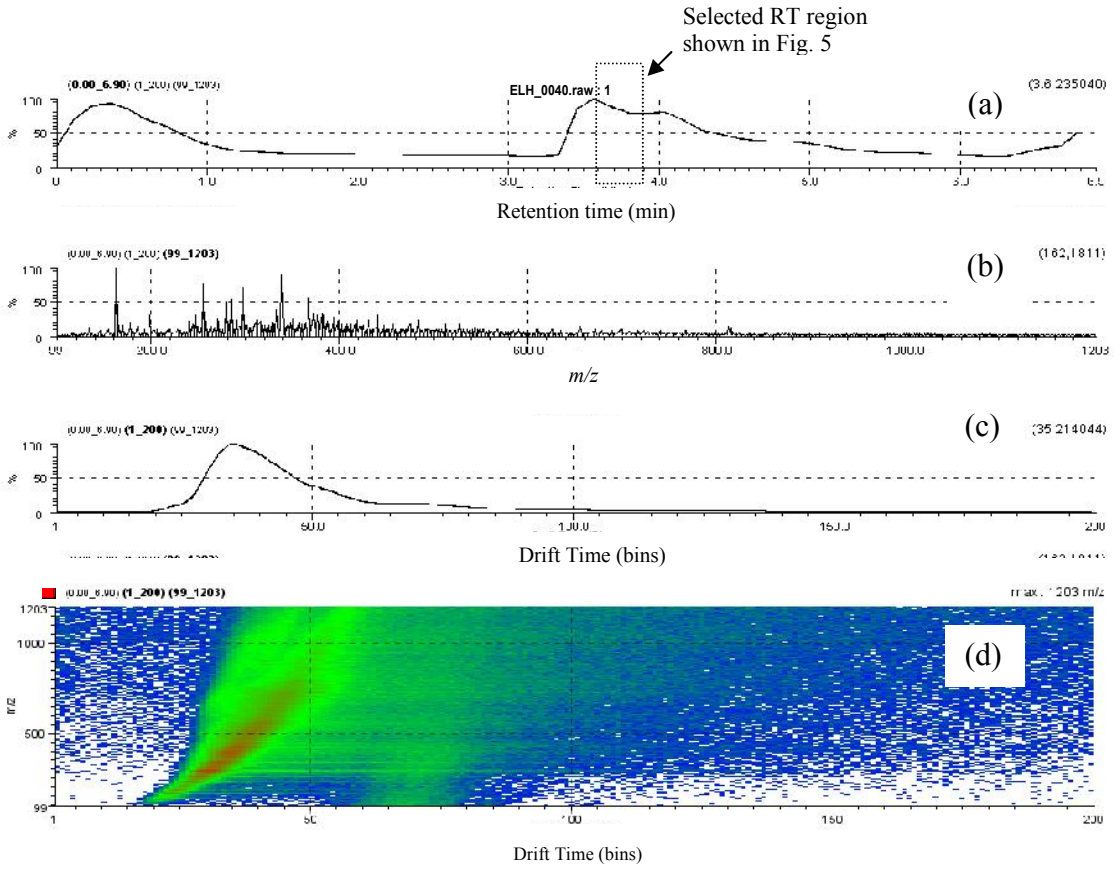
Selected RT region
shown in Fig. 5
ELH_0040.raw: 1
(a)
Retention time (min)
(b)
m/z
(c)
Drift Time (bins)
(d)
Drift Time (bins)

Figure 3

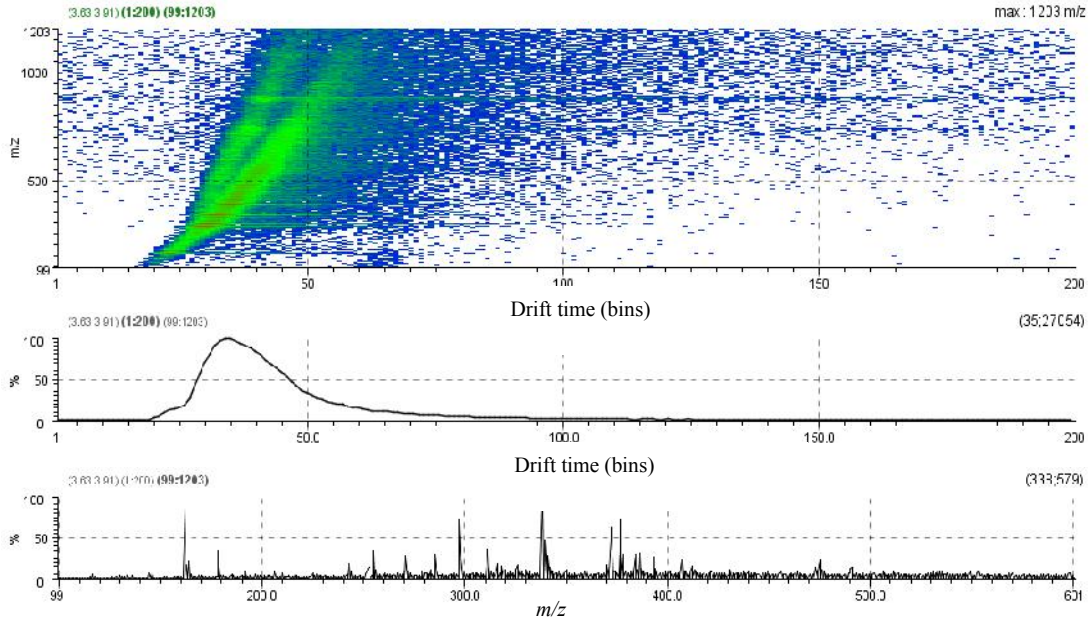
max : 1203 m/z
m/z
Drift time (bins)
(35;2754)
%
Drift time (bins)
(333;579)
%
m/z

Figure 4

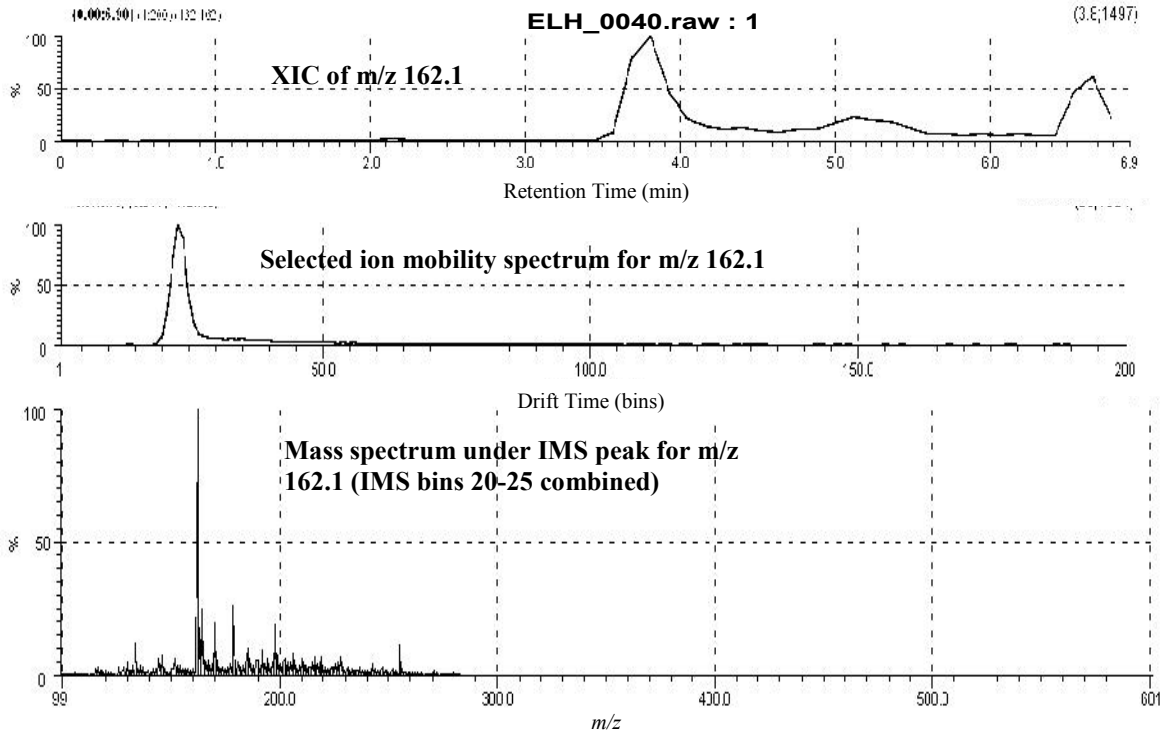
ELH_0040.raw : 1
XIC of m/z 162.1
Retention Time (min)
Selected ion mobility spectrum for m/z 162.1
Drift Time (bins)
Mass spectrum under IMS peak for m/z 162.1 (IMS bins 20-25 combined)
m/z

Figure 5

APPENDIX 3:

Direct analysis of pharmaceutical formulations from non-bonded reversed-phase thin layer chromatography plates by desorption electrospray ionisation-ion mobility-mass spectrometry

***Rapid Commun. Mass Spectrom*. 2009; 23: 2597.**

Emma L. Harry[1], James C. Reynolds[1], Anthony W. T. Bristow[2], Ian D. Wilson[3], Colin S. Creaser[1*]

[1] *Centre for Analytical Science, Department of Chemistry, Loughborough University, Leicestershire, LE11 3TU.*

[2] *AstraZeneca, Charter Way, Silk Road Business Park, Macclesfield, Cheshire, SK10 2NA, UK.*

[3] *AstraZeneca, Alderley Park, Macclesfield, Cheshire, SK10 4TF, UK.*

* Corresponding author:

Email. c.s.creaser@lboro.ac.uk

Tel. +44 (0)1509 222552

Fax. +44 (0)1509 223925

Abstract

The direct analysis of pharmaceutical formulations and active ingredients from non-bonded reversed-phase thin layer chromatography (RP-TLC) plates by desorption electrospray ionisation (DESI) combined with ion mobility-mass spectrometry (IM-MS) is reported. The analysis of formulations containing analgesic (paracetamol), decongestant (ephedrine), opiate (codeine) and stimulant (caffeine) active pharmaceutical ingredients is described, with and without chromatographic development to separate the active ingredients from the excipient formulation. Selectivity was enhanced by combining ion mobility and mass spectrometry to characterise the desorbed gas-phase analyte ions on the basis of mass-to-charge (*m/z*) ratio and gas-phase ion mobility (drift time). Varying the solvent composition of the DESI spray using a step gradient was employed to optimise the desorption of active pharmaceutical ingredients from the RP-TLC plates. The combined RP-TLC/DESI/IM-MS approach has potential as a rapid and selective technique for pharmaceutical analysis by orthogonal gas-phase electrophoretic and mass-to-charge separation.

Keywords:

Ion mobility-mass spectrometry; reversed-phase thin layer chromatography; DESI; Gradient DESI.

Desorption electrospray ionisation provides a means by which analytes can be sampled from the surface under ambient conditions, ionised and detected.[1]

Introduced in 2004 by Takats *et al.*[2] DESI lends itself to the analysis of molecules that are amenable to conventional electrospray ionisation (ESI). DESI has been reported for the analysis of both polar and non-polar analytes, including proteins and peptides,[3] pharmaceuticals,[4] metabolites,[5] lipids,[6] and biological tissues.[7] The desorption of analytes directly from surfaces by DESI is achieved by directing electrosprayed droplets at the surface under interrogation, producing ESI type spectra within a few seconds with the appropriate choice of desorbing solvent. Several ionisation mechanisms have been proposed including the well established chemical sputtering or droplet pick-up mechanism,[8] in which analytes on the surface are picked up by the impacting droplets, followed by gas phase ion formation via electrospray mechanisms. Alternative mechanisms involve charge transfer between a gas phase ion and analytes on the surface and gas-phase ion/molecule reactions.[9]

Thin layer chromatography (TLC) remains a widely used technique for the separation of mixtures for both qualitative and quantitative analysis, but has limitations with respect to the identification of the separated analytes. To overcome this limitation there have been many attempts to couple TLC with MS using ionization techniques such as fast atom bombardment (FAB) and matrix assisted laser desorption ionisation (MALDI).[10] In this context, DESI as a sample introduction method for MS seems ideally suited to combination with TLC and its use has been described with normal phase silica gel[11] and cellulose[12] plates for the study of medicinal herbs[13], dyes,[13-14] alkaloids,[15] proteins and peptides[16] and pharmaceutical formulations.[17] The application of DESI to the analysis of analytes from hydrophobic, reversed-phase

TLC plates with bonded silica phases has been investigated for the analysis of dyes[18-20]and caffeine extracted from beverages.[21] More recently, Wiseman *et al* reported the use of pressurised planar electrochromatography using reversed-phase C_{18} plates for the study of steroids.[22] DESI/MS has also been employed for the chemical imaging of dyes separated on TLC plates.[11] The desorption of analytes from non-bonded, reversed-phase TLC plates by DESI has not been previously reported and presents additional challenges because the plates cannot be pre-cleaned to reduce background contamination prior to analyte deposition and there may be interference from stationary phase molecules being desorbed together with the analyte.

Ion mobility spectrometry is a gas-phase electrophoretic technique which allows ionized analytes to be characterised on the basis of their ion mobility (K), defined by the reduced mass (μ), charge (e) and collision cross section (Ω) (*i.e.,* size and shape) of the ion (Eqn 1)[23]

$$K = \left(\frac{3ze}{16N}\right)\left(\frac{2\pi}{\mu k_B T}\right)^{1/2}\left(\frac{1}{\Omega_D}\right) \qquad \text{Eqn 1}$$

where N is the number density of the buffer gas, k_B is the Boltzmann constant and T is the temperature. The time (t_d) taken for an analyte ion to traverse a drift cell (of length l), under the influence of a weak electric field (E) and in the presence of a buffer gas is determined by the mobility of the ion (Eqn 2), so mixtures of analyte ions may be separated on the basis of their relative drift times which are typically on the millisecond timescale.

Eqn 2

$$t_d = l/\mathrm{K.E}$$

The combination of ion mobility spectrometry with mass spectrometry (IM-MS), allows gas-phase ions generated in the DESI ion source to be separated first by their mobility in a drift cell and then by mass-to-charge ratio in the mass analyser, providing a multidimensional separation with increased selectivity for the analytes of interest.

DESI/IM-MS has been reported for the direct analysis of active ingredients in pharmaceutical formulations, demonstrating the benefits offered by the additional dimension of IM.[24] Further studies described the use of DESI/IM-MS for the analysis of peptides[25] and conformational studies of folded and denatured states of proteins.[26] In more recent investigations, DESI was coupled with a travelling-wave based ion mobility-mass spectrometer for the analysis of drugs.[27]

In this paper, we describe the use of DESI/IM-MS for the detection of active pharmaceutical ingredients deposited and developed on non-bonded reversed-phase TLC plates. A step gradient of the desorption solvent was used to optimise the DESI solvent composition.

Experimental

Materials

Acetonitrile (HPLC gradient grade) and water (HPLC grade) were purchased from Thermo Fisher Scientific (Loughborough, UK). Mass spectrometry grade (puriss, p.a) formic acid was purchased from Sigma-Aldrich (Gillingham, UK). Generic Co-codamol tablets containing 500 mg paracetamol and 8 mg codeine and a generic cold and flu tablets containing 250 mg paracetamol, 25 mg caffeine and 8mg ephedrine were purchased over the counter.

Sample preparation

Tablets were crushed and extracted in water (2 mL) and filtered (Whatman filter paper, qualitative). The extracted solution was manually spotted onto the reversed-phase hydrocarbon impregnated silica gel TLC plates (Analtech Uniplates, Newark, USA; 10 x 20 cm, 250 microns) in 1µL aliquots up to 6µL in total volume. The plates were developed in a saturated chamber with 50/50 (v/v) methanol-water.

DESI/IM-MS analysis

The DESI/IM-MS ion source region is shown in Figure 1. All experiments were carried out employing a prototype IM-quadrupole time-of-flight mass spectrometer (Waters Corporation, Manchester) which has been described in detail elsewhere.[24] The atmospheric pressure ionisation (API) region of a Z-spray electrospray ionisation

source was modified for DESI by attaching a section of TLC plate to a manipulator, allowing horizontal, vertical and rotational manipulation of the plate, which was located in the atmospheric pressure ionisation region of the mass spectrometer at an approximate 45° angle relative to the spray tip and cone. A Waters Alliance 2790 chromatograph (Waters Corporation, Manchester, UK) was coupled to the modified DESI ion source of the IM-Q-ToFMS spectrometer to provide the DESI solvent flow. A split was employed to reduce the solvent flow rate to the DESI probe (typically 25 μL/min) from the higher flow through the LC system (200 μL/min). The area of sample desorbed when the DESI probe and sample position were optimised was approximately 1 mm in diameter. Variable solvent composition experiments were carried out in which the TLC plate was analysed using three different solution compositions using the following step gradient: 10% A (0-1.5 min), increased to 50% A (1.5-3.0 min) and then to 90% A (3.0-4.5 min), where A = 0.1% aqueous formic acid and B = 0.1% formic acid in acetonitrile. At each gradient step change the DESI source was moved in the vertical plane ensuring that an area of the TLC plate under interrogation had not previously been exposed or desorbed. Solvent and gas flow directed at the ionisation surface also creates a washing effect. The vertical movement of the sample stage ensured that that the solvent plume from the previous row was not interrogated.

The IM-Q-ToFMS was operated in positive ion mode with the ESI capillary voltage set to 3.5 kV; cone voltage 40 V; source temperature 120 °C; desolvation gas, N_2 gas flow 250 L/hr; desolvation gas temperature, 180 °C. Ions from the DESI source were directed into the trap region at the head of the ion mobility drift cell and periodically gated into the drift cell, which was operated in the pressure region of 1.0 to 3.0 Torr N_2, using a gate electrode pulse (3.50 V, 200 μs pulse width and 15ms pulse period).

The IM drift tube consisted of a multi-plate ion guide (15.2 cm in length) to which a voltage gradient (14.24 V/cm and a supplement RF voltage 3.8 V) were applied. Ions passing through the drift region were then directed through the quadrupole and collision cell into the reflectron TOF mass analyser. The quadrupole was operated in wide band pass mode (*m/z* 50-1000) and the collision cell without any collision gas. Ion mobility spectra were acquired by collecting data from 200 TOF pushes (45 μs per bin) and plotting drift time (scan number) against mass-to-charge ratio (*m/z*). IM-MS data were typically accumulated for 5 s, with a 2 s interscan delay. Acquired data were presented as a plot of time against ion intensity; total ion mobility response or selected ion mobility responses. Masslynx version 4.1 (Waters Corporation, Manchester, UK) was used to control the IM-MS instrument and for data acquisition and processing.

Results and discussion

Pharmaceutical formulations containing paracetamol, caffeine, codeine and ephedrine were analysed by DESI/IM-MS directly from the surface of non-bonded RP-TLC plates, generating mass-to-charge and mobility data for the desorbed ions. Optimisation of the positioning of the sample relative to the atmospheric pressure ionisation region of the mass spectrometer, including the spray tip and cone (Figure 1) was found to be a critical parameter influencing analyte signal intensity. The optimum position was determined by manipulation of the sample in the horizontal, vertical and rotational planes with the maximum analyte response observed at an

angle of 45° relative to the spray tip and cone. A further parameter found to effect analyte responses significantly was the DESI solvent flow rate. An increase in flow correlated with an increase in analyte signal response and the amount of analyte desorbed from the RP-TLC plate surface. The signal intensity for the active ingredients paracetamol and codeine showed a nine-fold increase when the DESI solvent flow rate was increased from 2 μL/min to 5 μL/min. A further increase in ion intensity was observed up to a flow rate of 50 μL/min, but only a small increase in signal response was observed at flow rate above an optimised flow of 25 μL/min. The TLC plates showed a clear "wetting effect", with a solvent layer forming on the surface under interrogation by the incident electrospray, which facilitates the extraction of analytes from the surface into the thin liquid layer.

High noise levels were observed in the resulting DESI mass spectra, presumably as a result of interferences present on the plate or ablation of the hydrocarbon stationary phase, which was a non-bonded phase and could not, therefore, be washed prior to sample loading. IM-MS data were acquired by repetitive scanning of nested data sets, with mass spectra (45 μs/scan) and IM spectra (~13 ms) scanned repetitively throughout the LC run. Spectra were accumulated to yield 200 mass spectra and one ion mobility spectrum every 7 s. The ion mobility drift time is plotted as 'bins', where each bin corresponds to an acquired mass spectrum. The nested data acquisition of IM and MS data results in an analysis incorporating a gas-phase electrophoretic separation of the ESI generated ions on the basis of charge state and collision cross section (i.e. size and shape), between the mass analysis, all within the timescale of the MS run.

Total ion and selected ion mobility responses for the active pharmaceutical ingredients extracted from a generic cold and flu tablet, including ephedrine, paracetamol and caffeine, deposited on the TLC plate without solvent development, are displayed in Figure 2. Selected ion responses for protonated ephedrine (*m/z* 168; Figure 2(a)), paracetamol (*m/z* 152; Figure 2(b)), and caffeine (*m/z* 195; Figure 2(c)) showed drift times of 0.90 ms (bin 20), 0.95 ms (bin 21) and 1.04 ms (bin 23) respectively. The selected ion responses are much cleaner and sharper then the total ion mobility spectrum with peak widths at half height of 5 bins (ephedrine), 3 bins (paracetamol) and 4 bins (caffeine) compared to 11 bins for the total ion mobility spectrum. The corresponding mass spectra are also shown in Figure 3. The mass spectrum obtained by combining all 200 bins (Figure 3(d)) corresponds to the mass spectrum expected in the absence of IM separation and contain a large number of desorbed ions across the whole mass range. In contrast, when the mass spectra obtained by combining bins at the drift times (bins 15-24, 18-23 and 21-25; Figure 2) of the active ingredient peaks (Figures 3(a), (b) and (c)) are compared to the mass spectrum from the combined total ion mobility response, the enhanced selectivity for the actives is observed. The resulting mass spectra show fewer ions and, in the case of paracetamol (*m/z* 152) and caffeine (*m/z* 195), the $[M+H]^+$ ion is the base peak. Paracetamol was the most abundant component in the cold and flu tablet (250 mg per tablet); however, caffeine (25 mg per tablet) showed the highest IM-MS response, as a result of higher DESI ionisation efficiency from the TLC plate. On the basis of the amount of active ingredient spotted on the plate the limit of detection (LOD) (3:1 signal-to-noise) was estimated to be 16 $\mu g/cm^2$, 34 $\mu g/cm^2$ and 239 $\mu g/cm^2$ for caffeine, ephedrine and paracetamol respectively.

Total ion and selected ion mobility responses obtained from the DESI/IM-MS analysis of paracetamol and codeine extracted from a generic Co-codamol tablet, following separation by TLC, are displayed in Figure 3, together with an image of the developed reversed-phase plate. LOD were again estimated on the basis of the amount spotted for both the active ingredients within the co-codamol tablet. Paracetamol was found to have a LOD of 225 μg/cm^2 and codeine 9 μg/cm^2. This lower limit of detection for paracetamol following chromatographic separation may be due to the distribution of paracetamol in the developed and undeveloped spots or reduced ion suppression due to separation of the excipient components from the active pharmaceutical ingredient. The drift time for paracetamol (Figure 4(a)) was 0.90 ms (bin 20) showing good IM reproducibility for the RP-TLC/DESI/IM-MS analysis of paracetamol (Figure 2(b)). The sharp peak observed in the *m/z* 152 selected ion response for paracetamol (Figure 4(a)) contrasts with the broad total ion mobility response when all 200 bins were averaged, shown in Figure 4(b). The mass spectrum obtained by averaging the spectra in the range bin 19-23 (Figure 4(c)) has *m/z* 152 as the base peak. Comparing this spectrum with that shown in Figure 4(d), which is equivalent to the DESI-MS analysis without mobility selection, demonstrates the effectiveness of the orthogonal IM and MS analysis in simplifying and improving spectral quality. Analysis of the developed codeine spot also shows an increased selectivity for the active ingredient. Figure 5 displays the total ion response and the selected ion response for *m/z* 300, assigned to protonated codeine with a drift time of 2.3 ms. The corresponding mass spectra are shown in Figure 5(c) and 5(d). Comparing the mass spectrum corresponding to the codeine selected ion response with the total ion response shows that the additional separation of ion mobility improves selectivity for codeine. It should be noted that the paracetamol (Figure

4(a)), and codeine (Figure 5(a)), selected ion mobility responses were fully resolved by the ion mobility separation.

Method development experiments, although essential are often time consuming and relatively expensive. In this work, the solvent composition of the DESI spray was varied by employing a step gradient to determine the optimum solvent for desorption. Extracted Co-codamol was spotted onto the TLC plate, which was analysed sequentially using three different solvent compositions (90:10, 50:50, 10:90, acetonitrile:water with 0.1% formic acid). Figure 6 shows signal response (*m/z* 300) versus % organic solvent. Signal responses were determined from the mass spectra corresponding to the selected ion mobility response for codeine combining bins across the peak at half height. It can be seen that codeine displayed increasing signal response as the organic component of the spray was reduced, which correlates with the high aqueous solubility of codeine (1 g in 0.7 mL at 25 °C). A greater % of water would facilitate extraction of codeine from the surface of the TLC plate into the wetted surface layer.

Chemical imaging of the developed codeine spot was carried out by rastering across the spot to obtain a 1-D image. The DESI sampling stage was moved in increments of 0.5 mm in the vertical plane to move the DESI plume across the spot and IM-MS spectrum were acquired and accumulated at each point. Ion mobility spectra, consisting of 200 mass spectra (bins), were averaged and the selected ion mobility response for *m/z* 300 extracted from the data. The image obtained for the mass spectral ion intensity of *m/z* 300 at the drift time for codeine, is displayed in Figure 7. The codeine response for the TLC spot shows a maximum intensity at 16 mm

corresponding to the R_f of codeine (R_f = 0.16). The 1-D image allows peak areas to be calculated for quantitative analysis by DESI.

Conclusion

This study has demonstrated that active pharmaceutical ingredients can be desorbed by DESI directly from non-bonded RP-TLC plates, with or without separation from the excipient components. Variation of the solvent composition of the DESI spray using a step gradient allows the optimisation of the method for analytes can be achieved with reduced development times. The combined RP-TLC/DESI/IM-MS approach has been shown to have potential to enhance selectivity for analytes compared to DESI/MS alone. Improved mass spectral quality was observed in all cases when IM separation was used in conjunction with mass spectrometry as a result of the orthogonal mobility and mass-to-charge separation.

Acknowledgements

We thank AstraZeneca UK for financial support and Waters Corporation, Manchester, for operational support of the IM-Q-ToFMS.

References

[1] Pasilis SP, Kertesz V, Van Berkel GJ, Schulz M, Schorcht S. *Anal Bioanal Chem*. 2008; **324**: 391.

[2] Takats Z, Wiseman JM, Gologan B, Cooks RG. *Science*. 2004; **306**: 471.

[3] Bereman MS, Nyadong L, Fernandez FM, Muddiman DC. *Rapid Commun. Mass Spectrom*. 2006; **20**: 3409.

[4] Takats Z, Wiseman JM, Cooks RG. *J. Mass Spectrom*. 2005; **40**: 1261.

[5] Chen H, Pan Z, Talaty N, Raftery D. Cooks RG. *Rapid Commun. Mass Spectrom*. 2006; **20**: 1577.

[6] Manicke NE, Wiseman JM, Ifa DR, Cooks RJ. *J Am Soc Mass Spectrom*. 2008; **19**: 531.

[7] Kertesz V, Van Berkel GJ, Vavrek M, Koeplinger KA, Schneider BB, Covey TR. *Anal. Chem*. 2008; **80**: 5168.

[8] Costa AB, Cooks RG. *Chem. Commun*. 2007:3015

[9] Venter A, Nefliu M, Cooks RG. *Trends in Analytical Chemistry*. 2008; **27**: 284.

[10] Wilson ID. *J. Chromatogr. A*. 1999; **856**: 429.

[11] Van Berkel GJ, Kertesz V. *Anal. Chem*. 2006; **78**: 4938.

[12] Pasilis SP, Kertesz V, Van Berkel GJ, Schulz M, Schorcht S. *Anal Bioanal Chem*. 2008; **324**:
391.

[13] Pasilis SP, Kertesz V, Van Berkel GJ. *Anal. Chem*. 2007; **79**: 5956.

[14] Kertesz V, Van Berkel GJ. *Rapid Commun. Mass Spectrom* . 2008; **22**: 2639.

[15] Van Berkel GJ, Tomkins BA, Kertesz V. *Anal. Chem*. 2007; **79**: 2778.

[16] Pasilis SP, Kertesz V, Van Berkel GJ. Schulz M, Schorcht S.*J. Mass Spectrom*. 2008; **43**: 1627.

[17] Van Berkel GJ, Ford MJ, Deibel. *Anal. Chem*. 2005; **77**: 1207.

[18] Yao Lin S, Huang MZ, Chang HC, Shiea J. *Anal. Chem*. 2007; **79**: 8789.

[19] Ford MJ, Van Berkel GJ. *Rapid Commun. Mass Spectrom*. 2004; **18**; 1303.

[20] Ford MJ, Kertesz V, Van Berkel GJ. *J. Mass Spectrom*. 2005; **40**: 866.

[21] Ford MJ, Deibel MA, Tomkins BA, Van Berkel GJ. *Anal.Chem*. 2005; **77**: 4385

[22] Janecki DJ, Novonty AL, Woodward SD, Wiseman JM, Nurok D. *Journal of Planar Chromatography*. 2008; **21**: 11.

[23] Creaser C, Griffiths JR, Bramwell CJ, Noreen S, Hill CA, Thomas CLP, *Analyst*. 2004; **129**: 984.

[24] Weston DJ, Bateman R, Wilson ID, Wood TR, Creaser CS. *Anal. Chem*. 2005; **77**: 7572.

[25] Kaur-Atwal G, Weston DJ, Green PS, Crosland S, Bonner PLR, Creaser CS. *Rapid Commun. Mass Spectrom.* 2007; **21**: 1131.

[26] Myung S, Wiseman JM, Valentine SJ, Takats Z, Cooks RG, Clemmer DE. *J. Phys. Chem. B*. 2006; **110**: 5045.

[27] Williams P, Scrivens JH. *Rapid Commun. Mass Spectrom*. 2008; **22**: 187.

Legends to figures

Figure 1. (a) Schematic diagram of DESI source and mass spectrometer interface, (b) photograph of the ion source region.

Figure 2. Ion mobility spectrum and selected ion mobility responses for the DESI/IM-MS analysis of a generic cold and flu tablet obtained from a RP-TLC plate without development, using DESI with a solvent composition of 50:50 (v/v) acetonitrile:water with 0.1% formic acid at a flow rate of 25 µl/min. (a) *m/z* 168 (ephedrine), (b) *m/z* 152 (paracetamol), (c) *m/z* 195 (caffeine), and (d) total ion mobility spectrum.

Figure 3. Mass spectra corresponding to selected ion mobility responses for the DESI/IM-MS analysis of a generic cold and flu tablet obtained from a RP-TLC plate without development (a) bins 15-24 (ephedrine), (b) bins 18-23 (paracetamol), (c) bins 21-25 (caffeine), and, (d) mass spectrum obtained by combining all 200 bins acquired during the ion mobility separation.

Figure 4. Ion mobility spectrum and selected ion mobility response for the DESI/IM-MS analysis of a generic Co-codamol tablet obtained from a RP-TLC plate following chromatographic development, using DESI with a solvent composition of 50:50 (v/v) acetonitrile:water with 0.1% formic acid at a flow rate of 20 µl/min. (a) selected ion response for *m/z* 152 (paracetamol), (b) total ion mobility spectrum, (c) mass spectrum corresponding to the selected ion response for *m/z* 152 (bins 19-23), (d) mass spectrum obtained by combining all 200 bins acquired during the ion mobility separation.

Figure 5. Ion mobility spectrum and selected ion mobility response for the DESI/IM-MS analysis of a generic Co-codamol tablet (conditions as Figure 4), (a) selected ion response for *m/z* 300 (codeine), (b) total ion mobility spectrum, (c) mass spectrum corresponding to the selected ion response for *m/z* 300 (bins 48-59), (d) mass spectra corresponding to the total ion response.

Figure 6. RP-TLC/DESI/IM-MS analysis of an extracted Co-codamol tablet employing a step gradient for the DESI analysis (90:10, 50:50, 10:90, acetonitrile:water with 0.1% formic acid): signal response versus % organic solvent for *m/z* 300 ion (codeine).

Figure 7. RP-TLC/DESI/IM-MS selected ion response for scanned 1-D image, showing signal distribution along a lane of the codeine TLC spot (*m/z* 300 and bin 53). Dashed line represents scan direction.

Figures

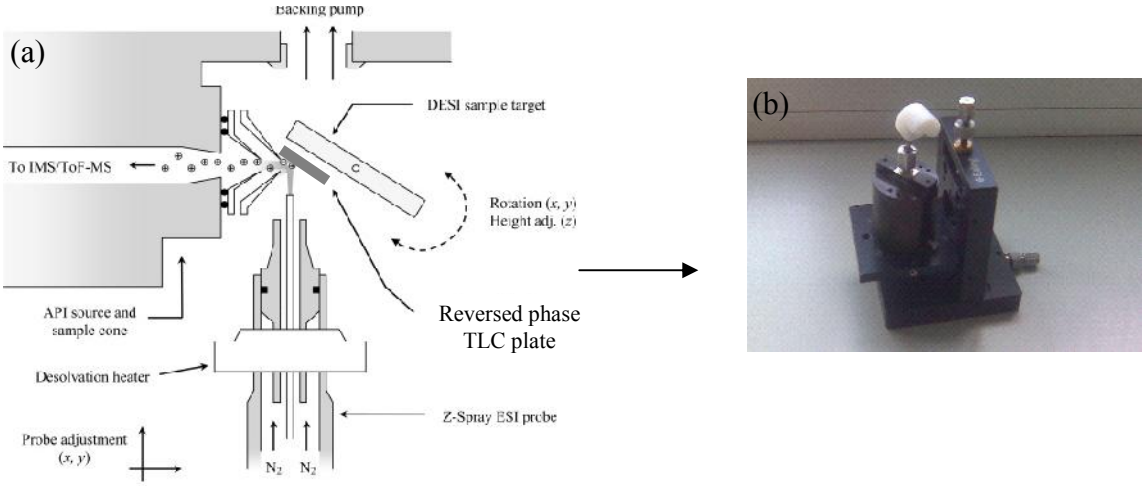

Figure 1

Figure 2

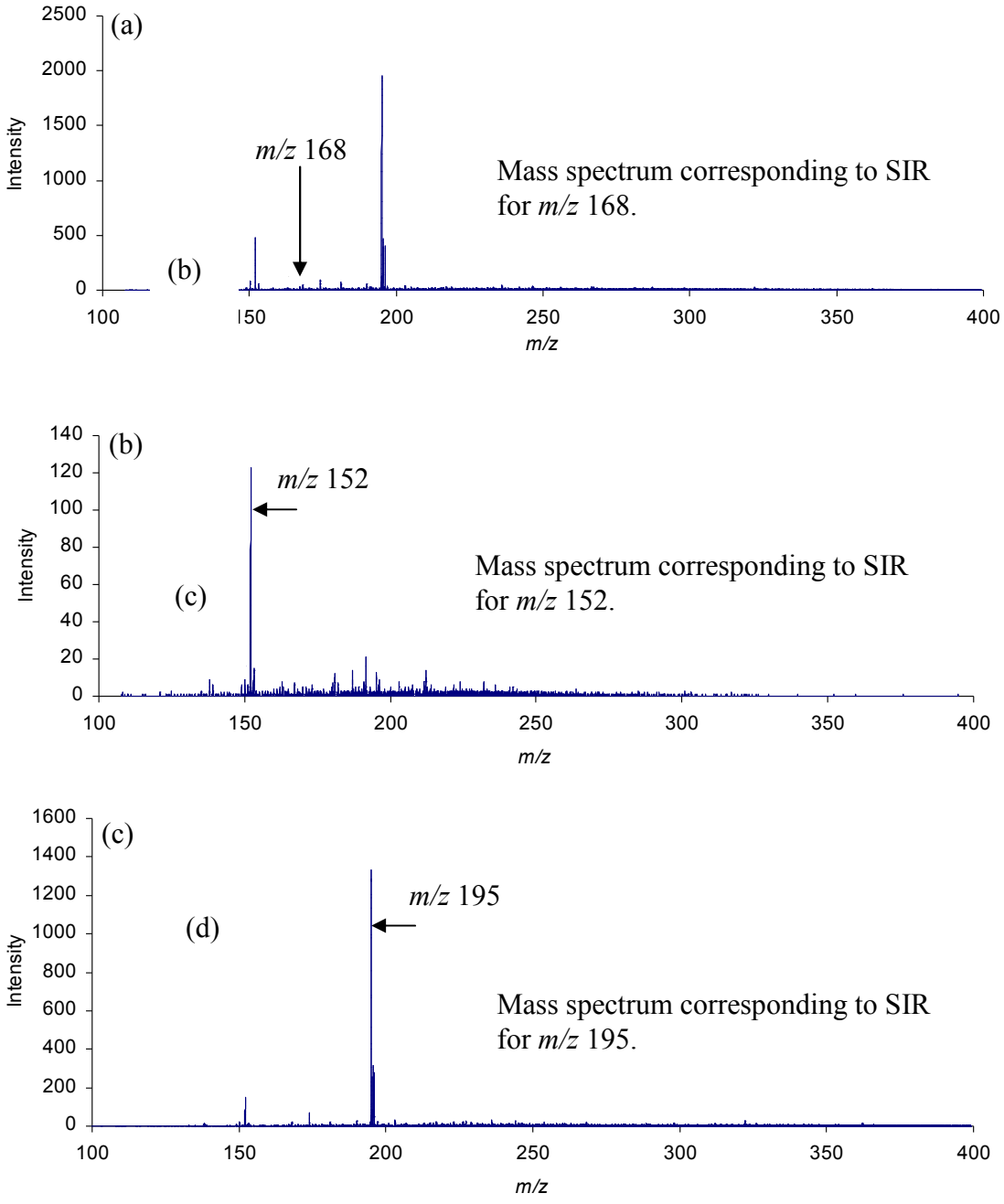
(a)
(b)
(c)
(d)
m/z 168
m/z 152
m/z 195
Mass spectrum corresponding to SIR for m/z 168.
Mass spectrum corresponding to SIR for m/z 152.
Mass spectrum corresponding to SIR for m/z 195.
Intensity
m/z

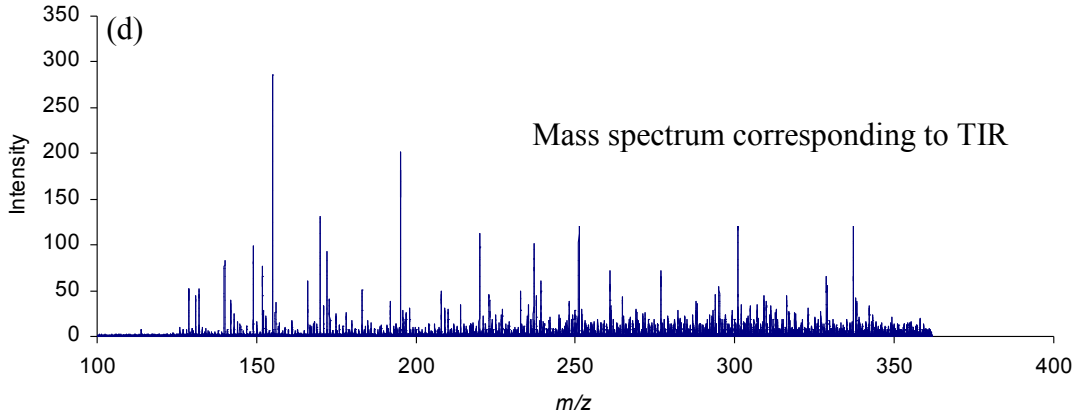
(d)
Mass spectrum corresponding to TIR
Intensity
m/z

Figure 3

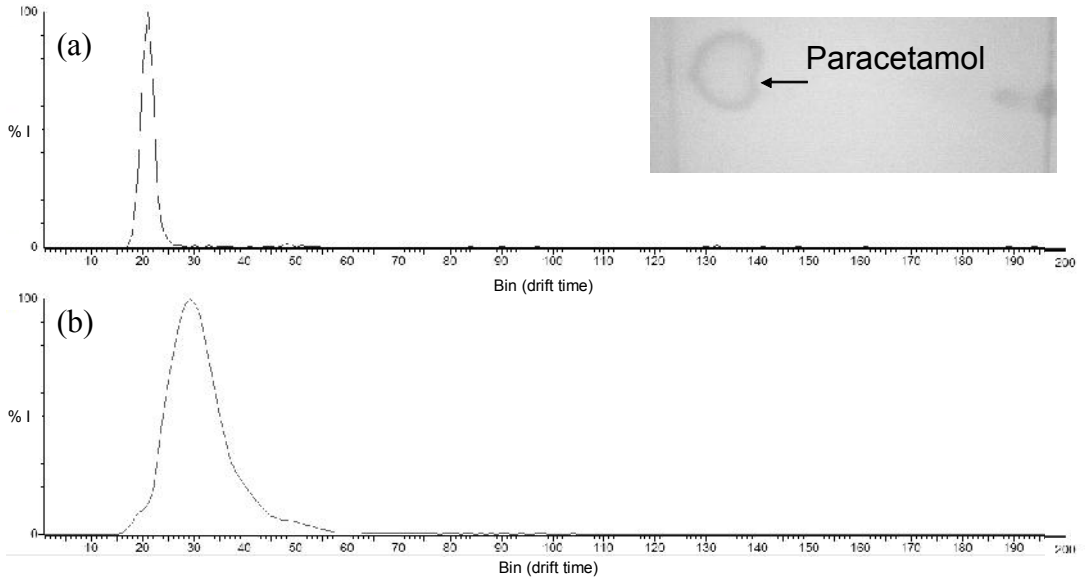
(a)
Paracetamol
Bin (drift time)
(b)
Bin (drift time)

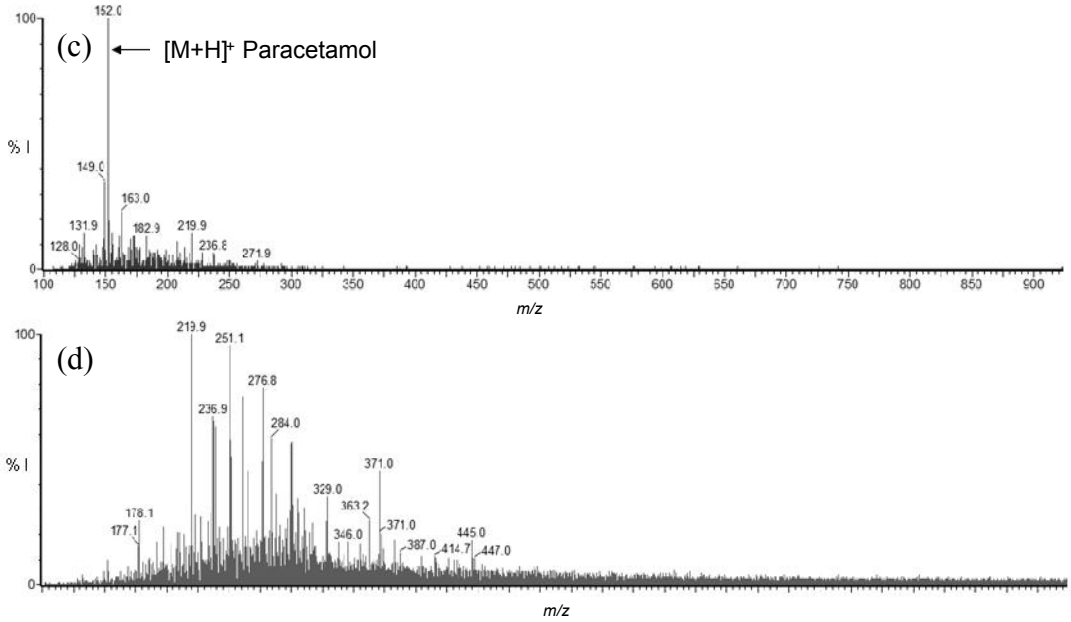
(c)
[M+H]+ Paracetamol
m/z
(d)
m/z

Figure 4

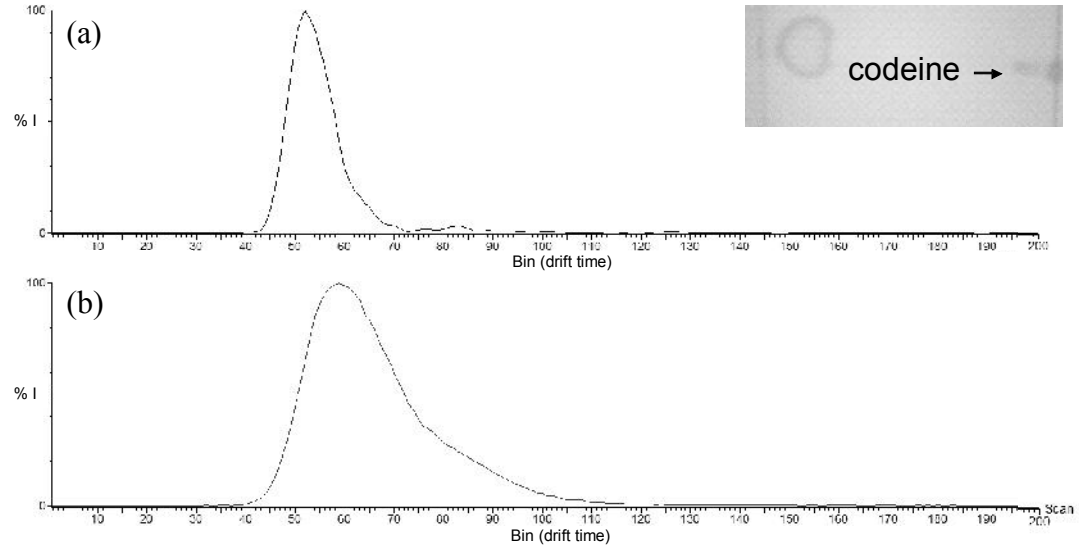

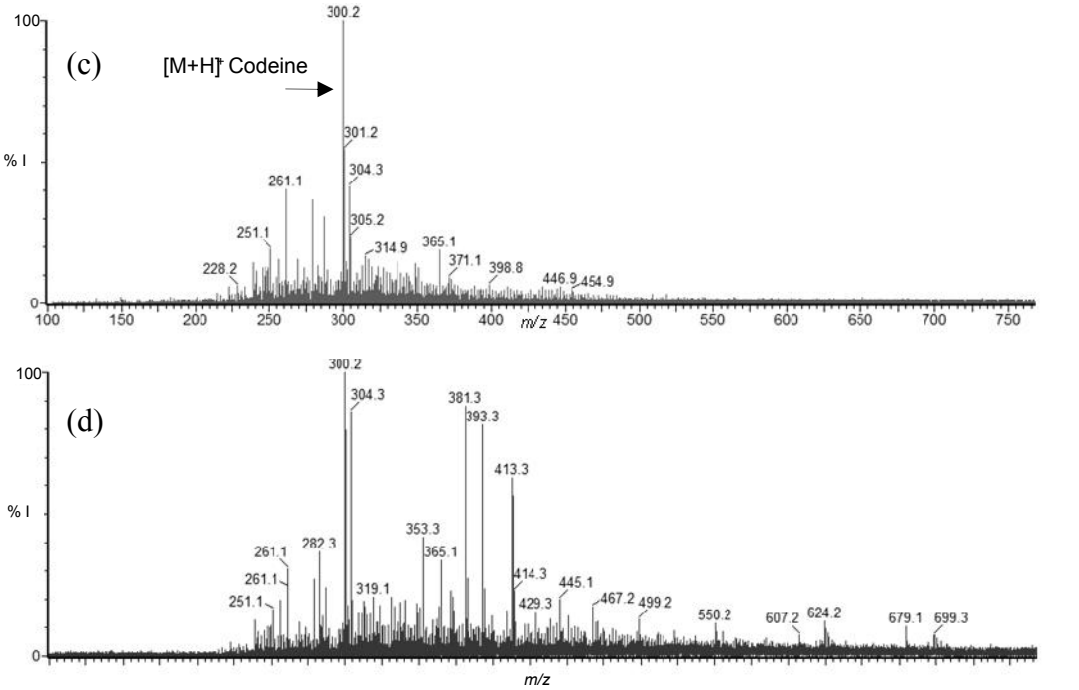

Figure 5

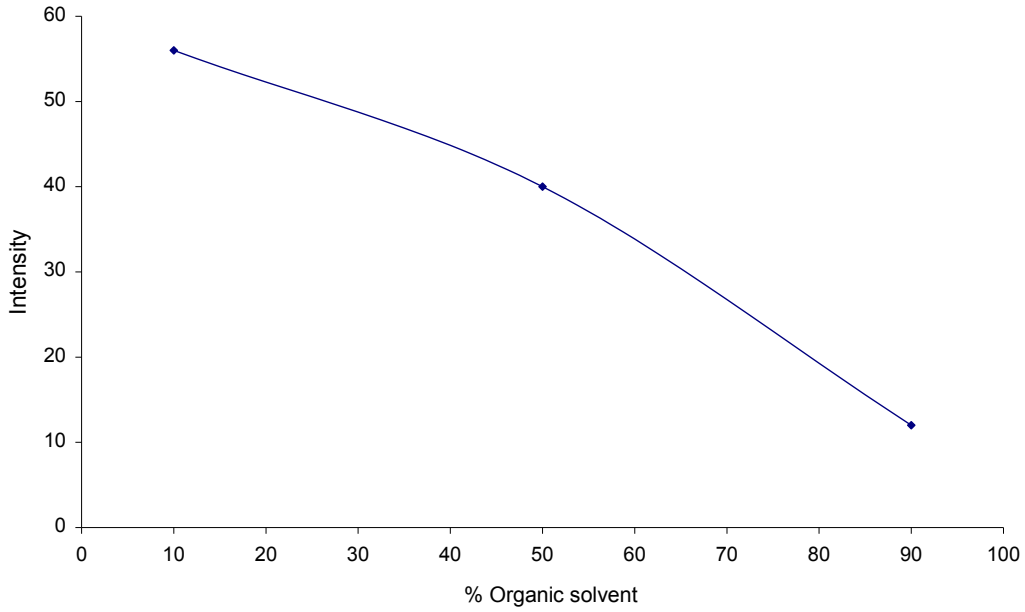

Figure 6

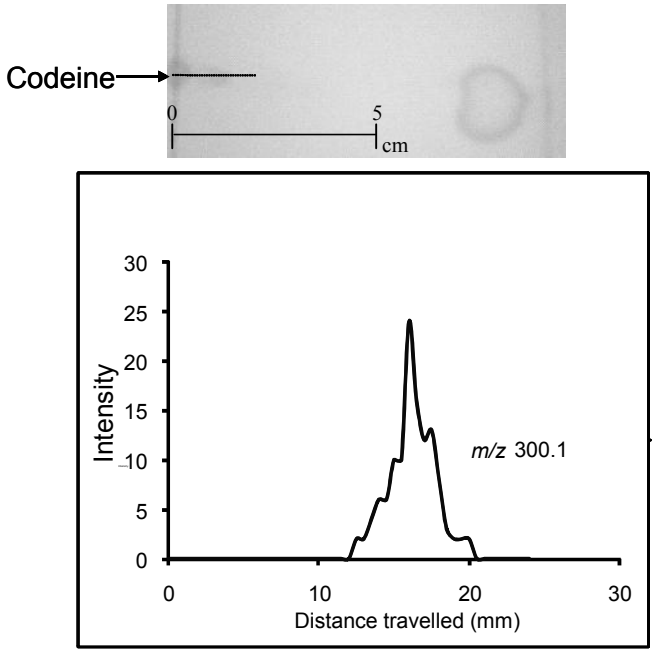

Figure 7

APPENDIX 4:

Real-time reaction monitoring using ion mobility-mass spectrometry

***Analyst*. 2011; 136: 1728.**

Emma L. Harry[1], Anthony W.T. Bristow[2], Ian D. Wilson[3] and Colin S. Creaser[1*]

[1] *Centre for Analytical Sciences, Department of Chemistry, Loughborough University, Leicestershire, LE11 3TU.*

[2] *AstraZeneca, Charter Way, Silk Road Business Park, Macclesfield, Cheshire, SK10 2NA, UK.*

[3] *Clinical Pharmacology, Drug metabolism and Pharmacokinetics Dept., AstraZeneca, Alderley Park, Macclesfield, Cheshire, SK10 4TG, UK.*

* Corresponding author:

Email. c.s.creaser@lboro.ac.uk

Tel. +44 (0)1509 222552

Fax. +44 (0)1509 223925

Summary

The potential of ion mobility (IM) spectrometry in combination with mass spectrometry (MS) for real-time reaction monitoring is reported. The combined IM-MS approach using electrospray ionization affords gas-phase analyte characterization based on both mass-to-charge (*m/z*) ratio and gas-phase ion mobility (drift time). The use of IM-MS analysis is demonstrated for the monitoring of the reaction products formed when 7-fluoro-6-hydroxy-2-methylindole is deprotonated by aqueous sodium hydroxide. Real-time reaction monitoring was carried out over a period of several hours, with the reaction mixture sampled and analysed at intervals of several minutes. Results indicate that spectral quality is improved when employing IM-MS, compared to mass spectrometry alone, as the complexity of the reaction mixture increases with time. The combined IM-MS approach has potential as a rapid and selective technique to aid pharmaceutical process control and for the elucidation of reaction mechanism.

Introduction

Process understanding and validation is an essential requirement for process control, to assure quality and purity in the manufacture of chemicals and pharmaceuticals. The Food and Drug Administration (FDA) has recognised that process knowledge is key to quality and, through better understanding, to building a cause and effect model that improves process control.[1] The pharmaceutical industry also requires quick, efficient, sensitive and high throughput methods for both quality control and quality assurance of drug products. Real-time reaction monitoring can provide detailed information about the course of a reaction and in turn aid process understanding. Current techniques employed for real-time reaction monitoring include, liquid chromatography (LC),[2] mass spectrometry,[3] infrared spectroscopy,[4] nuclear magnetic resonance[5] and near infrared spectrometry[6] However, there is a need to develop new approaches for real-time reaction monitoring that provide enhanced quantitative and structural information on reaction intermediates and products.

Ion mobility spectrometry (IM) is a gas phase electrophoretic technique which allows ionised analytes to be characterised on the basis of their ion mobility (K) in the presence of a buffer gas and under the influence of a weak electric field. K is defined by the reduced mass (μ), charge (e), and collision cross section (Ω), which is determined by the size and shape of the ion, according to Eq. (1)[7]

$$K = \left(\frac{3ze}{16N}\right)\left(\frac{2\pi}{\mu k_B T}\right)^{1/2}\left(\frac{1}{\Omega_D}\right) \qquad \text{Eq. 1}$$

Where N is the number density of the buffer gas, k_B is the Boltzmann constant and T is the temperature. The drift time (t_d) of an ion is the time taken to transverse a drift cell (of length l), under the influence of the electric field (E) and in the presence of the buffer gas, and is determined by the mobility of the ion. Mixtures of analyte ions may, therefore, be separated on the basis of their relative drift times which are typically in the millisecond timescale Eq. (2)

$$t_d = l/\mathrm{K.E} \qquad \text{Eq. 2}$$

The combination of ion mobility spectrometry with mass spectrometry (IM-MS) allows gas-phase ions generated in an electrospray ion source to be separated first by their ion mobility in a drift cell and then by mass-to-charge ratio in the mass analyser. The technique also lends itself to the acquisition of nested data sets, in which MS spectra are acquired at regular intervals (45-60 μs) during each IM separation (~15 ms), thereby reducing analysis times whilst having the potential to improve selectivity and data quality compared to MS analysis alone.[8]

IM has evolved into a technique for sensitive detection of many trace compounds and a wide range of chemical species such as chemical warfare agents,[9] biomolecules,[10] drugs of abuse[11] and inorganic substances.[12] IM has also been reported for the online monitoring of monomer concentrations in (semi-) batch emulsion polymerisation reactors,[13] the monitoring of yeast fermentation,[14] part per billion level process monitoring of ammonia in process streams[15] thus indicating the potential of IM as a rapid and precise measurement device for the monitoring of processes. More recently IM has been reported in pharmaceutical applications ranging from cleaning

verification of manufacturing equipment,[16] direct formulation analysis[17-19] and protection of pharmaceutical workers health and safety.[20] These studies suggest that IM combined with MS, may have potential for enhancing pharmaceutical process understanding and process control.

In this communication, we demonstrate proof of principle for the use of IM-MS for reaction monitoring applied to the direct, real-time analysis of the products formed when 7-fluoro-6-hydroxy-2-methylindole is deprotonated by sodium hydroxide. The use of orthogonal IM and MS analysis yields data comparable to mass spectrometry alone, but with the addition of an ion mobility dimension.

Experimental

Chemicals.

Acetonitrile (HPLC gradient grade) and water (HPLC grade) were purchased from Thermo Fisher Scientific (Loughborough, UK) Mass spectrometry grade (puriss, p.a) formic acid and sodium hydroxide (ACS reagent, ≥ 97.0%) pellets were purchased from Sigma-Aldrich (Gillingham, UK). 7-fluoro-6-hydroxy-2-methylindole was provided by AstraZeneca (Macclesfield, UK).

Sample preparation and real time monitoring.

Stock solutions of 7-fluoro-6-hydroxy-2-methylindole were prepared at concentrations of 0.1, 1, 3, 5, 10, 15, 20 and 50 μg ml^{-1} in 49.5/49.5/1 (v/v/v) acetonitrile/water/formic acid for calibration procedures.

7-fluoro-6-hydroxy-2-methylindole (125 μg ml^{-1}) was prepared in acetonitrile and stirred for 10 minutes on ice. Aqueous sodium hydroxide (40 m moles) was prepared in deionized water and added to the indole reaction vessel over a two minute period to initiate the deprotonation reaction. The reaction vessel was maintained at a temperature between -5 and 0 °C for the first six hours of the reaction, after which the reaction vessel was left overnight to warm to room temperature. Aliquots (20 μl) of the reaction mixture were removed from the reaction vessel and diluted to a concentration within the linear dynamic range of the analysis in 49.5/49.5/1 (v/v/v) acetonitrile/water/formic acid to quench the reaction for IM-MS analysis and infused into the ESI source at 5 μl min^{-1}. For real-time reaction monitoring, spectra were recorded at regular intervals during the deprotonation of the indole. Thus, a time zero spectrum was acquired before the addition of the sodium hydroxide and further

spectra were acquired at 60, 80, 160, 220 minutes and 24 hr and 7 days after addition of the sodium hydroxide.

Instrumentation.

Direct infusion IM–MS experiments were performed on a Synapt HDMS spectrometer (Waters Corporation, Manchester, UK), operated in positive ion mode with the ESI capillary voltage set to 3 kV and the cone voltage to 27 V. The nitrogen desolvation and cone gas flow rates were set to 500 and 30 L h^{-1} respectively, with a source temperature of 120 °C and desolvation gas temperature set to 300 °C. The ion mobility region contains three (trap, IM, and transfer) travelling wave stacked ion guides (TWIGS). The trap ion guide was used to accumulate ions and periodically then release an ion packet into the IM ion guide for mobility separation. A full description of the mode of operation of stacked ring ion guides with travelling waves is given elsewhere.[21] The travelling wave velocity was set to 300 ms^{-1} with a pulse height of 12 V in all acquisitions. Ions were injected into the IM TWIG from the trap TWIG for 200 μs in every ion mobility separation. Each ion mobility spectrum consists of 200 sequential ToF mass spectra (acquisition time typically less than 15 ms). The quadrupole was operated in wide band pass mode (*m/z* 50-1000) and the collision cell contained no collision gas. IM–MS data were obtained by combining the ion mobility spectra acquired in a 120 s infusion. Acquired data were presented as a plot of time against ion signal intensity; total ion mobility response or selected ion mobility responses. Masslynx version 4.1 software (Waters corporation, Manchester, UK) was used to control the IM-MS instrument and for data acquisition. Data mining was carried out using DriftScope version 2 (Waters corporation, Manchester, UK).

Results and Discussion

7-fluoro-6-hydroxy-2-methylindole (I) is converted to the O-linked indole product, 4-[(4-fluoro-2-methyl-1H-indol-5-yl)oxy]-2-methyl-1H-indol-5-ol (II), in the presence of air and sunlight, and through the addition of aqueous sodium hydroxide. Further deprotonation of indole phenolate by the sodium hydroxide leads to the formation of higher O-linked polymeric products, resulting in an increase in sample complexity over time. The reaction was studied to provide process understanding for pharmaceutical development. Reaction monitoring was carried out by IM-MS and MS with electrospray ionization, to follow the rate of polymerization of the indole I to II and other O-linked products, generating mass-to-charge and mobility data for the analyte ions present in the reaction mixture.

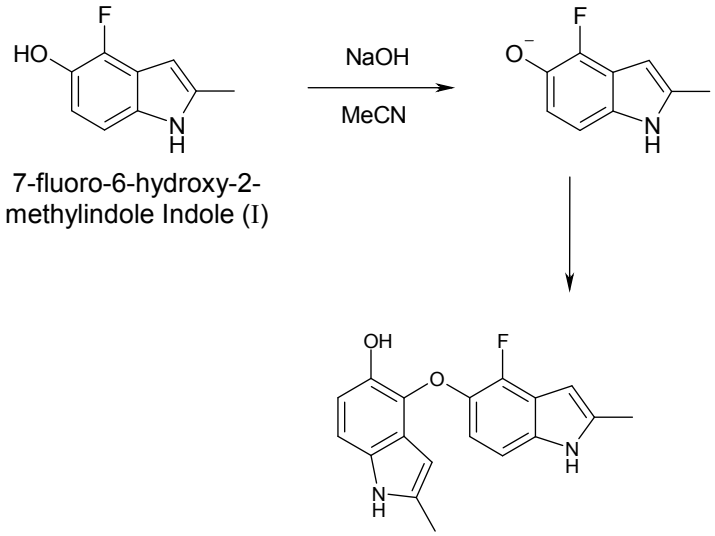

7-fluoro-6-hydroxy-2-methylindole Indole (I)

(II)

Initial investigations were directed at the optimization of the composition of the solvent system used to quench the aliquots of reaction mixture extracted from the

reaction vessel for analysis. Three solvent systems were investigated: 100 % acetonitrile (ACN), 50/50 (v/v) ACN/water and 49.5/49.5/1 (v/v/v) ACN/water/formic acid. Experiments carried out in 100 % ACN, gave a low signal response for all ions, with a total ion mobility response ion count approximately an order of magnitude less than the 50/50 (v/v) ACN/water and ~30 times less than the 49.5/49.5/1 (v/v/v) ACN/water/formic acid solvent system, for an initial indole concentration of 2.5 μg ml^{-1}. The presence of formic acid quenches the base catalysed reaction and enhances ionization efficiency, so 49.5/49.5/1 (v/v/v) ACN/water/formic acid was used for reaction monitoring with spectral acquisition carried out immediately after sample dilution.

Calibration curves were created from the indole standards for both IM-MS and MS analysis. IM-MS analysis has a lower linear dynamic range than MS because of detector saturation, but the analysis of the calibration standards showed a linear response in the concentration range 0.1 - 5 μg ml^{-1} for the indole, with an R^2 value of 0.9941. To ensure experiments were carried out within the linear dynamic range of the instrument, sample aliquots removed from the reaction vessel were diluted to a concentration within the linear dynamic range for the analysis. IM-MS data were acquired by repetitive scanning of nested data sets, with mass spectra (45 μs/scan) and IM spectra (~13 ms) scanned repetitively throughout, spectra were accumulated to yield 200 mass spectra and one IM spectrum every 7 seconds. The IM drift time is plotted as 'bins', where each bin corresponds to an acquired mass spectrum.

The total ion and selected ion mobility responses for the IM-MS analysis of the indole reaction mixture one hour after addition of aqueous sodium hydroxide are displayed

in Figure 1. The selected ion response for the protonated indole, II (*m/z* 311.13; Figure. 4.3(a)), shows a sharp peak, compared to the total ion mobility response, which is centered at a drift time of 5.72 ms and has a peak width at half height of 25 bins. The corresponding mass spectra are shown in Figure 4.4.

The mass spectrum obtained by combining all 200 bins (Figure 4.4(a)) corresponds to the spectrum expected in the absence of IM separation and contains a large number of ions across the whole mass range. In contrast, when the mass spectrum obtained in IM-MS mode by combining bins 128-130 (drift time range 5.7-5.8 ms; Figure. 4.4(b)) is compared with the mass spectrum in the absence of ion mobility separation, the relative intensity of the $[M+H]^+$ ion for II (*m/z* 311.13) has been enhanced selectively and is observed as the base peak in the ion mobility-selected mass spectrum.

The complexity of the reaction mixture one hour after addition of sodium hydroxide is illustrated in Figure 3, which shows the *m/z* versus ion drift time (bins) space, averaged over the whole IM-MS analysis, allowing good visualisation of the full IM-MS analysis data. The protonated monomer (I), O-linked dimer (II) and O-linked trimer ions are highlighted showing that these ions are resolved on the basis of mass-to-charge and drift time. The drift time of an ion may be used to determine the collision cross section (Ω, Eq. 1), which may be correlated with modelled or predicted structures[20-24], so IM-MS data has the potential for the structural analysis of mass-selected transient intermediates and products in complex reaction mixtures for enhanced process understanding.

The indole the reaction mixture was monitored by MS and IM-MS over a period of seven days. The reaction of indole monomer (I, *m/z* 166) to O-linked dimer (II, *m/z* 311) following addition of aqueous sodium hydroxide was fast, indicated by the reaction mixture rapidly turning from a straw coloured to a dark brown solution. The reaction continues via further addition of indole phenolate, with elimination of fluorine, to produce higher polymeric products. Figure 4 displays the time dependent ion intensities for the protonated ions derived from the reactant and products under MS and IM-MS analysis: *m/z* 166 (monomer, I), *m/z* 311 (O-linked dimer, II), *m/z* 456 (O-linked trimer), *m/z* 601 (O-linked tetramer), *m/z* 746 (O-linked pentamer) and *m/z* 891 (O-linked hexamer). Products and reactants ions were observed under both MS and IM-MS conditions. The ion intensities were lower in IM-MS mode, because of the transmission efficiency through the IM drift cell, but the instrumental sensitivity was sufficient to for monitoring reaction reactant and products throughout the course of the reaction. Ion counts were generated by combining selected bins (mass spectra) from the ion responses for each ion of interest at half height across the mobility peak. The O-linked dimer formation quickly reached a maximum intensity after the addition of sodium hydroxide and decreased thereafter as seen in Figure 4. The decrease in dimer ion intensity was associated with further polymerisation to form higher multimers. The formation of O-linked trimer reached a maximum at the same time as the dimer, but ion intensity showed only a slow decline during the first 80 minutes, followed thereafter by a sharper decline. The O-linked tetramer, pentamer and hexamer ion intensities rose more slowly, with the tetramer reaching an ion count maximum after 60-80 minutes in both the MS and IM-MS modes. The total ion current for all ions summed falls with time reflecting the difference in mass spectrometric response between the O-linked multimers and the monomer. These data

suggest that the monomer was progressively converted to the higher oligomers over time. The close similarity of the ion intensity trends observed in both the MS and IM-MS modes demonstrates that no loss of information is observed in IM-MS mode, whilst the greater selectivity and potential for structural analysis that IM measurement brings to the analysis has the potential to enhance ion assignments and process understanding.

Conclusion

This study has demonstrated that ion mobility-mass spectrometry can be employed as a rapid means to analyse a model chemical reaction mixture, offering the potential for real time reaction monitoring. The IM-MS approach has been shown to have potential to enhance visualization of the data selectivity for analytes compared with MS alone, as a direct result of the orthogonal mobility and mass-to-charge separation.

Acknowledgments

We thank AstraZeneca UK for financial support and Claire Scott, AstraZeneca UK, for helpful discussions.

References

[1] US Food and Drug Administration, Process Validation: General Principles and Practices, Draft Guidance 2008.

[2] T. Radhakrishna, D. Sreenivas Rao and G. Om Reddy*, Journal of Pharmaceutical and Biomedical Analysis*. 2001, **26**, 617–628.

[3] S. Rudaz, S. Souverain, C. Schelling, M. Deleers, A. Klompb, A. Norris, T.L. Vu, B. Ariano and J.L. Veuthey, *Analytica Chimica Acta.* 2003, **492**, 271–282.

[4] J. Tewari, V. Dixit and K. Malik, *Sensors and Actuators B.* 2010, **144**,104–111.

[5] K. Bakeev, *Process Analytical Technology, Spectroscopic Tools and Implementation Strategies for the Chemical and Pharmaceutical Industries*. JohnWiley & Sons, 1st edn., 2005, pp159.

[6] J. Hammond, B. Kellam, A.C. Moffata and R.D. Jee, *Anal. Commun*. 1999, **36**, 127–129.

[7] G. Eiceman and Z. Karpas*, Ion Mobility Spectrometry*, CRC press, 2nd edn., 2005.

[8] E.L. Harry, D.J. Weston, A.W.T. Bristow, I.D. Wilson and C.S. Creaser, *J. Chromatogr. B*, 2008, **871**, 357-361.

[9] W.E. Steiner, S.J. Klopsch, W.A. English, B.H. Clowers and H.H. Hill, *Anal. Chem*. 2005, **77**, 4792–4799.

[10] B.C. Bohrer, S.I. Merenbloom, S.L. Koeniger, A.E. Hilderbrand and D.E. Clemmer, *Annual Review of Analytical Chemistry*. 2008, **1**, 293-327.

[11] T. Keller, A. Mikib, P. Regenschetic, R. Dirnhofer, A. Schneider and H. Tsuchihashib. *Forensic science international*. 1998, **94**, 55-63.

[12] G.A. Eiceman, C.S. Leasure and V.J. Vandiver. *Anal. Chem*. 1986, **58**, 76–80.

[13] W. Vautz, W. Mauntz, S. Engell and J.I. Baumbach, *Macromol. React, Eng*. 2009, **3**, 85-90.

14. M. Kolehmainen, P. Rönkkö and O. Raatikainen. *Analytica Chimica Acta*. 2003, **484**, 93-100.

[15] T. Bacon and K. Webber. Acid and Halogen Gas Monitoring Utilizing Ion Mobility Spectroscopy (IMS), Technical Note, *Molecular Analytics*. 2005.

[16] R. Debono, S. Stefanou, M. Davis, and G. Walia. *Pharmaceutical technology*. 2002, **72**, 78.

[17] D.J. Weston, R. Bateman, I.D. Wilson, T.R. Wood, and C.S. Creaser. *Anal. Chem*. 2005, **77**, 7572-7580.

[18] M.D. Howdle, C. Eckers, A. Laures, C.S. Creaser, *J. Am. Soc. Mass Spectrom*. 2009, **20**, 1-9.

[19] G.A. Eiceman, S. Sowa, S. Lin, and S.E. Bell. *J. Hazard. Mater*. 1995, **43**, 13.

[20] R.M. O'Donnell, X. Sun and P.B. Harrington, *Trends in Analytical Chemistry*. 2008, **27**, 44-53.

[21] K. Giles, J. L. Wildgoose, D. J. Langridge and I. Campuzano, *Int. J. Mass Spectrom*. 20010, **298**, 10-16**.**

[22] T.W. Knapman, J.T. Berryman, I. Campuzano, S.A. Harris and A.E. Ashcroft**,** *Int. J. Mass Spectrom*. 2010, **298**, 17-23.

[23] M.F. Mesleh, J.M. Hunter, A. A. Shvartsburg, G. C. Schatz, and M. F. Jarrold, *J. Phys. Chem.* 1996, **100**, 16082-16086.

[24] T. Wyttenbach, G. von Helden, J.J. Batka Jr., D. Carlat, M.T. Bowers, *J. Am. Soc. Mass Spectrom*. 1997, **8**, 275-282

Legends to Figures

Figure 1. Ion mobility spectra for the IM-MS analysis of 7-fluoro-6-hydroxy-2-methylindole reaction mixture: (a) total ion mobility spectrum, (b) selected ion mobility response for *m/z* 311

Figure 2. Mass spectra for the IM-MS analysis of 7-fluoro-6-hydroxy-2-methylindole reaction mixture: (a) mass spectrum obtained by combining all 200 bins acquired during the ion mobility separation and (b) mass spectrum corresponding to the selected ion response for *m/z* 311 (bins 128-130)

Figure 3. 2D plot of drift time (bins) vs *m/z* for full data set of IM-MS analysis of indole reaction mixture, one hour after addition of aqueous sodium hydroxide, (a) indole monomer (*m/z* 166, I), (b) O-linked dimer (*m/z* 311, II) and (c) O-linked trimer (*m/z* 452).

Figure 4. MS and IM-MS analysis of the reaction of 7-fluoro-6-hydroxy-2-methylindole following the addition of aqueous sodium hydroxide. (a) signal response versus time in minutes for m/z 166 (monomer), m/z 311 (O-linked dimer), m/z 456 (O-linked trimer), m/z 601 (O-linked tetramer), m/z 746 (O-linked pentamer) and m/z 891 (O-linked hexamer) using (a) MS and (b) IM-MS.

Figures

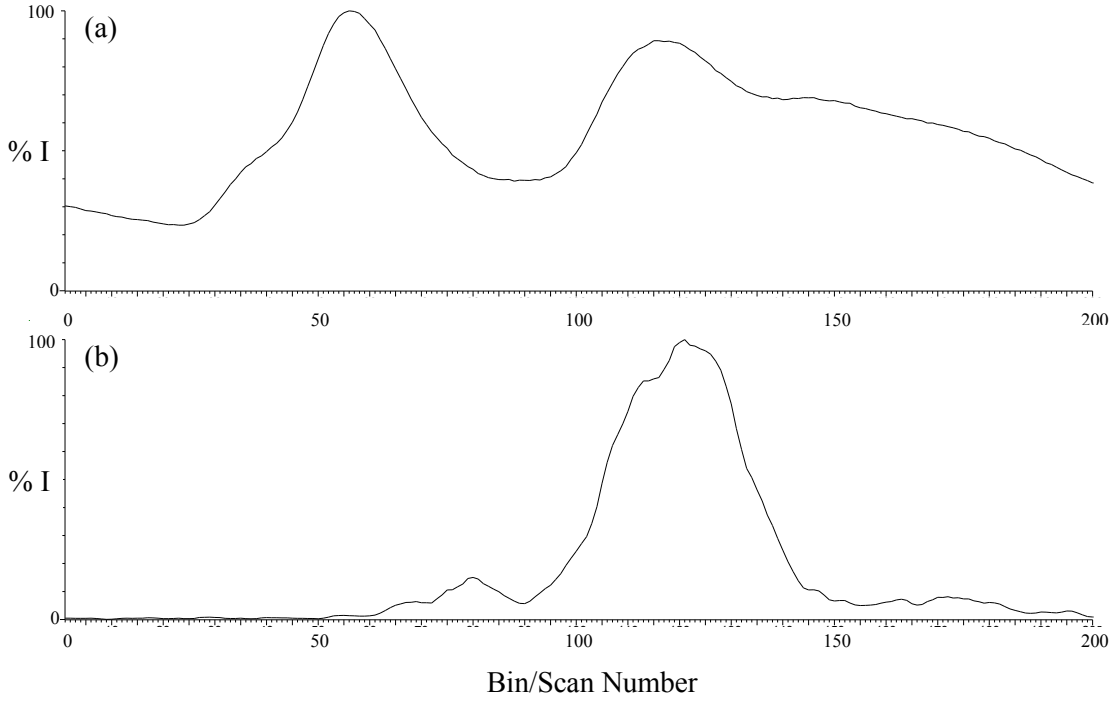

Figure 1

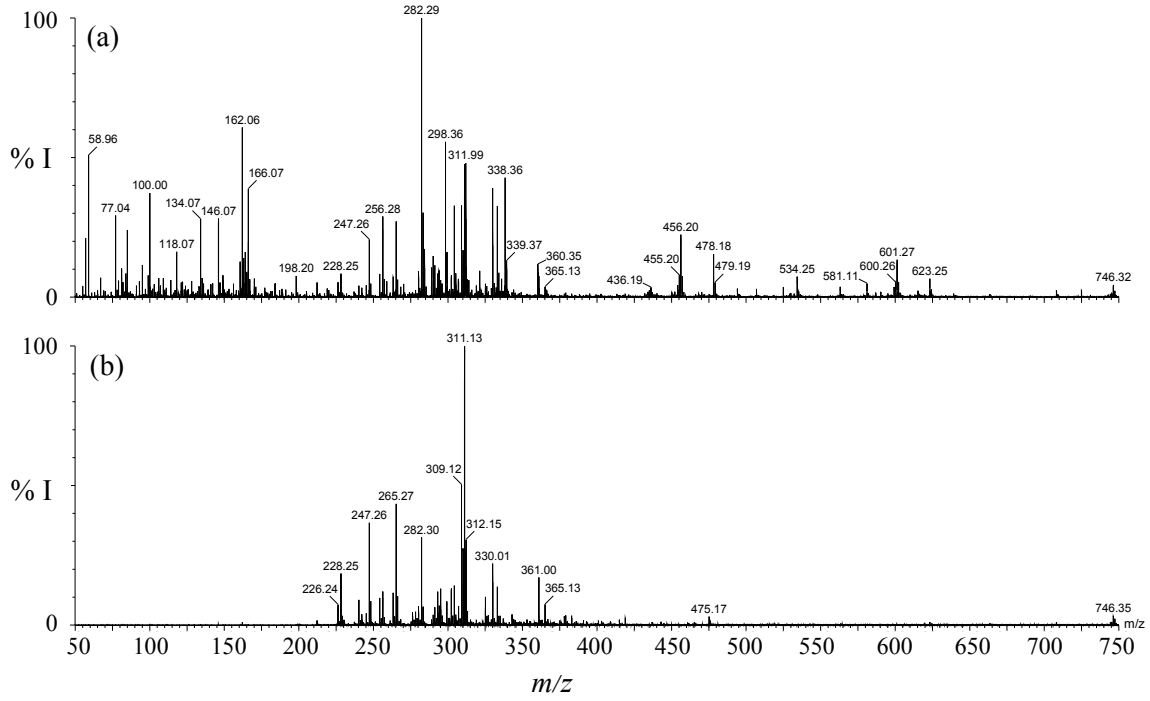
100
(a)
% I
0
282.29
58.96
162.06
298.36
311.99
166.07
338.36
100.00
134.07
146.07
77.04
256.28
247.26
339.37
118.07
456.20
478.18
360.35
455.20
601.27
198.20
228.25
365.13
479.19
534.25
600.26
623.25
436.19
581.11
746.32
100
(b)
% I
0
311.13
309.12
265.27
247.26
312.15
282.30
330.01
228.25
361.00
226.24
365.13
475.17
746.35
m/z
50
100
150
200
250
300
350
400
450
500
550
600
650
700
750
m/z

Figure 2

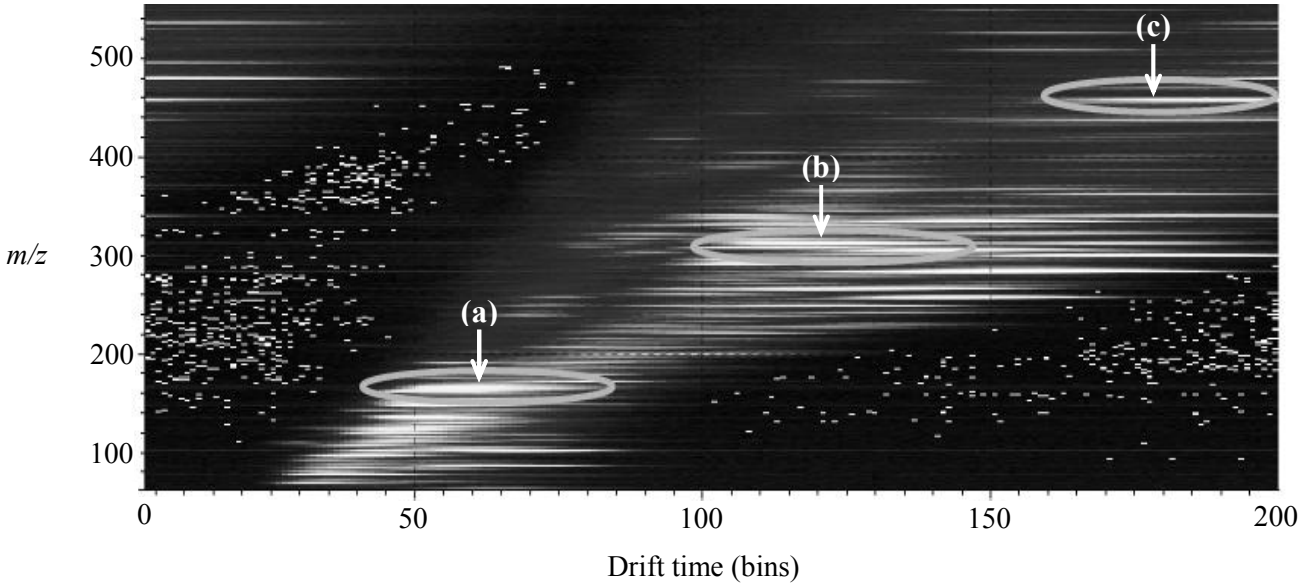

Figure 3

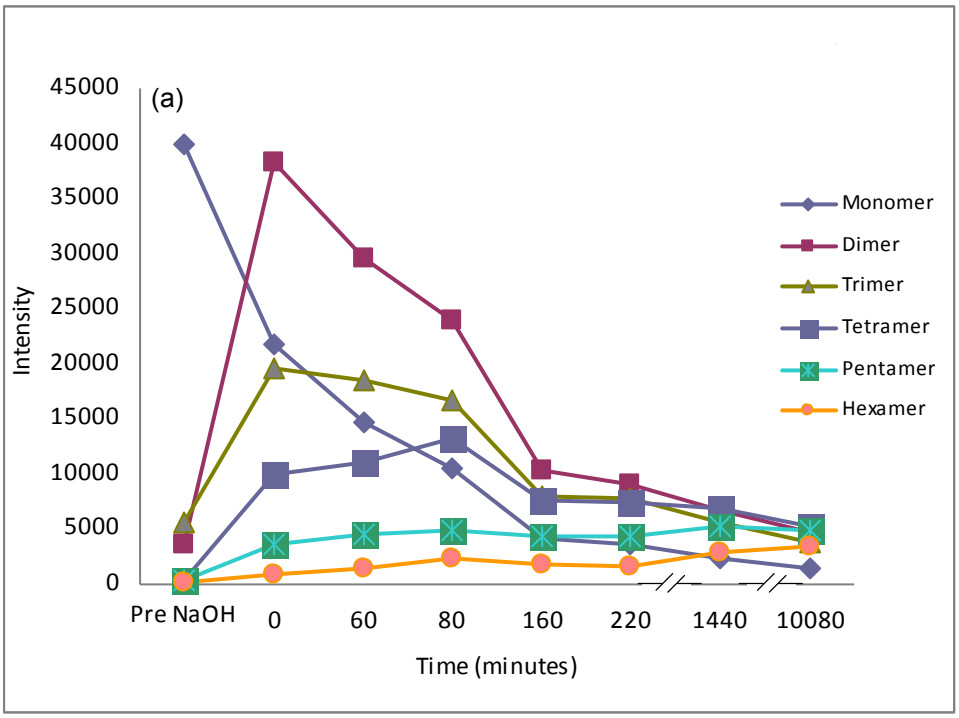
(a)
45000
40000
35000
30000
25000
20000
15000
10000
5000
0
Intensity
Pre NaOH
0
60
80
160
220
1440
10080
Time (minutes)
Monomer
Dimer
Trimer
Tetramer
Pentamer
Hexamer

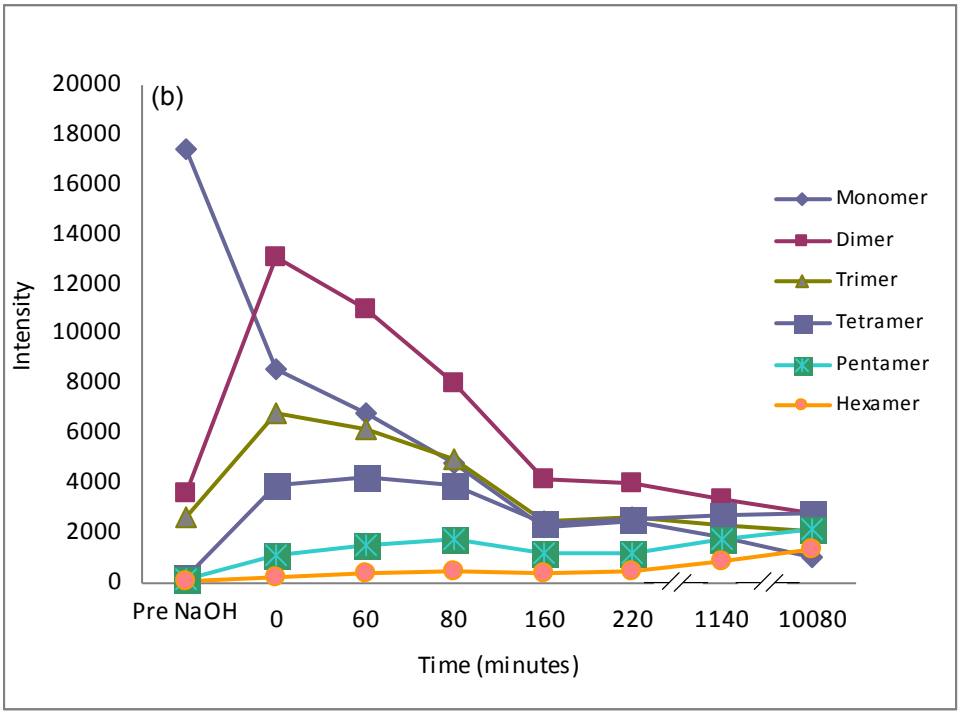
(b)
20000
18000
16000
14000
12000
10000
8000
6000
4000
2000
0
Intensity
Pre NaOH
0
60
80
160
220
1140
10080
Time (minutes)
Monomer
Dimer
Trimer
Tetramer
Pentamer
Hexamer

Figure 4.